Occurrence and Constitution of Natural and Synthetic Ferrihydrite, a Widespread Iron Oxyhydroxide

John L. Jambor

Leslie Research and Consulting, 316 Rosehill Wynd Tsawwassen, British Columbia, Canada V4M 3L9

John E. Dutrizac*

CANMET, 555 Booth Street, Ottawa, Ontario, Canada K1A OG1

Received November 25, 1997 (Revised Manuscript Received August 3, 1998)

Contents

I. Abstract

The importance of ferrihydrite in metallurgical processing and in the geochemical cycling of iron has been underestimated because of the difficulty in specific characterization, and because of the common designation of ferrihydrite as amorphous iron hydroxide, colloidal ferric hydroxide, $Fe(OH)_3$, etc. Ferrihydrite is generally classified according to the number of X-ray diffraction lines that the material gives: typically "2-line ferrihydrite" for material that exhibits little crystallinity, and "6-line ferrihydrite" for that which is best crystallized. The small grain size of ferrihydrite and its relatively poor crystallinity have thwarted attempts at the direct determination of its crystal structure, which in turn has meant that the chemical composition cannot be defined precisely. Recent X-ray spectroscopic studies, however, have indicated that the ferrihydrite structure has close similarities to those of the FeOOH-type minerals, specifically goethite and akaganéite, rather than to hematite. The widely reported nominal formula of ferrihydrite, $5Fe_2O_3{\cdot}9H_2O$, is thought to be excessively hydrous, and it has been demonstrated that almost all of the water can be replaced by adsorbed species in quantities that cannot be accommodated within the crystal structure. There is general contemporary agreement that the iron in ferrihydrite is octahedrally coordinated, but it also has been proposed that the octahedral coordination represents only the "core" structure, and that much of the surface of the ferrihydrite has iron in tetrahedral

10.1021/cr970105t CCC: $30.00
Published on Web 10/03/1998

John Leslie Jambor is the principal of Leslie Research and Consulting. He obtained his M.Sc. in geology at the University of British Columbia in 1960 and joined the Geological Survey of Canada. In 1966 he obtained his Ph.D. in mineralogy and crystallography from Carleton University, Ottawa. Upon transferring in 1976 from the Geological Survey to CANMET, formerly the Mines Branch, his main focus turned to applied mineralogical investigation of ore deposits and ore and processing products, and subsequently to environmental mineralogy related to acid mine drainage. Since leaving CANMET in 1993, he has operated as a conslutant to the minerals industry, particularly in the field of environmental issues. He is Adjunct Professor at the Department of Earth Sciences, University of Waterloo, and at the Department of Earth and Ocean Sciences, University of British Columbia.

John Dutrizac received his B.A. Sc. and Ph.D. degrees in 1963 and 1967 from the University of Toronto. Upon graduation, he worked briefly in industry before joining CANMET in 1968. His principal research interests are the leaching of sulfide minerals in ferric ion media, zinc processing with its associated iron precipitation problems, and copper electrorefining, especially the characterization of copper anodes and anode slimes. He retains an active interest in the history of metallurgical processing and has published several papers on this topic, in addition to over 175 technical papers. Dr. Dutrizac is a past President of the Metallurgical Society of CIM and has been a recipient of several international awards.

coordination. These "coordination-unsaturated" surface sites are highly amenable to the adsorption of foreign species and, combined with the large surface area, may account for the high adsorptive capacity of ferrihydrite. The adsorption of various ions generally retards the transformation of ferrihydrite to goethite or hematite.

II. Introduction

Iron is the fourth most abundant element in the earth's crust and is the second most abundant metal.[1] Iron occurs in a diversity of minerals including sulfides, oxides, hydroxides, and complex hydroxide anion species such as jarosite, $KFe_3(SO_4)_2(OH)_6$. Weathering results in the presence of iron in natural waters, soils, and oxidized ore cappings. Because of its relative abundance, iron is a common constituent of virtually all ores and concentrates treated by the metallurgical industry. The processing of base metal sulfide ores by flotation techniques generates large tonnages of tailings which commonly contain abundant pyrite and/or pyrrhotite. The oxidation of the iron sulfide minerals in tailings ponds releases an acidic iron sulfate drainage, the neutralization of which generates poorly characterized iron hydroxide species. In addition, the processing of base metal sulfide concentrates by hydrometallurgical methods solubilizes at least part of the inevitably associated iron content. At some point in the processing circuit, the dissolved iron must be removed by hydrolytic precipitation. Although the industry has developed sophisticated techniques to precipitate the iron as easily filterable jarosite, goethite, or hematite,[2] precipitation of some iron hydroxide is commonly practiced either to reduce the iron concentration to very low levels or to eliminate specific impurities from the circuit.[3]

Traditionally, the iron hydroxide precipitates encountered in the metallurgical industry have been described as amorphous ferric hydroxide, colloidal ferric hydroxide, $Fe(OH)_3$, etc. Significantly, however, the precipitates do not have the composition $Fe(OH)_3$, and they are not amorphous although their X-ray diffracting properties are poor. It is now recognized that many of these precipitates are actually ferrihydrite, and their widespread occurrence makes ferrihydrite an important species in the natural environment, in tailings management, and in metallurgical processing.

In their seminal paper on the iron compound later to become known as ferrihydrite, Towe and Bradley[4] introduced their topic as follows:

> In the past colloidal ferric oxides and hydroxides have been the subject of a great deal of interest and several distinct phases have been identified and characterized. In addition to these more definite phases, however, there exists a widely occurring group of amorphous and paracrystalline-to-crystalline compounds referred to in various ways but most frequently as "hydrous ferric oxide" or "ferric hydroxide". The data concerning such materials are often contradictory, as are interpretations regarding their mineralogical composition.

Towe and Bradley were able to characterize their synthetic phase sufficiently that correspondence with a naturally occurring analogue was no longer in doubt. The latter was referred to as the "Towe–Bradley phase" in the title of the paper by Chukhrov et al.,[5] but the new name ferrihydrite, alluding to the composition, was introduced within the text. The name ferrihydrite was used again by Chukhrov et al.,[6] and was in further use by 1973.[7] Childs[8] reported that approval of the new name by the International Mineralogical Association (IMA) did not take place until 1975, but his inference is probably

Table 1. Oxides, Hydroxides, and Oxyhydroxides of Iron

mineral	nominal formula	phase	nominal formula
goethite	α-FeOOH	synthetic	$Fe(OH)_2$
akaganéite[a]	β-FeOOH	synthetic	β-Fe_2O_3
lepidocrocite	γ-FeOOH	synthetic	ϵ-Fe_2O_3
feroxyhite	δ-FeOOH	synthetic	FeOOH
hematite	α-Fe_2O_3		
maghemite	γ-Fe_2O_3		
magnetite	Fe_3O_4		
wüstite	FeO		
bernalite	$Fe(OH)_3$		
ferrihydrite	$Fe_5HO_8 \cdot 4H_2O$		

[a] Cl may be an essential constitutent.[11]

based on the abstract that appeared in New Mineral Names;[9] Chukhrov et al. stated in their 1973 paper[10] that IMA approval had been obtained prior to publication.

Of the 14 iron oxides, hydroxides, and oxyhydroxides that have been more or less well-defined, 10 are known to occur in nature and these are presented in Table 1. The most common are goethite, hematite, and magnetite, each of which can occur in sufficient abundance to be a rock-forming mineral. Lepidocrocite, ferrihydrite, and maghemite can be designated as intermediate in that each is known from many localities, but all occur much less frequently and in much less abundance, to the point of rarity, in comparison to goethite, hematite, and magnetite. Nevertheless, the intermediate minerals are in turn common, both in distribution and quantity, relative to the sparseness of wüstite, akaganéite, feroxyhyte, and bernalite, with the last known only from one locality.

The diagnostic criteria for the various iron oxides are given in Table 2. Ferrihydrite is always extremely fine grained, which in part accounts for the continued debate about its structure and composition. The only other megascopic feature that may be useful for identification is the mineral's reddish brown color (hue ranges between 7.5YR and 2.5YR).[12] Although the color of most minerals can vary with crystal size, morphology, and element substitutions (and that of ferrihydrite is no exception), color can be a characteristic feature. Nevertheless, no experienced researcher would attempt to identify ferrihydrite solely on the basis of its megascopic or microscopic properties, and even the utilization of laboratory techniques such as X-ray diffraction does not always provide an unequivocal identification. The reason for the possible ambiguity is that ferrihydrite is always poorly crystalline or disordered. Thus, it is common, if not standard, to have preceding the name a descriptive qualifier such as "2-line" ferrihydrite or "6-line" ferrihydrite. Such qualifiers refer to the number of characteristic X-ray diffraction peaks that the mineral or synthetic phase has yielded; the relationship is that the fewer and broader the X-ray peaks, the poorer the crystallinity. The above discussion suggests that ferrihydrite is of considerable importance in minerals processing and extractive metallurgy. The discussion also indicates that the properties of ferrihydrite are not unequivocally defined and that this lack of definition impedes the identification and

Table 2. Diagnostic Criteria for Iron Oxide Minerals[†]

mineral	color (Munsell)	usual crystal shape	most intense XRD lines[d]	DTA events, °C	IR bands, cm^{-1}	magnetic hyperfine field (T)		
						295 K	77 K	4 K
ferrihydrite	reddish brown, 5YR−7.5YR	hexagonal plates[a]	2.54, 2.24, 1.97, 1.73, 1.47	endotherm 150		–	–	47−50
hematite	bright red, 5R−2.5YR	hexagonal plates	2.70, 3.68, 2.52	nil	345, 470, 540	51.8	54.2/53.5[e]	54.2/53.5[b]
maghemite	red to brown	cubes	2.52, 2.95	exotherm 600-800	400*, 450*, 570, 590, 630	50	–	52.6
magnetite	black	cubes	2.53, 2.97	see footnote *c*	400, 590	49.1/46.0[b]	–	–
goethite	yellowish brown, 7.5YR−10YR	needles, laths	4.18, 2.45, 2.69	endotherm 280-400	890, 797	38.2	50.3	
lepidocrocite	orange, 5YR−7.5YR	laths	6.26, 3.29, 2.47, 1.937	endotherm 300-350	1026, 1161, 753	–	–	45.8
akaganéite	yellowish brown, 5YR−10YR	somatoids, rods	3.33, 2.55, 7.47	endotherm 270	840, 640	–	47.1, 46.7, 45.3	48.9, 47.8, 47.3
feroxyhyte	reddish brown, 5YR−7.5YR	fibers, needles	2.54, 2.22, 1.69, 1.47	endotherm 250	1110*, 920, 790, 670	42.0	53.0	53.5
bernalite	dark green	pyramidal to pseudooctahedral	3.784, 1.682, 2.393, 2.676, 1.892	exotherm 190-200		42.0		55.7

[†] Adapted from Schwertmann and Cornell;[13] bernalite and its accompanying data added here.[14–17] [a] Poorly developed. [b] For tetrahedral and octahedral Fe, respectively. [c] Magnetite converts via maghemite or directly to hematite, depending on particle size. [d] Arranged in order of decreasing relative intensity; values in angstroms. [e] With and without Morin transition (spin flip at 260 K), respectively.

characterization of the species in processing operations. In an effort to address these issues, a systematic review of the literature on ferrihydrite was carried out to identify its modes of occurrence, to characterize its composition and crystal structure, and to discuss some of its properties of relevance to the minerals industry.

III. Occurrences of Ferrihydrite

A. Extraterrestrial Occurrences

The presence of limonite in altered chondrite meteorites was known prior to the work of Tomeoka and Buseck[18,19] and Keller and Buseck,[20] but the quantity was insufficient to account for the apparent amount of Fe(III) as determined by chemical analysis. Selected-area electron-diffraction patterns of the iron oxide showed two broad rings at *d* values characteristic of 2-line ferrihydrite. Tomeoka and Buseck[19] suggested that the ferrihydrite, which is intergrown intimately with fine-grained phyllosilicates and amounts to ~34% of the iron in the Orgueil meteorite, is preterrestrial rather than a terrestrial weathering product. Brearley[21] obtained electron diffraction rings at 2.45, 2.15, 1.99, and 1.41 Å, characteristic of 4-line ferrihydrite, from a hydrated iron oxide that makes up about 10 vol % of the matrix of the Kakangari chondrite. Brearley accepted the contention of Tomeoka and Buseck that the ferrihydrite in the chondrite they examined was of preterrestrial origin, but concluded that the occurrence of ferrihydrite within pores in the matrix of the Kakangari chondrite did not exclude a possible terrestrial genesis for the mineral. Subsequently, Brearley and Prinz[22] reported the presence of 3-line (2.54, 2.20, and 1.54 Å) ferrihydrite in a ureilite and proposed that ferrihydrite formed initially from pentlandite, and then from magnetite, in the earliest stages of preterrestrial aqueous oxidation.

The presence of ferrihydrite as a preterrestrial alteration mineral is strongly supported by textural features, and this genesis seems to have been accepted without challenge. It has been further suggested[23,24] that ferrihydrite-bearing clay silicates (smectites) warrant serious consideration as analogues for soils on Mars. This suggestion is based on the identification of ferrihydrite as the interlayer ferric component in Fe(III)-doped smectites prepared in the laboratory and on the recognition that spectroscopic analyses of the doped smectites and the soils on Mars exhibit important similarities.

Altered basaltic glass (palagonite) on Mauna Kea volcano on the island of Hawaii is a good spectral analogue of Martian bright regions. Nanophase ferric oxide, which is a generic term for ferric oxide/oxyhydroxide particles having nanoscale (<20−50 nm) particle dimensions, was found by Morris et al.[25] to be responsible for the ferric doublet detected in the Mössbauer spectrum and for the visible-wavelength ferric absorption edge observed in the reflectivity spectra. The nanophase ferric oxide, either hematite or its mixture with ferrihydrite, was concluded to be the primary pigmenting agent of the bright soils and dust of Mars.

B. Ferrihydrite in Waters and Sediments

In their original descriptions of ferrihydrite, Chukhrov et al.[5,10] noted that the mineral occurs as deposits associated with cold-water springs, and as a supergene alteration product, at several localities throughout the former USSR. In the 1973 description, 11 localities were specifically named, and all were reported to have near-neutral pH, outlet temperatures of 5−7 °C, and to involve the participation of the bacteria *Gallionella ferruginea*, *Leptothrix ochracea*, and *Toxothrix trichogenes*. Chukhrov et al. also cited occurrences in mine workings, on volcanic rocks at the edge of a caldera in which the temperature of a water spring issuing from the floor was 30−40 °C, as precipitates from a thermal spring (80 °C, pH 5.8−6.1), in iron-bearing sediments from the Red Sea depression, and in ferruginous sediments affected by thermal waters in the Kuril Islands. It was concluded that ferrihydrite is geologically young (Pleistocene or younger) and that it transforms to hematite on aging, and to goethite in the presence of solutions containing iron(II).

Ferrihydrite has been noted in the water column of lakes[26] and was reported to be the main crystalline form of the Fe(III) precipitates in the recent bottom sediments of lakes in the Muskoka and Sudbury areas of Ontario,[27] in the Niagara Basin of Lake Ontario,[28,29] and at Narrow Lake, north of Edmonton, Alberta.[30] Some of these sediments contain up to 1.5 wt % P, with much of it adsorbed as PO_4 on the ferrihydrite. At a site in New Zealand, adsorbed P in ferrihydrite was noted by Childs et al.[31] to decrease downstream relative to the P contents in the mineral at the spring-fed source, whereas the reverse occurred for Si, Al, Ca, and C. Schwertmann et al.[32] reported that the bottom sediments in two Finnish lakes (pH 6.7−6.9) contain as much as 50 wt % Fe, present largely as various proportions of ferrihydrite and goethite. Locally increased proportions of ferrihydrite were attributed to a higher rate of Fe(II) supply from the groundwater, and to a higher rate of oxidation as a function of water depth and bottom-sediment permeability.

Aeration of water, including that for drinking purposes, commonly leads to the precipitation of ferrihydrite.[33−35] Ferrihydrite also forms as incrustations in water wells and on metallic objects immersed in wells,[36] and has been noted as coatings on the walls and bases of paddy races in Japan,[37] and as coatings on pebbles in ferriferous streams.[38] Ivarson and Sojak[39] described the occurrence of abundant *Gallionella* in the effluents and ochreous deposits of partly blocked field drains at several Ontario sites. Although only "amorphous" iron oxides were detected by X-ray diffraction, the apparent lack of detection of ferrihydrite was possibly related to the timing of the study, which was only shortly after the recognition of ferrihydrite as a mineral.

Henmi et al.[40] suggested that poorly crystallized siliceous ferrihydrite precipitates, for which the Si−O stretching band of the infrared spectrum shifted as Si increased and Fe decreased, might represent a series with hisingerite $Fe_2^{3+}Si_2O_5(OH)_4 \cdot 2H_2O$. In ferrihydrite containing 3−7 wt % Si, Carlson and

Schwertmann[33] noted a broad absorption band at 960−975 cm^{-1}, which does not occur either in pure ferrihydrite or in a mechanical mixture with amorphous silica (1080 cm^{-1}); the 960−975 cm^{-1} band was therefore attributed to Fe−O−Si bonds. Experimental tests by Carlson and Schwertmann showed that Si concentrations of 7−12 mg/L inhibited the crystallization of lepidocrocite and goethite in favor of ferrihydrite.

Chukhrov[41] proposed that hematite in red-bed deposits originated by the alteration of ferrihydrite that had been transported as particulate matter to the depositional site, and subsequently spontaneously altered to hematite. The presence of ferrihydrite in marine sediments has been inferred (on the basis of extractions with 0.2 M ammonium oxalate solution) by Canfield,[42] and the detection of a ferrihydrite-like phase in Pacific Ocean deep-sea iron−manganese oxide crusts was reported by Murad and Schwertmann.[43] Ferrihydrite, feroxyhyte, akaganéite, goethite, hematite, magnetite, maghemite, and chromite were found in polymetallic nodules from the East Pacific basin.[44] Dill et al.[45] found that ferrihydrite occurred sparingly in metalliferous muds associated with several "hot spots" on the East Pacific Rise (18° S); the mineral formed during the initial stages of oxide precipitation, and subsequently was altered to goethite during diagenesis. The presence of the sole clay mineral, nontronite, was ascribed to the reaction of ferrihydrite with hydrothermal silica. Iron-rich plumes at the East Pacific Rise contain particulate oxyhydroxides consisting mainly of ferrihydrite,[46] and hydrothermal iron-rich crusts recovered from several volcanic "hot spots" in the southwestern Pacific consist largely of ferrihydrite.[47] The crusts were formed by the interaction of seawater and hydrothermal fluids discharged from the volcanoes. Brown et al.[48] and Sawicki et al.[49] noted the coexistence of siderite and ferrihydrite in a microbial biofilm that formed on the wall of an excavated vault, deep underground in the Lac du Bonnet batholith in Manitoba. They suggested that this type of mechanism for the precipitation of Fe(II) and Fe(III) in close proximity may have a bearing on the geological development of banded iron formations, a suggestion expanded upon by Brown et al.[50]

C. Ferrihydrite in Soils

Ferrihydrite typically forms where oxidation of Fe(II) is rapid, and thus it is perhaps not surprising that the first reported occurrence of ferrihydrite in soils was for weathered crusts on basalts in Hawaii.[51] Ferrihydrite has since been detected as an important constituent in Spodosols,[52−54] in loess,[55] as the precursor to hematite in rubified (hematitic) soils,[56] in a peat bog,[57] in bog iron,[58] in soil concretions[59] and hardpan,[60] in oxidized surface layers of saline sulfidic soils of Australia,[61] and as the oxidized coatings on diabase and sandstone in Antarctica.[62] Numerous additional references to the presence of ferrihydrite in soils are given in the review papers by Childs[8] and Schwertmann,[12,63] who cite publications on well-documented occurrences in hydromorphic (gley) soils, in placic horizons,[64] in podzols,[65,66] in Spodosols and Spodosol-like soils, in soils derived from volcanic ash and tephra,[67] in rice-paddy soils,[68] and in iron pans. Childs[8] noted that long periods of weathering usually lead to the formation of goethite and hematite, and that

> the emerging general impression is that ferrihydrite is a common component of...soils undergoing rapid early weathering, of soils containing soluble silicate or organic materials that inhibit the formation of more crystalline iron oxides (and hence stabilize ferrihydrite), and of soils that are subject to periodic reduction and oxidation (including paddy soils).

The various properties of ferrihydrite that affect the character of soils are reviewed by Childs.[8] Aside from the obvious role as a cementing and pigmentation agent, it has been shown by Parfitt[69] that ferrihydrite is comparable to allophane as an adsorber of phosphate. The presence of humic compounds is known to inhibit crystal growth, and high C/Fe ratios result in the formation of ferrihydrite rather than goethite or lepidocrocite.[57,70] Adsorption of organic complexes increases the solubility of ferrihydrite and decreases the cementation and stability properties of the soils.[71,72] The decrease ensues because ferrihydrite in soils in temperate regions has a positive charge and is attracted to the permanently negatively charged sites on clay−mineral surfaces;[73] addition of organic carbon reduces the positive charge of the ferrihydrite, and gradually may even reverse it at high-carbon contents.[71]

Most ferrihydrite occurs in pedogenic environments that are moist and cool. Under warmer or dryer conditions, ferrihydrite generally transforms to goethite or hematite. The rate of this conversion and the various factors that affect it are discussed in the section on transformations.

D. Mine Wastes and Acid Mine Drainage

Oxidation of pyrite in coal commonly leads to the generation of acidic effluents and downstream precipitation of ochreous, iron-rich deposits. Numerous occurrences of ferrihydrite in such precipitates, mainly from coalfields in Ohio, have been reported.[74,75] Ferrihydrite is one of the oxidation products in a suite of secondary minerals that formed in weathered Pb−Zn ores in the Tyne River Basin in northeast England.[76] Weathered uranium ore in the Alligator Rivers region of the Northern Territory of Australia contains U- and Th-bearing iron oxides, principally ferrihydrite and goethite.[77] At both locations, the dissolution of the ore minerals and downstream transportation ultimately lead to the precipitation of iron oxides, including ferrihydrite. Similarly, uranium minerals in the shallow ore zones of the Koongarra uranium deposit, Northern Australia, have been attacked by groundwaters, resulting in a zone of elevated U concentrations extending away from the ore zone in the direction of the groundwater flow. Chemical extractions indicated that the uranium is associated predominantly with ferrihydrite and other iron oxides, and laboratory experiments demonstrated that the transformation of ferrihydrite to more crystalline iron oxides substantially reduced the ability of the samples to adsorb uranium from solution.[78]

Weathered, arsenopyrite-rich gold ore that had been ground and treated with cyanide at the Yankee mine near Trentham, Victoria, Australia, was examined by Brown et al.[79] Using Mössbauer spectroscopy as the only tool for identifying the weathered products, they concluded that the principal secondary mineral is pharmacosiderite and that small amounts of scorodite, ferrihydrite, and goethite are also present.

The pore waters within sulfide-rich tailings are invariably highly charged with iron derived by the oxidation of pyrite (FeS_2) and pyrrhotite ($Fe_{1-x}S$). A characteristic feature of the surfaces of oxidized tailings impoundments is their rusty color, which results mainly from the destruction of iron sulfides and the consequent reprecipitation of the iron as secondary iron oxides. Goethite, and locally jarosite, are the predominant secondary minerals,[80] but ferrihydrite also occurs in small amounts.[81] Ferrihydrite also has been noted to form during the drying of the cores retrieved from tailings impoundments, thus indicating that the Fe-rich pore waters may yield ferrihydrite precipitates, but only after external influences are imposed.[82] Accordingly, caution is required in the sampling methodology and the interpretation of the results.

The seeps adjacent to tailings impoundments are common sites for ochreous precipitates. A plume of red-brown sludge near the margins of a retention pond at the Ranger uranium mine, Northern Territory, Australia, was found[83] to consist mainly of ferrihydrite, with lesser amounts of goethite and lepidocrocite. At low water levels, and accompanying higher water temperatures, additional goethite forms by direct precipitation and by transformation of the ferrihydrite.

Sediments receiving acid drainage from mine tailings at Rossport (north shore of Lake Superior), Burchell Lake (west of Thunder Bay), and Cranberry Lake (northwest of Sudbury) in Ontario, and from a coal refuse impoundment in Belmont County, Ohio, were found by Ferris et al.[84] to be laden with ferrihydrite. Johnson[85] suggested that concentrations of Cu and Zn released by the acid mine drainage were subsequently affected mainly by downstream adsorption on ferrihydrite. Mann and Fyfe[86] identified goethite, ferrihydrite, maghemite, hematite, and akaganéite at the cell walls of *Euglena* sp. extracted from sediments cored at a discharge channel of the Stanrock tailings area, Dennison Mines Limited, Elliot Lake, Ontario. At the Levant mine, Cornwall, England, ferrihydrite not only occurs as a mineral in an extensive secondary suite, but also is present in suspended flocculates in waters collected within the mine.[87] The flocculates in low-pH (<5) waters consist of goethite, ferrihydrite, lepidocrocite, and quartz, whereas near-neutral (pH 5−8) groundwaters contain a different assemblage in which jarosite is present and ferrihydrite is absent.

One of the technologies under investigation for the treatment of acid mine drainage involves the construction of artificial wetlands containing vegetation capable of sorbing toxic metals. More than 300 experimental wetlands have been established in Appalachia alone.[88] The characterization of the metal forms retained by the wetland substrates is generally on the basis of sequential extractions, but for one such constructed wetland, which receives AMD from an abandoned coal mine in McCreary County, Kentucky, the mineralogy of the precipitates has been determined.[89] Minerals precipitating in flumes and in entry wetland cells lacking vegetation included ferrihydrite, lepidocrocite, goethite, possibly an akaganéite-like mineral, and high Fe/S ratio iron-oxyhydroxysulfates (similar to schwertmannite). Within vegetated wetland cells lined with crushed limestone, well-crystallized gypsum, lepidocrocite, and Fe-oxyhydroxysulfate minerals with low Fe/S ratios were accompanied by gradual reductions in ferrihydrite and akaganéite. The overall composition of the precipitates suggested that the Fe chemistry is controlled primarily by the solubility of iron oxyhydroxides in flumes, and by S-enriched iron oxyhydroxides inside the wetland cells. Formation of jarosite and goethite seems to have been inhibited by the presence of organic constituents as well as the presence of iron oxyhydroxysulfates and gypsum. Karanthanasis and Thompson[89] determined that more than 95% of the Fe, 99% of the Mn, and ~100% of the Zn in the surface effluents were in inorganic forms, whereas ~99% of the Cu and ~40% of the Al were organically bound. This speciation pattern was consistent throughout the wetland.

E. Other Occurrences

Ferrihydrite is well-known as one of the products derived from the corrosion or atmospheric oxidation of iron and steel. As knowledge of the constitution and distribution of Fe oxides derived thusly is of enormous economic importance to the iron and steel industries and their users, much of the literature pertaining to ferrihydrite is concerned with this topic (refs 90−92, and the references therein). Ferrihydrite is also of economic importance in that it is one of the iron-based catalyst precursors used in converting coal to liquid fuel by direct coal liquefaction, and is also applied to the slurry phase in heavy-oil upgrading processes. The effectiveness of ferrihydrite in relation to some of the other iron oxides may be attributable in part to the fine particle size and high dispersion (lack of agglomeration) of ferrihydrite, especially the 6-line versus the 2-line variant. Studies of ferrihydrite as a catalyst thus have the objective, in large part, of determining how to maintain or increase its surface area, thereby minimizing catalyst loading. Addition of adsorbents, such as Si, can increase by hundreds of degrees the temperature at which ferrihydrite converts to hematite; as the conversion stage is also the main agglomeration stage, addition of an adsorbent, both as to type and doping level, can be cost-effective in decreasing catalyst loading. These studies have contributed significantly to the understanding of the nature of the transformation of ferrihydrite to hematite,[93] the effects of Mo, Si, and Al adsorption,[94,95] and the structure of ferrihydrite.[96,97]

Many references to ferrihydrite in the literature are concerned with the nature and behavior of the ferrihydrite-like cores in ferritin because the manner

in which the protein shell takes up, sequesters, and releases its iron is of great biological importance.[98] This and directly related biological topics, however, are not dealt with herein.

F. The Role of Ferrihydrite in the Geochemical Cycling of Iron

Oxyhydroxides of iron play a significant role in the geochemical cycling of iron, and in oxidizing environments the development of ferrihydrite is superseded only by that of goethite and hematite. Although ferrihydrite is unstable, and with time will convert to the more stable iron oxides, namely goethite or hematite, the transformation can be retarded by adsorption of various species, both inorganic and organic. It has long been suggested by Schwertmann and his colleagues that ferrihydrite is a necessary precursor to the solid-state formation of hematite.[13,99] The limited range of stability of ferrihydrite relative to hematite and goethite, however, has resulted in the absence of ferrihydrite in all but the most recent part of the geological column. In modern natural environments there seems little doubt that the abundance of ferrihydrite is underestimated because of its lack of detection rather than its lack of presence. Ferrihydrite is unquestionably a mineral name that is more familiar to soil scientists than to those in the earth sciences community. Until very recently, few geochemists or mineralogists seemed to be aware that the "amorphous $Fe(OH)_3$" phase widely used in geochemical calculations is an inaccurate representation of ferrihydrite.

Natural precipitation of ferrihydrite is perceived to be limited by the need for rapid oxidation of Fe^{2+} to bypass the formation of the FeOOH phases. A further perceived limitation is that although the pH range for ferrihydrite precipitation extends from slightly acidic to slightly alkaline conditions, which encompasses all but the most extreme of natural aqueous environments, the pH range is nevertheless more restricted than that which permits goethite precipitation. The ferrihydrite occurrences outlined in the preceding text, however, show that the mineral is widely distributed in various soils and sediments, and forms from iron-laden water from which precipitation is rapid. Accelerated oxidation of iron by microbial activity seems to be a favorable condition, but is not essential.

Two of the most significant roles of ferrihydrite in the geochemical cycle are as an adsorbent of various trace elements and as a control on the concentration of iron in surface waters. Adsorption onto ferrihydrite and other iron oxides has been shown to play an important role in the transportation of Pb from continental waters to the oceans.[100] As has been noted by Coston et al.[101] sorption of metal ions in natural systems is thought to be dominated by surface reactions with Fe and Al oxyhydroxides and organic coatings,[102] and this association between contaminant metals and the oxyhydroxides has been used as an indicator of contaminant levels in sediments. In lacustrine sediments, the deportment of arsenic may be largely controlled by the association with ferrihydrite (readily extractable amorphous Fe oxyhydroxide).[103] Adsorption in natural systems is generally pH-dependent, both for ligands[104] and metals. Minor fluctuations in pH in natural systems may play a significant role in controlling the adsorption−desorption reactions associated with ferrihydrite. Fuller and Davis,[34] for example, observed diurnal fluctuations in the arsenate content of two streams, the pH of which varied by as much as 0.5 units daily in the pH 8 to 9 range because of photosynthesis. Arsenate adsorption decreased as the pH increased, and it was suggested that fluctuations in pH might have an even greater effect on trace metals such as Zn, Cu, and Cd.

It seems highly probable that many of the literature references to amorphous or colloidal iron hydroxides deal with ferrihydrite in all but name. Kimball et al.,[105] for example, reported on the deportment of As, Cd, Cu, Mn, Pb, and Zn in acid mine drainage associated with a phase variously described as "ochre-colored colloids" and "colloidal hydrous Fe oxides", but ferrihydrite per se was not mentioned in the paper. Ferrihydrite is difficult to identify explicitly in routine determinative procedures, and occurrences of the mineral have been underestimated either because of a lack of detection or because, in some cases, the occurrence has been cloaked by a pseudonym such as "amorphous iron hydroxide".

The role of diurnal fluctuations should not be underestimated as a key factor in the genesis of ferrihydrite in nature. McKnight et al.[106] have proposed that diurnal fluctuations of iron in streamwaters contribute to the preponderance of "amorphous iron hydroxides" relative to the better crystallized forms. It is well-established that particulate[107] and colloidal iron oxyhydroxides undergo inorganic[108,109] and organic-dependent photoreduction; the reaction occurs both in freshwater[110] and seawater.[111,112] The Fe(II) produced by photoreduction is transient[113,114] and is rapidly oxidized, with the resultant precipitation of ferrihydrite. Thus, although a need for somewhat special circumstances to produce ferrihydrite is implied, it is apparent that the requirements for ferrihydrite precipitation can be fulfilled on an enormous scale on a daily basis.

IV. Crystal Structure of Ferrihydrite

A. Historical Models

Towe and Bradley[4] synthesized ferrihydrite by preparing a 0.06 M solution of $Fe(NO_3)_3 \cdot H_2O$ and hydrolyzing it at 85 °C. The resulting wine-colored sol was centrifuged and dried at 50 °C and/or 110 °C. As well, the iron micelle of ferritin, a protein macromolecule similar to ferrihydrite that functions in the storage of iron and is found especially in the liver and spleen, was isolated by dissolution of its protein shell. X-ray and electron-diffraction patterns of the centrifuged product showed no differences from untreated ferritin.

Data obtained by Towe and Bradley[4] are summarized in Tables 3 and 4. Much of the remainder of their paper is a discussion of their proposed structural model which, although related to hematite, differs because of the large number of vacant Fe^{3+}

Table 3. Summary of Data Obtained by Towe and Bradley[4] for Ferrihydrite

density	3.96 g/cm^3	pycnometer determination of micellar material
composition	84 wt % Fe_2O_3	$3.7Fe_2O_3 \cdot 6.9H_2O$, ideally 3.75 $Fe_2O_3 \cdot 6.75H_2O$ or $Fe_5O_{7.5} \cdot 4.5H_2O = Fe_5HO_8 \cdot 4H_2O$
infrared spectrum	3450 cm^{-1} strong 1620 cm^{-1} weak	attributed to molecular H_2O; no features at 3600−3700 cm^{-1} or 800−850 cm^{-1} attributable to hydroxyl
DTA	strong exotherm ~100 °C endotherm ~425 °C	loss of H_2O conversion to hematite
X-ray	9 lines recorded	see Table 4; electron diffraction gave only two broad bands at ~2.55 and 1.47
unit cell	$a = 5.08$, $c = 9.4$ Å	rhombohedral, related to hematite, with hexagonal closest packing of oxygens

Table 4. X-ray Diffraction Data for Synthetic Ferrihydrite[4]

I_{obs}[a]	d_{meas}[b]	d_{calc}	hkl	I of corresponding line of hematite
uncertain	4.7	4.70	002	vw
uncertain	4.2	4.40	100, 101	–
uncertain	3.3	3.24	102	–
s	**2.54**	2.54	110	80
m	**2.47**	2.46	111	–
m-s	**2.24**	2.24	112	70
m(broad)	**1.98**	1.97	113	–
w	**1.725**	1.73	114	80
m	**1.515**	1.51	115	–
s	**1.47**	1.47	300	80
vw	**1.34**	1.33	116	<40
vw	**1.23**	1.24	304	10
uncertain	1.18	1.275	008	–
uncertain	1.05	1.04	306	–

[a] Abbreviations: s, strong; m, medium; w, weak; vw, very weak. [b] Boldface added here to distinguish the conclusively observed diffraction lines.

sites and concomitant ferric iron disorder in ferrihydrite and the four-layer repeat of hexagonal anion packing rather than the six in hematite.[41,122,116]

Van der Giessen,[117] working independently from Towe and Bradley,[4] synthesized ferrihydrite at 20 °C by the addition of ammonia to a solution of ferric nitrate. The product was similar to that of Towe and Bradley, and Van der Giessen proposed a cubic cell with $a = 8.37$ Å; he did not elaborate on a structure, and the diffraction data were subsequently reinterpreted by Atkinson et al.[118] as arising from goethite rather than ferrihydrite.

Chukhrov et al.[41] raised objections to the Towe−Bradley structure model, and in their paper Chukhrov et al. introduced the name *protoferrihydrite* for the less-crystallized variant that gives only two diffraction peaks, at about 2.5 and 1.5 Å. Protoferrihydrite is not an approved mineral name, and although its usage persists,[49] the phase is now generally referred to simply as ferrihydrite or 2-line ferrihydrite.

Harrison et al.[119] studied the ferrihydrite-like iron-rich cores of ferritin macromolecules and proposed a hexagonal cell with $a = 2.96$, $c = 9.4$ Å. The structural model proposed by Harrison et al. corresponds to a composition of FeOOH, and involves oxygen and hydroxyl ions in a close-packed structure in which Fe^{3+} is randomly distributed among all the octahedral and tetrahedral sites. In contrast, Brady et al.[120] concluded, from their study of ferrihydrite synthesized by the hydrolysis of ferric nitrate solution, that all of the iron is tetrahedrally coordinated.

As is apparent from the above, there seems to be little point in discussing in detail the individual structures that have been proposed: electron-diffraction and X-ray patterns give only a few data points, and these are insufficient to constrain models except in the broadest sense. As noted by Drits et al.:[121] "Several structural models have been suggested for ferrihydrite ...[but] none of these is generally accepted because the scarcity of XRD maxima makes it difficult to determine its actual structure by XRD." Other than the study by Russell[122] on the role of OH in ferrihydrite, there was in essence a two-decade hiatus that ended with the new structural proposal by Eggleton and Fitzpatrick.[123] This new proposal, based on results obtained using sophisticated laboratory equipment, ushered in the era of contemporary models.

B. Contemporary Models

Eggleton and Fitzpatrick[123] reviewed the data pertaining to previous structural models, and summarized the various related studies that had taken place during the 1970s. Most of the studies had involved ferritin and synthetic precipitates, but Coey and Readman[124] used natural ferric hydroxide gel precipitated near freshwater springs to determine its magnetic properties.

The X-ray patterns of 2-line and 6-line ferrihydrite as obtained by Eggleton and Fitzpatrick[123] are shown in Figure 1, in which it is evident that the 110 peak for 2-line ferrihydrite is shifted to higher d values relative to the peak for 6-line ferrihydrite (2.56 and 2.52 Å, respectively). Eggleton and Fitzpatrick interpreted the asymmetry on the low-angle side of the 110 peak in 6-line ferrihydrite to be the result of incorporation of some 2-line ferrihydrite; as a subtraction of 40% of the intensity of the 2-line pattern removed most of the asymmetry from the 6-line pattern, all succeeding crystal-structure calculations were based on the "corrected" data.

Derivation of a ferrihydrite structure model was based largely on consideration of the X-ray powder data. Transmission electron micrographs of some 6-line crystals had shown a prominent 9.4-Å lattice repeat, but in some crystallites the regularity was interrupted by shorter (4.7 Å) or longer (13 Å) repeats. The model was also influenced by the results of X-ray absorption edge spectroscopy: comparison of the spectra of 6-line ferrihydrite with those for $FePO_4$ (all Fe^{3+} tetrahedral), maghemite (38% tetrahedral Fe^{3+}), and hematite and goethite (all octahedral Fe^{3+}), gave results that were interpreted as indicating similar amounts of tetrahedral Fe^{3+} in maghemite and 6-line ferrihydrite.

The Eggleton and Fitzpatrick model is based on double-hexagonal close packing of oxygens (*ABAC*),

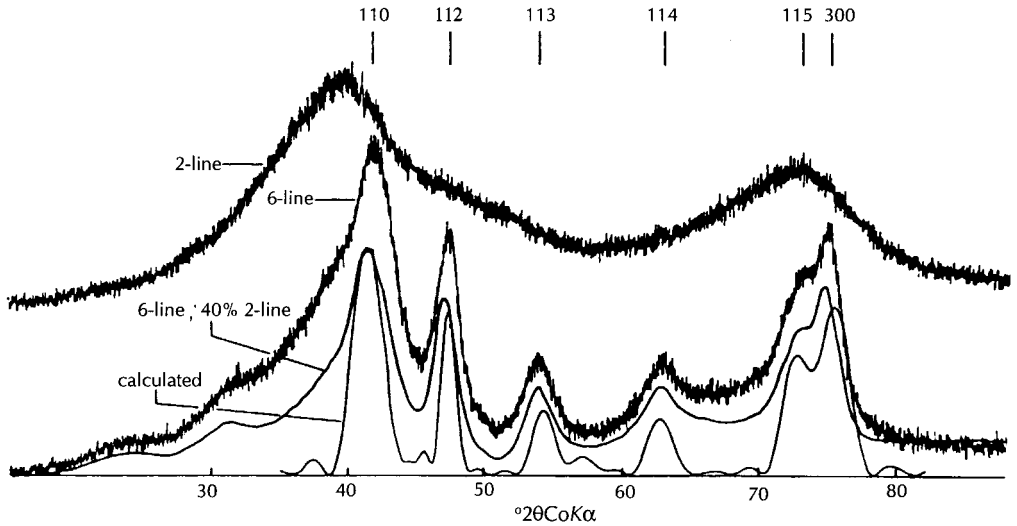

Figure 1. X-ray powder diffraction data: observed traces for 2-line and 6-line ferrihydrites, smoothed trace for 6-line with 40% 2-line ferrihydrite subtracted, and pattern calculated assuming 40-Å-size crystals. (after ref 123.)

Table 5. Indices, *d* Values, and Observed [F_o] and Calculated [F_c] X-ray Diffraction Structure Factors for 6-Line Synthetic Ferrihydrite[123]

hkl	*d*	[F_o]	[F_c]
002	4.7	15	24
003	3.13	32	9
110	2.52	52	55
111	2.47	—[a]	8
004	2.35	—[a]	21
112	2.23	38	38
113	1.98	29	28
005	1.88	<50[b]	33
114	1.72	34	30
115	1.51	50	51
300	1.46	87	89
116	1.33	27	29
220	1.27	28	32
305	1.18	18	19
225	1.07	27	30

[a] Obscured by 110. [b] Based on profile height at 57 °2θ Co Kα.

as in the structure by Harrision et al.[119] Whereas the Harrison et al. model assumed equal and random occupancy of all octahedral and tetrahedral sites, in the Eggleton and Fitzpatrick model two sheets of octahedrally coordinated iron are connected by two sheets having mixed tetrahedral−octahedral iron (in the ratio 5:2), with the cations randomly distributed over the available sites. After some adjustments, the results from the Eggleton and Fitzpatrick model yielded the calculated structure factors given in Table 5, and the calculated X-ray powder pattern shown as the lowermost profile in Figure 1. The unit cell is trigonal, space group $P31m$, with $a = 5.08$, $c = 9.4$ Å, but a smaller cell with $a = 2.96$ Å was found to satisfy the X-ray data equally well. The stoichiometry was concluded to be "FeO(OH), modified by the small crystal size and high surface water content to a composition of between $Fe_4(OH)_{12}$ and $Fe_5O_3(OH)_9$".

Cardile[125] attempted to resolve the question of tetrahedral Fe^{3+} in ferrihydrite by using high-resolution Mössbauer spectroscopy. However, little difference was found among the various models containing different proportions of octahedral and tetrahedral Fe^{3+}, and Cardile concluded that Mössbauer spectroscopy could not differentiate with confidence the two possible coordinations. In later work by Pankhurst and Pollard,[126] who used low temperatures and high applied fields, it was concluded that the Mössbauer spectra demonstrate an absence of tetrahedral Fe^{3+}.

Manceau et al.[127] concluded that inferences made by Eggleton and Fitzpatrick[123] to support the existence of tetrahedral Fe in ferrihydrite were invalid. For example, the observed transformation of ferrihydrite to maghemite on heating was cited by Eggleton and Fitzpatrick as indirect support for the existence of tetrahedral Fe, but Manceau et al. pointed out that ferrihydrite aged at moderate temperatures (<100 °C) transforms to hematite rather than maghemite, and that attempting to derive structural information from the thermal behavior of solids is a somewhat futile effort. Manceau et al.[127] also criticized the quality of the X-ray absorption spectra that had been obtained by Eggleton and Fitzpatrick[123] as "...insufficient to allow any conclusive finding; the interpretations had no firm physical basis and thus must be regarded as speculative." Manceau et al. stated that the spectral resolution required to analyze absorption edge spectra could be achieved only by using synchrotron radiation; results obtained by Manceau et al.[127] and Combes et al.[128,129] indicated 4-fold-coordinated Fe to be absent in ferrihydrite. This last point was not discussed in the response by Eggleton and Fitzpatrick,[130] who reiterated that the low-temperature transition of ferrihydrite to maghemite supported their contention that the structure of ferrihydrite contains tetrahedral Fe^{3+}.

Combes et al.[129] used X-ray absorption spectroscopy to determine the local structure of ferric ions during the formation of hematite from 2-line ferrihydrite at 92 °C. The results from EXAFS (extended X-ray absorption fine-structure) are shown in Figure 2, which is a plot of the radial distribution function (RDF) against aging time. Crystal-structure changes modify the position and relative intensity of the RDF peaks (Figure 2). Analysis of the EXAFS data indicates that the Fe−O distances slightly increase

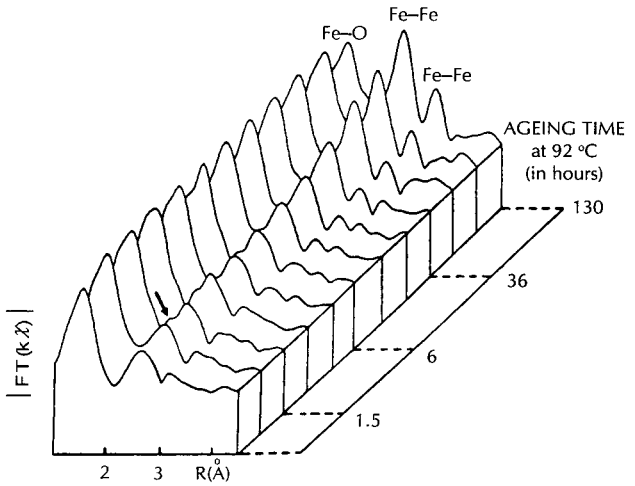

Figure 2. Partial RDF evolution as a function of aging time during the transformation of ferric gel to hematite at 92 °C (FT = Fourier transform). Left peak (Fe−O) corresponds to the oxygen shell surrounding the Fe atoms; second and third peaks (Fe−Fe) correspond to the nearest and next-nearest Fe atoms, on which a weak contribution from the next-nearest oxygens is superimposed. Phase at time 0 h is ferrihydrite, and that at 130 h is hematite. The arrow points to effects from a transition phase, as discussed in the text. (Diagram from ref 129.)

as aging proceeds, and after 25 h the distances are similar to those in hematite. For the Fe−Fe shells (Figure 2), the relevant RDF peaks increase with aging (Figure 2). Between 1.5 and 6 h a small shoulder appears on the first Fe−Fe peak (arrow in Figure 2), which corresponds to a short Fe−Fe distance (2.89 Å) characteristic of face-sharing octahedra. These octahedra coexist with octahedra linked by edges (3.05 Å) and vertexes (3.43 Å), but the presence of hematite is excluded. Thus, the material at this stage is referred to by Combes et al.[129] as the "transient phase". With increased aging the apparent number of Fe neighbors located at 2.89 Å progressively increases to a maximum of 1, at about 4 h; after 6 h of aging the Fe−Fe distance increases from 2.89 to 2.94 Å, at which stage crystallites of hematite (Fe−Fe = 2.95 Å) are detectable by X-ray diffraction. After 130 h, the structural parameters determined by EXAFS are those of bulk hematite. The nature of the "transient phase" and its relevance to the structure of ferrihydrite are not known; although the existence of the "transient phase" is acknowledged by Manceau and Combes,[131] it does not seem a topic of focus in the subsequent papers by Manceau and colleagues concerning the structure of ferrihydrite and, specifically, the transformation to hematite.[132]

The results of the above spectral study by Combes et al.[129] were obtained from the examination of gel which, although referred to in places as amorphous, gave an X-ray pattern with broad peaks corresponding to those of poorly crystalline 2-line ferrihydrite. Subsequent EXAFS study of 6-line, as well as 2-line, ferrihydrite was conducted by Manceau and Drits,[133] following which a new structural model for ferrihydrite was proposed by Drits et al.[121] In this model ferrihydrite is a mixture of ferrihydrite proper and ultradispersed hematite in which the coherent scattering domains of the mixture have mean dimensions of 20 Å in diameter and 14 Å in thickness; the 20 Å plane corresponds to the crystallographic *ab* plane, and the thickness is the *c* direction.[133] The approach used by Drits et al.[121] was, in its simplest terms, to obtain matches between the measured X-ray powder pattern and a calculated one, and between the observed and calculated EXAFS data for the Fe−(O,OH) contributions to the spectra.

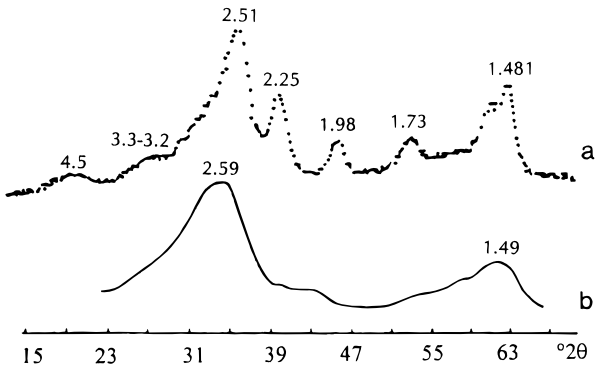

Figure 3. Experimental XRD patterns for 6-line (a) and 2-line (b) ferrihydrite. Cu Kα radiation and *d* values for peak heights in Å. (After ref 121, partly redrawn.)

The X-ray patterns obtained by Drits et al.[121] for 6-line and 2-line ferrihydrite are shown in Figure 3. The pattern for 6-line ferrihydrite actually contains eight lines, and a comparable pattern obtained by Childs[8] for a siliceous ferrihydrite that has better resolution and nine lines is shown in Figure 4. Drits et al.[121] noted that all X-ray patterns of ferrihydrite, regardless the degree of "crystallinity", have on the low-angle side of the line at 2.5 Å a diffuse intensity (near 2.6 Å) that results in an asymmetrical profile for the 2.5-Å line.

The simulated X-ray patterns for various previously proposed structure models are shown in Figure 5. The simulations assume that ferrihydrite consists of coherent scattering domains that, for the Towe-Bradley[4] and Harrison et al.[119] models, are 60 Å in diameter in the *ab* plane, and 4, 5, or 6 unit-cells thick ($H = \sim$38 Å to $\sim$56 Å). It is evident from Figure 5 that the Towe-Bradley and Eggleton and Fitzpatrick[123] structures do not provide a good agreement with the X-ray pattern for ferrihydrite; as well, the Harrison et al.[119] and Eggleton and Fitzpatrick[123] models do not match well the EXAFS data for Fe−(O,OH) contributions to the spectra (Figure 6). Particularly noticeable in the simulated X-ray patterns is the presence of prominent 001 diffraction lines (Figure 5), but these are absent in the observed patterns. For the EXAFS data, a conspicuous feature is that the indicated Fe−(O,OH) bond lengths in ferrihydrite and hematite are similar (Figure 6c); these lengths are characteristic of Fe in octahedral coordination. Thus, the Fe atoms in ferrihydrite can be concluded to occupy only octahedral sites, as in hematite.

To achieve a good match between the observed and simulated X-ray patterns of 6-line ferrihydrite, Drits et al.[121] concluded that a mixture consisting of three components is responsible for the observed diffraction effects: (i) defect-free ferrihydrite, (ii) defective fer-

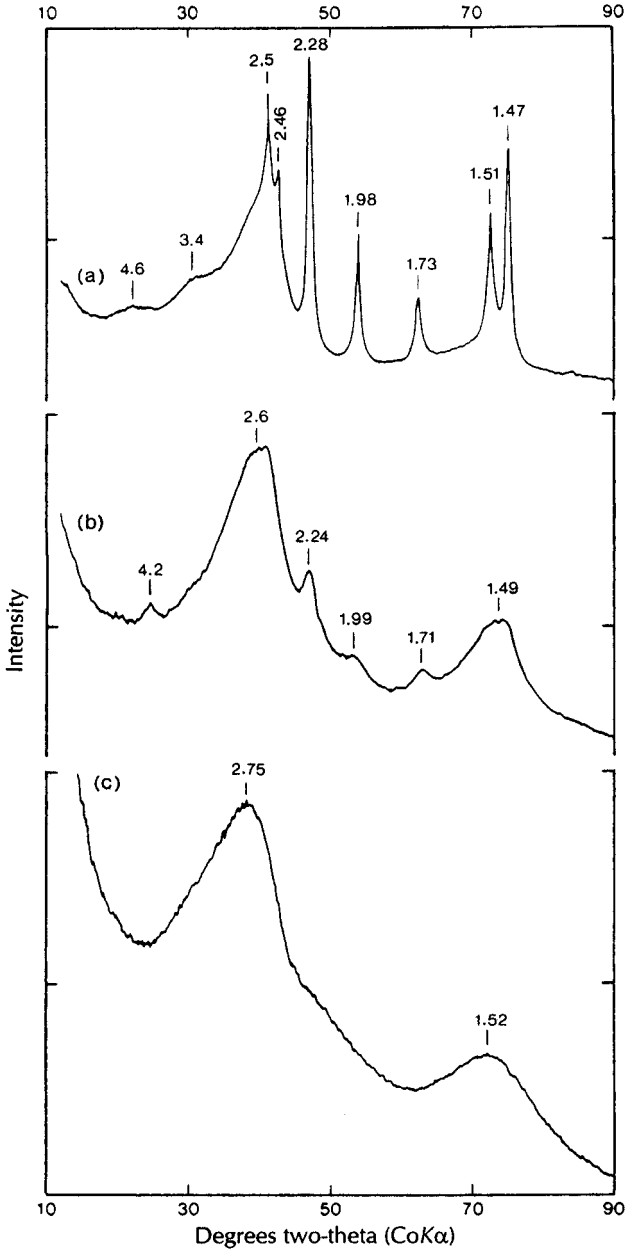

Figure 4. X-ray diffractograms of ferrihydrite: (a) "7-line" synthetic siliceous ferrihydrite; (b) natural siliceous ferrihydrite,[140] showing a small peak at 4.2 Å for goethite; (c) 2-line natural ferrihydrite.[37] Peaks are labeled in angstroms. (After ref 8, slightly modified.)

rihydrite, and (iii) ultradispersed hematite. The defect-free ferrihydrite consists of oxygens and hydroxyls in a close-packed arrangement in the pattern *AcBcAbCbA*..., where *A* and *B* are anion positions and *c* represents Fe sites. The Fe atoms in the *c* and *b* octahedral sites are distributed randomly, with a 50% probability of occupying a particular site. The unit cell is hexagonal, space group *P*31*c*, with $a = 2.96$ and $c = 9.40$ Å. Coherent scattering domains are 60 Å in diameter and contain 1−10 unit cells, each of which occurs with the same probability. The resulting simulated X-ray pattern is shown in Figure 7a. In this simulated pattern the strongest line, at 2.484 Å, consists of overlapping 100 and 101 peaks whose intensities are the reverse of those observed in experimental patterns; to achieve the appropriate

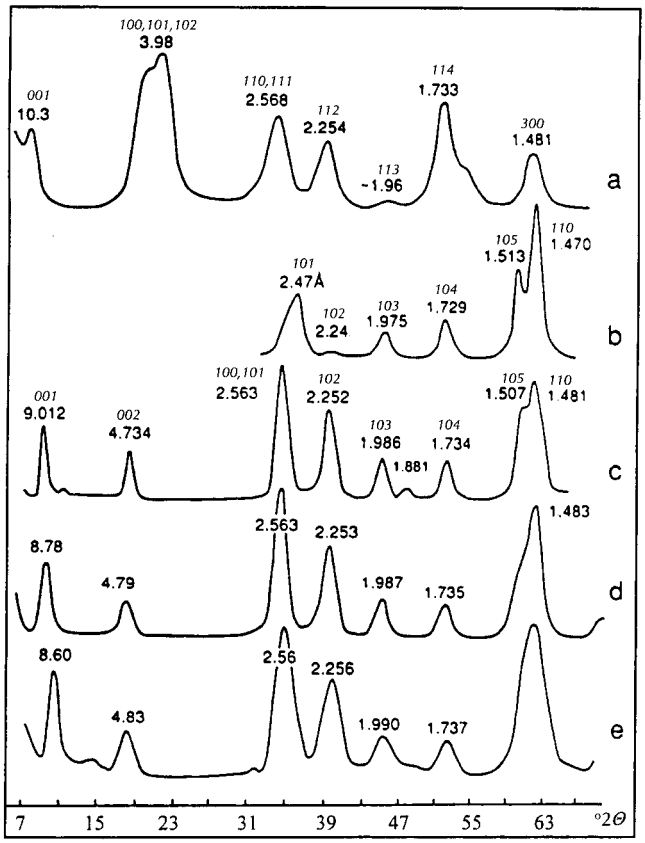

Figure 5. Comparison of XRD curves calculated for different ferrihydrite models: (a) Towe and Bradley[4] model with H = 45 Å; (b) Harrison et al. model[119] with H = 45 Å; (c) Eggleton and Fitzpartick[123] model with H = 70 Å; (d) Eggleton and Fitzpatrick[123] model with H = 45 Å; (e) Eggleton and Fitzpatrick[123] model with H = 36 Å. Cu Kα radiation, with *d* values for peak heights in angstroms, and *hkl* indices in italics. (After ref 133, with slight modification.)

intensities, stacking faults are introduced and the layer fragments *AcBcA* and *AbCbA* are assumed to occur randomly and with equal probability. This leads to the simulated pattern shown in Figure 7b. Note that diffraction lines at >2.5 Å are absent in Figure 7b, and to account for the experimentally observed lines at ~4.2 and ~3.3 Å, Drits et al.[121] assumed that the Fe atoms in each of the *AcBcA* and *AbCbA* fragments can be ordered, thus leading to superlattice reflections and a doubling of the *A* axis to ~5.13 Å.

To account for the asymmetrical appearance of the ferrihydrite diffraction line at ~2.5 Å (i.e., the less steep slope on the low-angle side of the peak), Eggleton and Fitzpatrick[123] assumed the constant presence of 40% admixed 2-line ferrihydrite. In the simulated X-ray diffraction profiles, however, Drits et al.[121] found that the addition of 2-line ferrihydrite did not remove the asymmetry. Because hematite is the only iron oxide-oxyhydroxide known to have its strongest peak at 2.6−2.7 Å, as well as lacking companion strong peaks at high *d* values (e.g., as for lepidocrocite), it was thought by Drits et al.[121] that the presence of ultradispersed hematite could account for the asymmetry of the relevant peak in ferrihydrite. The simulated X-ray pattern that combines the ferrihydrite components and hematite is shown in

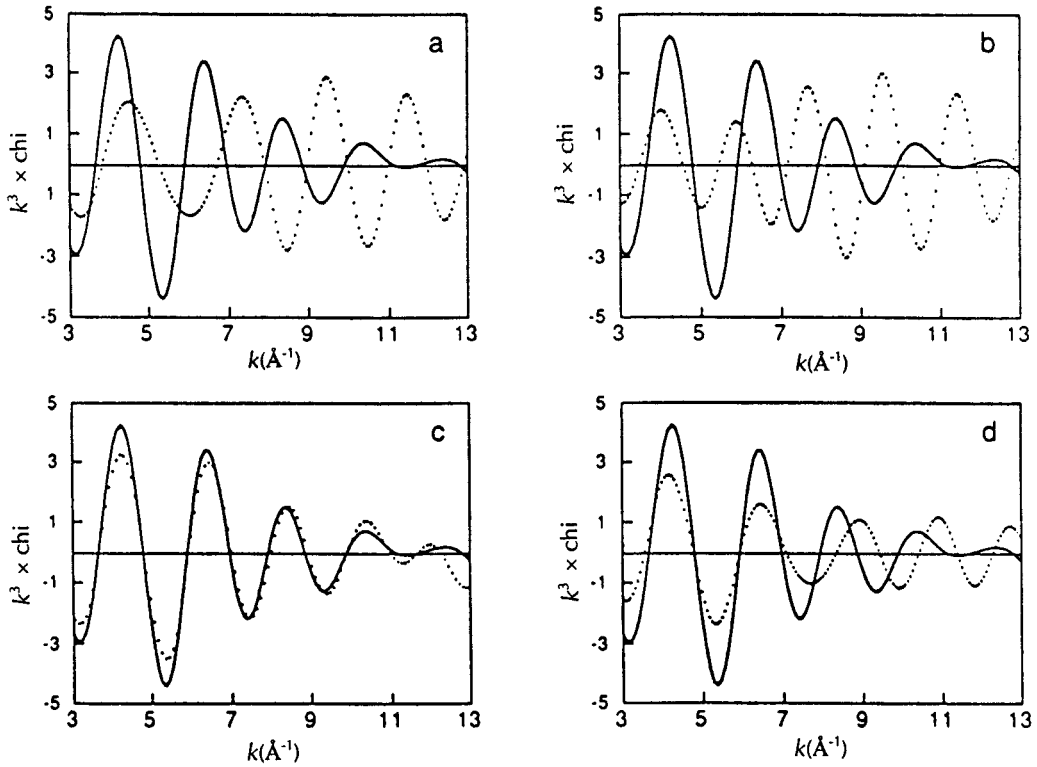

Figure 6. Experimental Fourier filtered Fe−(O,OH) contribution to EXAFS for 6-line ferrihydrite (solid line) compared to (dotted lines): (a) the contribution calculated for Harrison et al.[119] model; (b) calculated for Eggleton and Fitzpatrick[123] model; (c) the experimental contribution for hematite; (d) the contribution calculated for 1.4 oxygens at 1.86 Å + 1.9 oxygens at 1.95 Å + 1.9 oxygens at 2.12 Å. (After ref 133.)

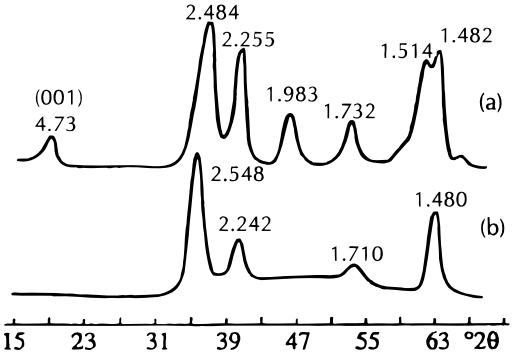

Figure 7. XRD patterns calculated for the ferrihydrite model with (a) 3D ordered structure and (b) disordered alternation of *ABA* and *ACA* fragments. (Slightly modified from ref 132.)

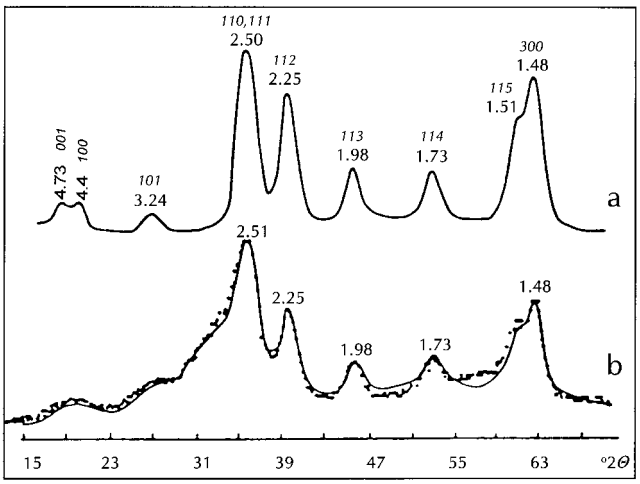

Figure 8. XRD curves for ferrihydrite: (a) calculated for a mixture of the defect-free ferrihydrite having random Fe distribution, and defective ferrihhydrite having ordered Fe distribution within *ABA* and *ACA* fragments; (b) comparison of the experimental XRD curve (dotted line) with the curve (solid line) calculated for the mixture of three components, defect-free and defective ferrihydrite having random and ordered Fe distribution plus ultradispersed hematite. The peak at 3.24 Å orginates from the defective ferrihydrite structure, and was indexed by assuming a periodicity along the *Z* axis of $c/2 = 4.7$ Å. Cu Kα radiation, with *d* values in angstroms, and *hkl* in italics. (Slightly modified from ref 121.)

Figure 8b. In summary, ferrihydrite was concluded by Drits et al. [121] to consist of a defect-free component with hexagonal unit-cell parameters $a = 2.96$, $c = 9.40$ Å, a defective component that has a hexagonal supercell with $a = 5.126$ Å, and ultradispersed hematite whose coherent scattering domains have a mean dimension of 10−20 Å. The main difference between 2-line and 6-line ferrihydrite is that the 2-line type consists of extremely small coherent scattering domains (20−30 Å).

Contemporaneous with, and independent of, the study by Drits et al.,[121] St. Pierre et al.[134] examined ferrihydrite using EXAFS, and the structure was investigated by Zhao et al.[97] using EXAFS and XANES (X-ray absorption near-edge structure) spectroscopy. St. Pierre et al. concluded that 2-line and 6-line ferrihydrite were similar, but the 2-line variety possessed a higher vacancy concentration. The results obtained by Zhao et al.[97] indicated that as much as 25% of the iron ions could be in tetrahedral coordination, although only at the particle surface; the bulk of the iron was concluded to have a structure

Table 6. EXAFS Pre-edge Peak Areas for Ferrihydrite Samples and Model Compounds[a]

sample	preparation condition	area (A) pre-edge (A = 0.01)
Fe_3O_4 (magnetite)	lab synthesized commercial catalyst	0.141
ferrihydrite I	as-received	0.127
	exposed to moist air	0.110
2-line ferrihydrite	cake	0.091
	oven-dried (50 °C)	0.116
2-line ferrihydrite	freeze-dried	0.112
	freeze- and vacuum-dried	0.137
6-line ferrihydrite	freeze-dried	0.118
	freeze- and vacuum-dried	0.122
siliceous ferrihydrite	freeze- and vacuum-dried	0.122
	vacuum-dried	0.119
aluminous ferrihydrite	vacuum-dried	0.124
α-FeOOH (goethite)	lab synthesized	0.077
α-Fe_2O_3 (hematite)	lab synthesized	0.074

[a] Modified from Zhao et al.[96]

similar to that for the octahedral oxyhydroxides. That the lower coordination sites at the particle surface were coordination-unsaturated was indicated by the XANES results, which also showed that exposure of dehydroxylated ferrihydrite to air increased the average coordination number because of adsorption of water molecules from the air.

The nature of the coordination-unsaturated (CUS) sites and their role in the transformation of ferrihydrite was elaborated upon by Zhao et al.[96] In XAFS spectroscopy, the "pre-edge" (preabsorption edge) spectrum is sensitive to coordination symmetry (but see also the discussion in ref 135). For iron atoms with 6, 5, and 4 coordination, the ratio of the pre-edge peak areas is 1:2:3; thus, the peak area increases as the coordination decreases. Pre-edge spectral peak areas examined by Zhao et al.[96] were found to be significantly higher for ferrihydrite than for goethite and hematite (Table 6), but are fairly close to that of magnetite (Table 6). In goethite and hematite the iron is in octahedral coordination, whereas in magnetite there are 67% octahedral sites and 33% tetrahedral sites. Thus, Zhao et al.[96] estimated, assuming that the increase in the pre-edge peak area for ferrihydrite was due to tetrahedral sites only, that their ferrihydrite samples had 20−30% tetrahedral sites. Although the presence of these lower coordination sites seems to contradict the EXAFS results, from which it was concluded that the iron in ferrihydrite is octahedrally coordinated, as in goethite and lepidocrocite, the XANES spectra are in essence a bulk measurement to which the surface iron ions do not contribute significantly because they have only one complete O/OH shell. Thus, the different results for the "bulk" spectra and EXAFS spectra indicate that, rather than being uniformly distributed in the ferrihydrite structure, the lower coordination (tetrahedral) sites are predominantly at the ferrihydrite surface.

The above model, in which the "core" of the ferrihydrite particles consists of iron in octahedral coordination whereas the surface has considerable iron in tetrahedral coordination, helps to explain the seemingly contrasting structural properties versus the high adsorptive capacity and behavior of ferrihydrite. For the EXAFS pre-edge peaks, Zhao et al.[96] observed a clear-cut relationship; namely, the drier the sample of ferrihydrite, the larger the pre-edge peak area. In other words, the drier the sample, the lower the coordination at the ferrihydrite surface; i.e., some surface iron ions become coordination-unsaturated as a result of dehydroxylation. This phenomenon possibly explained the conclusions by Manceau et al.,[127] which were also based on EXAFS results, that no tetrahedrally coordinated iron is present in ferrihydrite. However, if the surface tetrahedral sites are increasingly formed as ferrihydrite evolves from a hydrogel state to an "anhydrous" state,[96] then observations on the extent of tetrahedral iron would be highly dependent on the hydration state of the sample examined. Shinoda et al.[136] examined both freeze-dried ferrihydrite and the equivalent precipitate in solution, and concluded that both have the same basic structure of linked FeO_6 octahedra. In solution, however, the number of linked units was found to be only about 60% of that in the powder.

Determining how impurity ions are absorbed by ferrihydrite, and how they affect its transformation, were the principal objectives that led Zhao et al.[96] to the eventual development of their structural model for ferrihydrite. Detailed EXAFS results on the surface chemistry of ferrihydrite were described by Waychunas et al.,[137−139] Fuller et al.,[140] and Manceau[141] for arsenate adsorption, by Waite et al.[142] for uranium adsorption, and by Charlet and Manceau[143] for chromium adsorption. The study by Waychunas et al.[137] led to the conclusion that the FeO_6 polyhedra in ferrihydrite must be slightly different than those in goethite, but that the Fe−O bond lengths in ferrihydrite are closer to those of goethite than to those in lepidocrocite or akaganéite. For the Fe−Fe interatomic distances, however, lengths in ferrihydrite are similar to those in akaganéite. Thus, the structure of ferrihydrite was considered to consist of octahedral chains in which the Fe^{3+} octahedra are joined by sharing edges, forming short double chains. Independently of the work by Waychunas et al.,[137] the distances between Fe−Fe nearest-neighbor pairs also led Shinoda et al.[136] to eliminate the possibility of face sharing or single corner sharing of the FeO_6 octahedra. Shinoda et al. [136] concluded that the octahedra are linked by edge and double corner sharing.

As ferrihydrite aged, Waychunas et al.[137] noted from the Fe−Fe correlations that the numbers of Fe

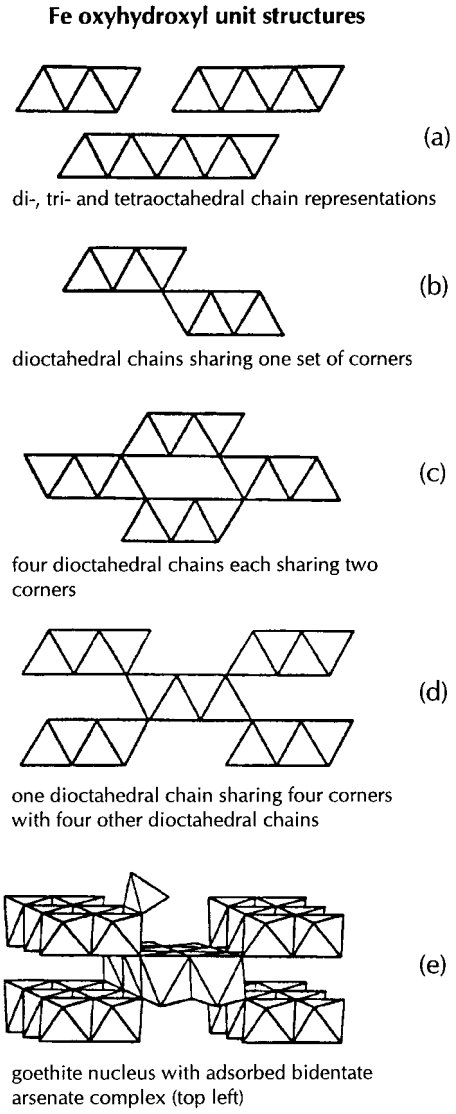

Figure 9. Model ferrihydrite structures. Schematic drawings of various octahedral chain models showing corner-sharing linkages between chains: (a) di-, tri-, and tetraoctahedral chains; (b) dioctahedral chains with one cross-linkage; (c) four dioctahedral chains each with two cross-linkages; (d) schematic drawing of the goethite structure (projected on 001); and (e) perspective drawing of a small unit of goethite structure with adsorbed bidentate arsenate on the groove surface. (From ref 137.)

neighbors increased; that is, Fe−O−Fe polymerization increased. Two Fe−Fe distances (3.04 and 3.45 Å) correlate with along-chain Fe−Fe neighbors (3.04 Å) and across-chain and interchain neighbors (3.45 Å). These values do not fit well with single-edge-sharing octahedral chains (Figure 9a), with dioctahedral chains, or with chains of trioctahedral or larger widths (Figure 9a). The data do, however, fit with an arrangement that involves cross-linked dioctahedral chains in a structure similar to that of goethite or akaganéite. In "young" ferrihydrite, therefore, only short, uncoupled chains joined by sharing edges are present, and interchain linkage is either absent or severely disordered. With aging, however, the chains lengthen, dioctahedral chains become more abundant, and these link to other chains by sharing corners to form a cross-linked structure (Figure 10). These increases in chain

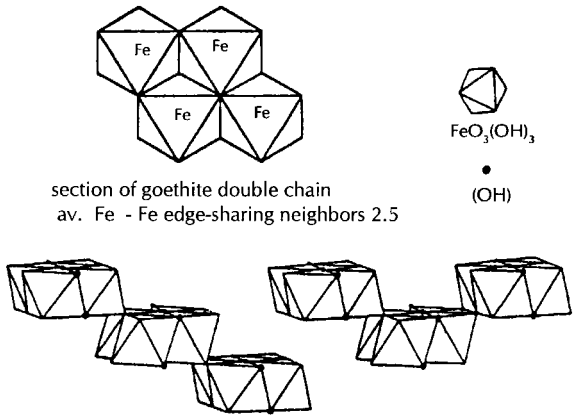

Figure 10. Schematic representation of the 2-line ferrihydrite structure. Top drawing shows plan view of linkages of iron octahedra to form short segments of dioctahedral chain. Bottom figure shows possible cross-linkages of dioctahedral chains. (After ref 145.)

length and in the amount of corner sharing of dioctahedral chains represent crystallite growth, a process which reduces the surface area and number of available adsorption sites.

A new structural model of ferrihydrite was proposed by Spadini et al.[144] In this structure, which was derived largely from the results of EXAFS spectroscopy, the fundamental units consist of microdomains of goethite. As noted above, however, Waychunas et al.[137] concluded that the FeO_6 polyhedra in ferrihydrite must be systematically different from those in goethite, and thus this structure remains to be proved. Likewise, it remains to be proved that the structure of 2-line ferrihydrite is strictly analogous to that of its better crystallized counterparts.

Although none of the contemporary models for a ferrihydrite structure is incontrovertible, significant progress has been made. First, there seems to be universal agreement that "amorphous iron hydroxide" is not amorphous. Usually there is at least a low degree of crystallinity detectable even by X-ray diffractometry. Crystallinity is nearly always evident in electron-diffraction patterns, or is detectable by spectroscopic methods. Nevertheless, amorphous iron hydroxide continues to be in widespread use in the literature as a term of convenience, commonly synonymous with 2-line ferrihydrite and commonly indicated as such.

Second, there seems to be universal agreement that the fundamental structure unit within ferrihydrite is the $Fe(O,OH)_6$ octahedron, and over the past five years a consensus seems to have emerged that the structure of ferrihydrite, although different from that of goethite, is generically of the goethite type rather than something radically different. General agreement on the nature of the specific atomic arrangements has not yet been attained, but it is likely that a widely accepted model will emerge soon. This prognostication can be made, with some assurance of fulfillment, because the recent EXAFS and XANES results have provided not only a foundation from which refinements can be undertaken, but also the impetus to seek a definitive structure. These refinements may involve supplementary EXAFS and

XANES investigations, especially on relatively well-crystallized, aged ferrihydrite, or they may involve the use of corroborating techniques such as detailed infrared spectroscopy.

Several other advances have been made in understanding ferrihydrite better. One in particular that merits mention with respect to structure is the recognition that ferrihydrite has, in essence, two structural aspects, one of which is the bulk or core structure, and the other pertains to the surface. The two are of course interlinked, for it is the lack of long-range order of the bulk structure that leads to the prominence of the surface structure. Nevertheless, this concept of duality is the crux of the structural model proposed by Zhao et al.[96] A similar, although less direct, distinction was made by Rea et al.,[145] who used Fe isotopic exchange to demonstrate that there are at least two types of iron sites in ferrihydrite. One of these, referred to as *labile* sites, rapidly approached equilibrium upon isotopic exchange of Fe, whereas the *nonlabile* population of sites exhibited a much slower rate of isotopic exchange. Although Rea et al.[145] assumed all iron to be in octahedral coordination, Mössbauer spectroscopy showed that the labile and nonlabile sites were different. The labile sites were interpreted to be the most distorted sites, thereby facilitating isotope exchange because of the weaker binding. Rea et al. concluded that

> ...it is reasonable to propose that the labile and nonlabile site populations can be assigned to locations within the structure with lesser and greater than average Fe−Fe octahedral coordination, respectively. The sites with lower coordination would presumably be on the ends of dioctahedral chains, whereas sites with greater Fe−Fe coordination would be located in the center of chains and perhaps at locations characterized by a high degree of chain cross-linking.

It is worth noting in the preceding excerpt that the labile sites are assigned to sites "...with lesser...than average Fe−Fe octahedral coordination". Although tetrahedral coordination is not mentioned, the general concept could be construed as having similarities to the CUS model proposed by Zhao et al.[96] in terms of adsorption response. Judging from the amount of published discussion that has been generated since the appearance of the paper by Waychunas et al.,[137] it seems highly likely that confirmation, refutation, or further debate about the CUS model and tetrahedral Fe in ferrihydrite will appear in the literature soon. In this regard, Waychunas et al.[139] already have stated that they were unable to confirm the existence of CUS sites in the (arsenic-bearing) system of their investigation. Although, Waychunas et al.[139] did not dismiss the CUS model, Manceau and Gates[135] reexamined the spectral results of Zhao et al.[96] and concluded that the suggested presence of 20−30% tetrahedral sites in ferrihydrite is excessive.

V. Chemical Composition

Chemical analyses are almost always a key criterion in establishing the general formula of a mineral, even if the precise crystal structure is not known. A good example is the clay minerals, most of which can be well-defined despite their small particle size and complex formulas. Ferrihydrite is much simpler in composition than are the clay minerals, but no single formula is widely accepted. Table 1 shows the composition as $Fe_5HO_8 \cdot 4H_2O$, which is from Towe and Bradley,[4] but Schwertmann and Cornell[13] additionally list $5Fe_2O_3 \cdot 9H_2O$, $Fe_6(O_4H_3)_3$, and $Fe_2O_3 \cdot 2FeOOH$ $2.6H_2O$ as alternatives. The last two formulas are from Chukhrov et al.[10] and Russell,[122] respectively, and to these can be added $Fe_{4.5}(O,OH,H_2O)_{12}$, which is a generalization of the two formulas given by Eggleton and Fitzpatrick.[123] The variation is remarkable when it is considered that ferrihydrite is easily synthesized in the laboratory. The problem, however, is that it has not been possible to put tight limits on the water content of the mineral by laboratory measurements, which give variable results, and the formula cannot be constrained as yet on the basis of a known crystal structure.

A few analyses reported for natural ferrihydrite are listed in Table 7. Silica is abundant in most analyses, but its nonessential character is suggested by the wide variation in percentages, and is proved by silica-free syntheses in the laboratory. The syntheses indicate that only Fe, O, and H are necessary, and Russell[122] has shown that an appreciable portion of the H is present as OH. In light of the more recent structural information that indicates a goethite-like structure for ferrihydrite, it seems inappropriate to write a component of the formula as Fe_2O_3 unless the intention is to focus on the hematitic fraction that Drits et al.[121] have concluded to be present within ferrihydrite. If hematite is indeed present in the major amounts suggested by Drits et al.,[121] then analyses of bulk samples are not particularly meaningful.

Eggleton and Fitzpatrick[123] reported that bulk compositions of ferrihydrite prepared from ferric nitrate solutions are $Fe_4(O,OH,H_2O)_{12}$ for the 2-line variety, and $Fe_{4.6}(O,OH,H_2O)_{12}$ for the 6-line type. For the first of these formulas the Fe:"O" ratio is 1:3, and for the second it is 1:2.6. In the FeO(OH) structure type, the ratio is 1:2. Dehydroxylation of surface sites in 6-line ferrihydrite would further move the 1:2.6 ratio toward the 1:2 ratio; thus $Fe_{4.6}(O,OH,H_2O)_{12} \rightarrow Fe_6(O,OH,H_2O)_{12}$, or $Fe_6O_6(OH,H_2O)_6 = n\text{FeO}(OH,H_2O)$. As in all preceding proposals, there is no proof that such a formulation is correct. Nevertheless, it is interesting to note that the addition of various adsorbates, such as Si,[146] Ge,[147] and Mo,[95] can substantially increase the temperature at which ferrihydrite transforms to hematite (Table 8). The same effect has been noted for natural siliceous ferrihydrite, and conversion to hematite has been reported to be arrested to temperatures exceeding 700 °C.[148] Conversion temperatures investigated by Childs et al.[149] for Si- and Ge-bearing samples have shown that the ferrihydrite structure can be maintained when <3 wt % of the total hydroxyl weight loss remains. Thus, in the formula $2FeO(OH,H_2O)_n$, one can assume losses such that $2FeO(OH,H_2O)_n \rightarrow n2FeO(OH,O)_n$. With further losses of all the hydroxyl, the formula becomes $2FeO(O_{0.5}\square_{0.5})$, which is equivalent

Table 7. Chemical Compositions of Natural Ferrihydrite

wt %	1[a]	2[a]	3[a]	4[a]	5[a]	6[b]	7[b]	8[c]
Fe_2O_3	62.97	57.35	58.60	54.38	63.03	78.71	42.36	70.93
FeO	3.63	0.41	2.20	2.16	0.67			
MnO	–	0.06	0.14	0.06	0.15	–	0.22	
MgO	tr	0.54	0.30	0.42	0.11	0.14	0.43	0.17
CaO	tr	4.00	1.00	2.43	1.06	0.38	1.65	0.84
Na_2O	–	–	–	–	0.24	–	0.99	
SiO_2	5.60	5.00	6.42	4.66	6.00	10.49	31.54	13.05
Al_2O_3	1.00	1.25	0.66	tr	3.00	0.05	9.64	<0.1
TiO_2	–	–	–	–	0.66	0.10	1.33	
H_2O^+	14.14	9.16	10.03	13.73	4.23	8.58	11.23	12.7
H_2O^-	11.00	22.46	20.53	15.00	18.13	20.82	19.50	23.0
Cl	0.00	tr	tr	0.13	–			
SO_3	1.37	0.00	0.00	0.00	0.36			
P_2O_5	–	–	–	7.21	–			
CO_2	–	–	–	–	2.14			
C	–	–	–	–	0.09			0.8
O≡Cl	–	–	–	0.03	–			
total	99.70	100.23	99.88	100.21	99.87	98.45	99.40	

[a] Analyses 1–5 from Chukhrov et al.[10] for ferrihydrite from cold springs. Na_2O includes K_2O. Five additional analyses are reported for ferrihydrite deposited from thermal waters. [b] Analyses 6 and 7 from Henmi et al.[40] for the most Si-rich and Si-poor of four analyses listed for oven-dried (105 °C) material; H_2O^- based on air-dry weight, Mn as MnO_2, Na_2O value includes K_2O 0.18. [c] Analysis 8 from Childs et al.,[37] one of four listed as elements (converted here to oxides, except for C); also reported, 0.1 wt % N.

Table 8. Approximate Temperatures of the Thermal Transformation of Ferrihydrite Having Different Si/Fe Molar Ratios to Hematite[146]

Si/Fe molar ratio	*T* (°C)
0.0	300
0.01	400
0.05	500
0.10	600
0.25	800
0.50	*a*
0.75	*b*

[a] Very poorly crystalline hematite, 800 °C. [b] No transformation product was observed at 800 °C.

to $Fe_2O_2(O,\square)$. One could assume, therefore, that the presence of hydroxyl is essential for maintaining the ferrihydrite structure, and as hydroxyl is lost, vacancies must be created to maintain the charge balance. As these vacancies increase, the structure becomes increasingly destabilized, so that at some small value of hydroxyl there is conversion to hematite.

The preceding scenario is in accord with most published opinions concerning the transformation of ferrihydrite on aging. The consensus, until recently, was that the conversion of ferrihydrite to goethite involves a solution–reprecipitation mechanism, whereas the conversion to hematite may be direct. In light of recent structural information, however, it is generally conceded that the magnitude of the required structure reorganization to hematite is too great to be accomplished by direct transformation.

VI. Identification Techniques for Ferrihydrite

A. X-ray Diffraction Determinative Methods

The X-ray patterns of "2-line" and "7-line" ferrihydrite are shown in Figure 4. All of the lines are indexable in accordance with the structural scheme proposed by Drits et al.;[121] viz., the first two lines in the best-crystallized sample correspond to the supercell reflections. The split peak at 2.54 and 2.46 Å, which is not usually resolved, corresponds to two indices in the main unit cell. The asymmetry to the left of the peak at 2.54 Å is the position for admixed hematite.

X-ray patterns for the chemically similar compounds ferrihydrite, feroxyhyte, and schwertmannite[150–153] are shown in Figure 11. The distinction between the three may be difficult when the crystallinity is poor (Figure 12). The diffraction line at ~2.0 Å is reported to be characteristic for ferrihydrite,[10] supposedly distinguishing it from poorly crystalline feroxyhyte.[154] The appearance of a diffraction line at 4.8–5.0 Å seems to be a good indication of the presence of schwertmannite. Childs[8] has pointed out that ferrihydrite, having four or fewer X-ray lines, may not be distinguishable from feroxyhyte or some other poorly crystalline iron oxide, and Farmer[155] has cautioned that 2-line ferrihydrite could be easily confused with hisingerite, an iron silicate that also occurs in soils. Childs,[8] however, noted that the 2 Å peak of ferrihydrite is relatively weak and broad, and typically is seen only for samples that also show the lines at 2.5, 1.7, and 1.5 Å. Manceau et al.[156] concluded that, even in their most disordered states, ferrihydrite and hisingerite have X-ray diffractograms that are sufficiently distinct to prevent confusion.

The use of *n*-line terminology seems to be somewhat generalized, and in the literature it seems to be common to refer to poorly crystalline ferrihydrite as 2-line, whereas material showing better crystallinity is typically categorized as 6-line ferrihydrite regardless of the actual number of lines observable. This informality can be criticized as being misleading to those unfamiliar with the nuances of ferrihydrite types, but it is defensible on the grounds that the number of lines recorded is subject to interpretation and to the resolving power of the equipment used in the X-ray recording. As long as the 2-line, 6-line, or *n*-line nomenclature is used informally, to designate a *variety* of ferrihydrite, arguments about the validity of the nomenclature are viewed here as unproductive.

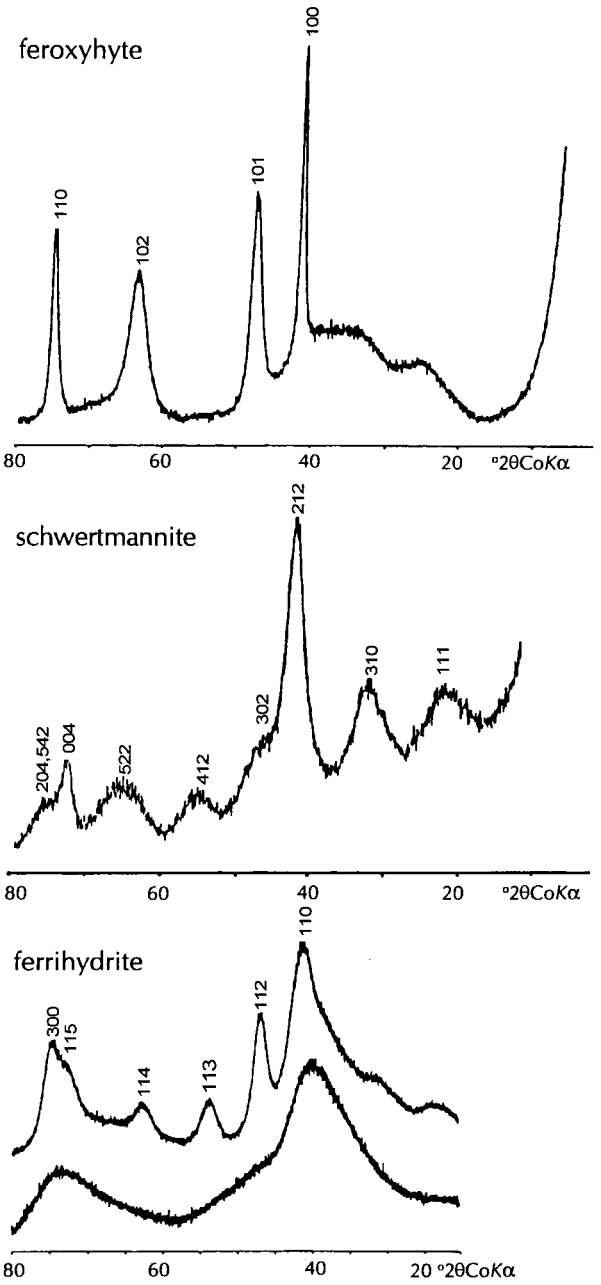

Figure 11. X-ray diffractograms for feroxyhyte, schwertmannite, and ferrihydrite. (Compiled and slightly modified from Schwertmann and Cornell;[13] note that the scale from 40° to 20° is compressed in the patterns for ferrihydrite.)

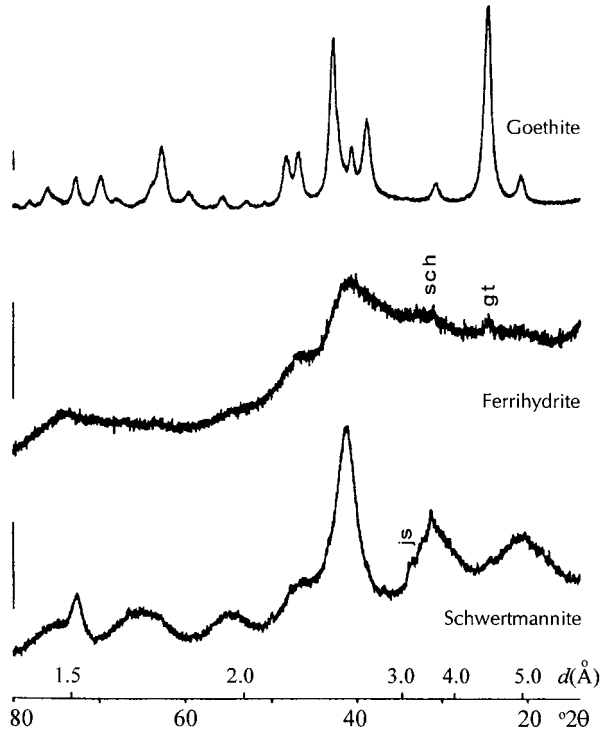

Figure 12. X-ray diffraction diagrams of goethite, ferrihydrite and schwertmannite from acid-drainage environments. Marked foreign mineral admixtures are jarosite (js), goethite (gt), and schwertmannite (sch); scale bars correspond to 400 counts per second. (Slightly modified after ref 153.)

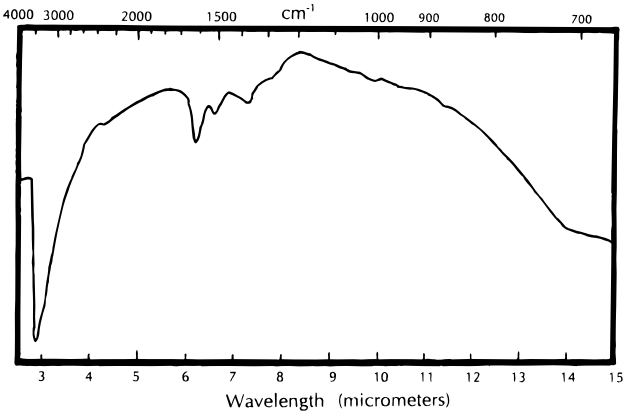

Figure 13. Infrared absorption spectrum of synthetic ferrihydrite. (Adapted from ref 4.)

The use of protoferrihydrite, however, is misuse of a mineral name, is contrary to the rules of mineral nomenclature, and is not to be condoned.

B. Infrared Spectrum

The infrared spectrum of Towe and Bradley's[4] synthetic ferrihydrite is shown in Figure 13. The absorption bands at 3450 and 1620 cm^{-1} were assigned to molecular water, and the absence of bands in the 3600−3700 and 800−850 cm^{-1} regions was interpreted to indicate an absence of hydroxyl. This interpretation was supported by Chukhrov et al.[10] and Schwertmann and Fischer.[7] For natural ferrihydrite, Chukhrov et al.[10] also noted an additional band in the region 930−1020 cm^{-1}; absorption increased in intensity as the silica content increased, and thus this band was ascribed to silica gel. The same band was later noted by Schwertmann and Thalman[157] and Carlson and Schwertmann[33,158] to shift with increasing Si content (Figure 14) and was interpreted to result from Fe−O−Si interactions in the ferrihydrite structure.

Russell[122] synthesized 5-line ferrihydrite and determined its infrared spectrum to be similar to that obtained by Towe and Bradley.[4] Upon evacuation, however, absorption bands were evident at 3615 and 3430 cm^{-1}, and were attributed to surface OH and structural OH, respectively. On treatment with D_2O, the OH groups were readily converted to OD groups. Comparison with other iron oxyhydroxides, especially akaganéite, led Russell[122] to suggest that the con-

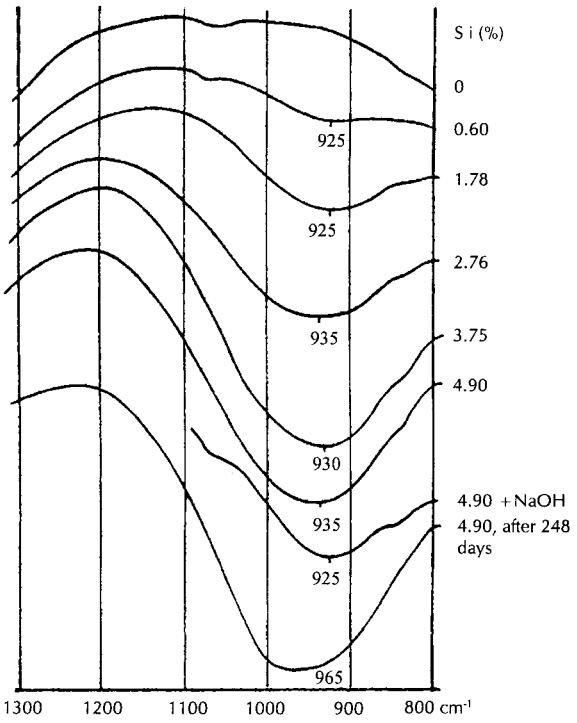

Figure 14. Infrared spectra of ferrihydrite, showing the effects of increasing amounts of silicon. (Adapted from ref 158.)

centration of OH in ferrihydrite may be a third to half that of FeOOH. Thus, if FeOOH is written as $Fe_2O_3 \cdot H_2O$, Russell suggested that the nominal formula of Towe and Bradley[4] for ferrihydrite could be rewritten as $Fe_2O_3 \cdot 2FeOOH \cdot 2.6H_2O$.

C. Mössbauer Spectroscopy

Natural and synthesized ferrihydrite and the cores of ferritin give identical Mössbauer spectra. Murad and Schwertmann[159] determined the spectra of natural ferrihydrite using ochreous precipitates from the type locality in Kazakhstan, from Hanover, Germany, and from three localities in Finland. The X-ray diffraction patterns of the samples varied from 2-line to 6-line ferrihydrite, and a similar range in X-ray diffraction properties was obtained from a series of synthetic ferrihydrites that had been prepared using three different methods of synthesis.

At room temperature (291 K) and at 130 K the Mössbauer spectra showed only a paramagnetic doublet, but at 4.2 K all spectra were completely split magnetically and appeared as sextets. The room-temperature doublet required fitting with at least two Lorentzian doublets with isomer shifts of 0.34 and 0.35 mm/s, and quadrupole splittings of 0.45 and 0.89 mm/s. The 4.2 K sextet could be fitted by three sextets, with identical isomer shifts for all sextets and slightly different quadrupole settings. Maximum absorption in the 4.2 K spectrum occurred near 500 kOe. Murad and Schwertmann[159] concluded that the Mössbauer results should not be taken as proof for the existence of discretely different iron sites in the ferrihydrite structure; rather, "the [broad] hyperfine field distributions of the magnetically split spectra... indicate continuous variations of parameters, and therefore of environments of the iron nuclei".

The general features of the Mössbauer spectrum of ferrihydrite were reviewed by Murad,[160,161] and interpretations of specific aspects of the spectra of synthetic ferrihydrite and corrosion-derived ferrihydrite were given by Chadwick et al.,[162] Madsen et al.,[163] Arshed et al.,[164] and Cianchi et al.[165,166] Pollard et al.[167] provided a comparison of the spectra of goethite, lepidocrocite, akaganéite, and 2-line and 6-line ferrihydrite at low temperatures and in the presence of applied magnetic fields. Wide hyperfine field distributions (half widths about 60 kOe) and low quadrupole splittings (<0.1 mm/s) were found to be indicative of ferrihydrite, though higher quadrupole splitting values (to 0.9 mm/s) are commonly reported.[92]

Chadwick et al.[168,169] synthesized ferrihydrite and Al-substituted ferrihydrite by rapid evaporation of concentrated ferric nitrate solutions. In the final stage, the evaporated solution was heated in an open oven for 2 h at 250 or 500 °C. Aluminum-substituted samples were prepared by starting from a mixed Al−Fe nitrate solution, and Al substitutions of 8−92% were claimed. Chadwick et al. reported that their Fe phase gave two very broad X-ray diffraction lines at 2.7 and 1. 5 Å, "...characteristic of ferrihydrite". It is interesting to note that the X-ray line at 2.7 Å, which is the strongest line for hematite, corresponds to that at 2.4−2.5 Å in "standard" 2-line ferrihydrite, but similar shifts in *d* values have been recorded by Murad[170] and Carlson and Schwertmann.[158] The products synthesized by Chadwick et al.[168,169] were reported to be brown and to give at 4.2 K a broad 6-line magnetically ordered Mössbauer spectrum with hyperfine parameters: isomer shift (relative to iron metal) = 0.47 mm/s, quadrupole splitting ≈ 0.0 mm/s, and hyperfine field = 49 T.

The influence of the degree of crystallinity on the Mössbauer spectrum of ferrihydrite was reported by Murad,[171] Murad and Schwertmann,[172] and Murad et al.[173] Unlike well-crystallized Fe oxides, no abrupt onset of magnetic order at a well-defined temperature occurs for ferrrihydrite; rather, the superparamagnetic and magnetically ordered components coexist over a wide temperature range.[160] Natural ferrihydrite is superparamagnetic at room temperature, and may remain so to temperatures as low as 23 K. Some well-crystallized samples, however, show partial magnetic order at 77 K, and at 4.2 K all ferrihydrite is completely magnetically ordered. According to Murad,[171] the average quadrupole splitting for paramagnetic ferrihydrite varies from about 0.7 to 0.85 mm/s, whereas for most Fe(III) oxides it is in the range 0.5−0.6 mm/s. Half-widths and maxima of quadrupole-split doublets shift to higher values as the grain size/crystallinity decrease. Murad[171] noted that poorly crystalline "siliceous" ferrihydrite in soils that were developed from recent basalts gave Mössbauer parameters similar, in the paramagnetic state, to those of well-crystallized ferrihydrite; there is, however, an indication that the so-called well-crystallized ferrihydrite may have been schwertmannite rather than ferrihydrite.[74]

Pankhurst and Pollard[126] examined the spectra of synthetic 2-line and 6-line ferrihydrite at 4.2 K in applied fields of up to 9 T. The 2-line ferrihydrite

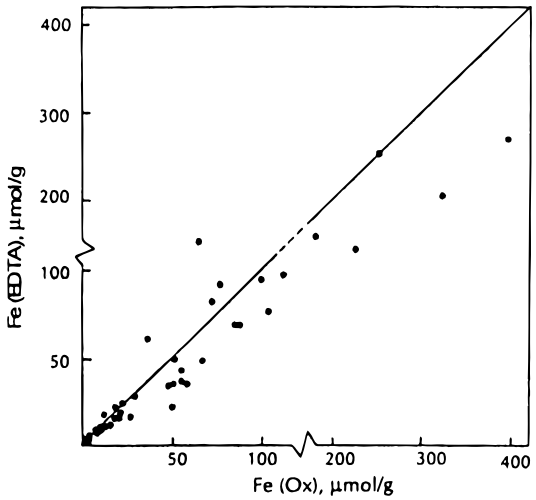

Figure 15. EDTA-extractable iron plotted against oxalate-extractable iron for 45 soil samples. Oxalate-extractable iron is the amount of iron extracted during 2 h shaking with 0.2 M oxalate, pH 3, in the dark, and EDTA extraction periods were 3−7 months. (After ref 174.)

was found to be ferrimagnetic, whereas the 6-line ferrihydrite was antiferromagnetic. The different magnetic states were concluded to exist simply because of random fluctuations arising from the small numbers of ferric ions per particle. Although Pankhurst and Pollard concluded that the iron in ferrihydrite is exclusively octahedrally coordinated, this conclusion was questioned by Zhao et al.,[96] who pointed out that small particle sizes affect the Mössbauer spectra in such a way that the possibility of tetrahedral sites in ferrihydrite cannot be excluded.

D. Differential Dissolution

Differential dissolution is a method widely used to determine the identity of iron oxides in soils.[174] For complete dissolution of all iron oxides, without distinction, the dithionite−bicarbonate−citrate treatment of Mehra and Jackson[175] is generally employed. For selective dissolution of poorly crystalline iron oxides (i.e., ferrihydride or "amorphous" phases), extraction by Schwertmann's ammonium oxalate treatment[176] is used almost universally. Maghemite can be preferentially dissolved by 0.2 M oxalic acid.[99] Ferrihydrite is readily soluble in ammonium oxalate at pH 3,[177] whereas goethite and hematite are much more resistant (goethite ≈ hematite < lepidocrocite). Thus, after a 2-h treatment with ammonium oxalate, and provided that sources of Fe^{2+} such as siderite are absent, the proportion of ammonium oxalate-extractable Fe to dithionite-extractable Fe (Fe_o/Fe_d) is generally taken to represent the proportion of ferrihydrite versus "crystalline" (hematite-goethite) iron oxides. A multiplier of 1.7 is generally used to convert Fe_o values to ferrihydrite concentrations on the assumption that oxalate dissolves only ferrihydrite and that dissolution is complete.[8] An awkward aspect of the oxalate treatment is that the solution is light-sensitive; thus, extractions must be done in darkness, or the solution receptacles must be wrapped in a light barrier such as aluminum foil.

Potassium or sodium pyrophosphate solutions have been used for many years for determining organic-complexed Fe in soils. The technique, which generally involves shaking the soil in a 0.1 M pyrophosphate solution at pH 10 for 16 h, is considered inaccurate because of the presence of suspended material in the extracts, and because the relationship to organic complexing is uncertain. Modifications or alternatives to the pyrophosphate and ammonium oxalate treatments have been proposed,[178,179] but have not been adopted widely. Recent refinements to the ammonium oxalate treatment have mainly involved the duration of the treatment or X-ray diffraction monitoring to determine coincident dissolution of the Fe oxides.[68,180,181] X-ray monitoring is particularly useful for soils that may contain magnetite, which also is soluble in oxalate.[182,183] The use of ammonium oxalate and EDTA, and the effects of adsorbed anions such as phosphate, were discussed by Borggaard;[184,185] the EDTA reagent, however, requires 3−7 months for extraction. For this reason, and because comparative tests on soils indicate that the amounts of Fe extractable by oxalate and by EDTA are similar (Figure 15), EDTA seems not to be used extensively.

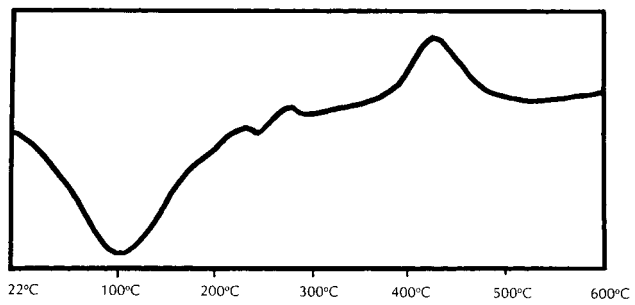

Figure 16. Differential thermal curve of ferric nitrate hydrolyzate run in static nitrogen atmosphere at 10 °C/min. Sample weight approximately 20 mg. (From ref 4.)

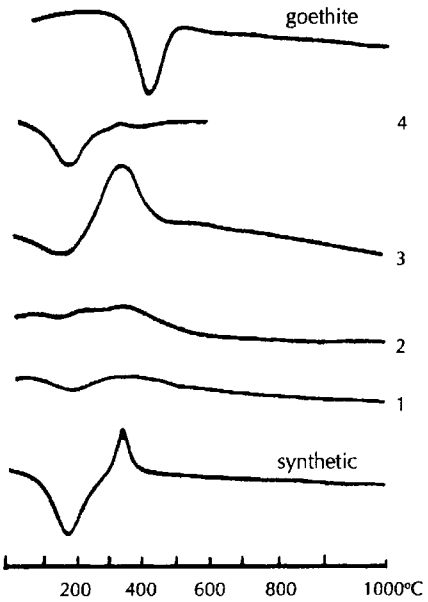

Figure 17. DTA curves of goethite, and natural (1−4) and synthetic ferrihydrite. (Modified after ref 10.)

E. Thermogravimetric and Differential Thermal Analyses

Thermogravimetric (TG) analysis of synthetic 6-line ferrihydrite was found by Saleh and Jones[186] to give

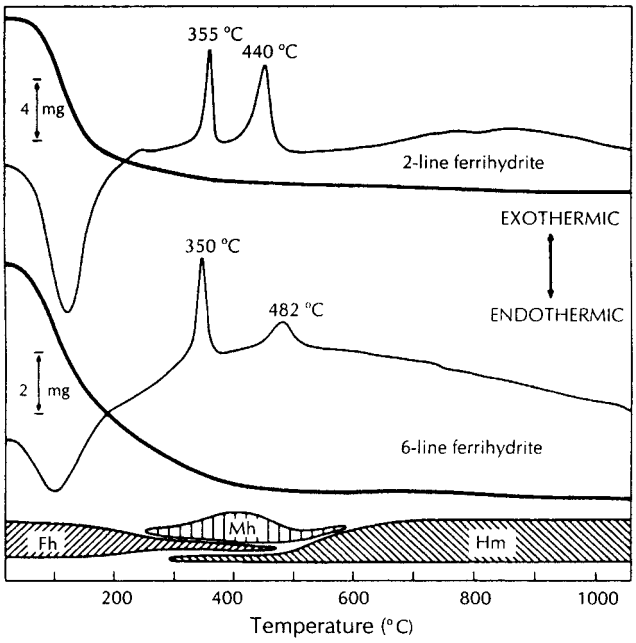

Figure 18. Differential thermal analysis curve (thin line), thermogravimetric curve (thick line), and thermal products (bottom) for 2-line and 6-line ferrihydrite: Fh, ferrihydrite, Mh, maghemite, Hm, hematite. (After ref 123.)

a weight loss of 22.4%. For synthetic 2-line and 6-line ferrihydrites, Eggleton and Fitzpatrick[123] obtained smooth and continuous weight losses of 19.65 and 25 wt %, respectively.

Differential thermal analysis (DTA) of pure synthetic ferrihydrite was reported by Towe and Bradley[4] and Chukhrov et al.[10] to give a low-temperature endotherm corresponding to the expulsion of water, and a moderately strong exothermic peak at 300−400 °C, the latter thought to mark the conversion to hematite or the recrystallization of hematite. Two additional but small exothermic peaks, one at about 225 °C and the other at about 275 °C, are evident in the DTA curve shown by Towe and Bradley (Figure 16). Chukhrov et al.[10] showed five DTA curves for natural and synthetic ferrihydrite; some of the curves for the natural material do not show a pronounced exothermic effect (Figure 17), but the reason for the difference was not discussed. However, silica-bearing synthetic ferrihydrite is known to give only a broad, weak exotherm at about 700 °C, thus suggesting that the natural samples examined by Chukhrov et al.[10] were siliceous ferrihydrites (only two of the four samples for which DTA curves are illustrated in Figure 17 were chemically analyzed, but both contain ~6 wt % SiO_2). Carlson and Schwertmann[158] suggested that the appearance of the high-temperature (~700 °C) exotherm indicated the presence of Si−Fe−O bonds; i.e., the incorporation of Si into the ferrihydrite structure.

Eggleton and Fitzpatrick[123] obtained two well-defined exothermic peaks in their DTA curves for unsubstituted ferrihydrites (Figure 18). Material heated to 310 °C was found to be ferrimagnetic, and

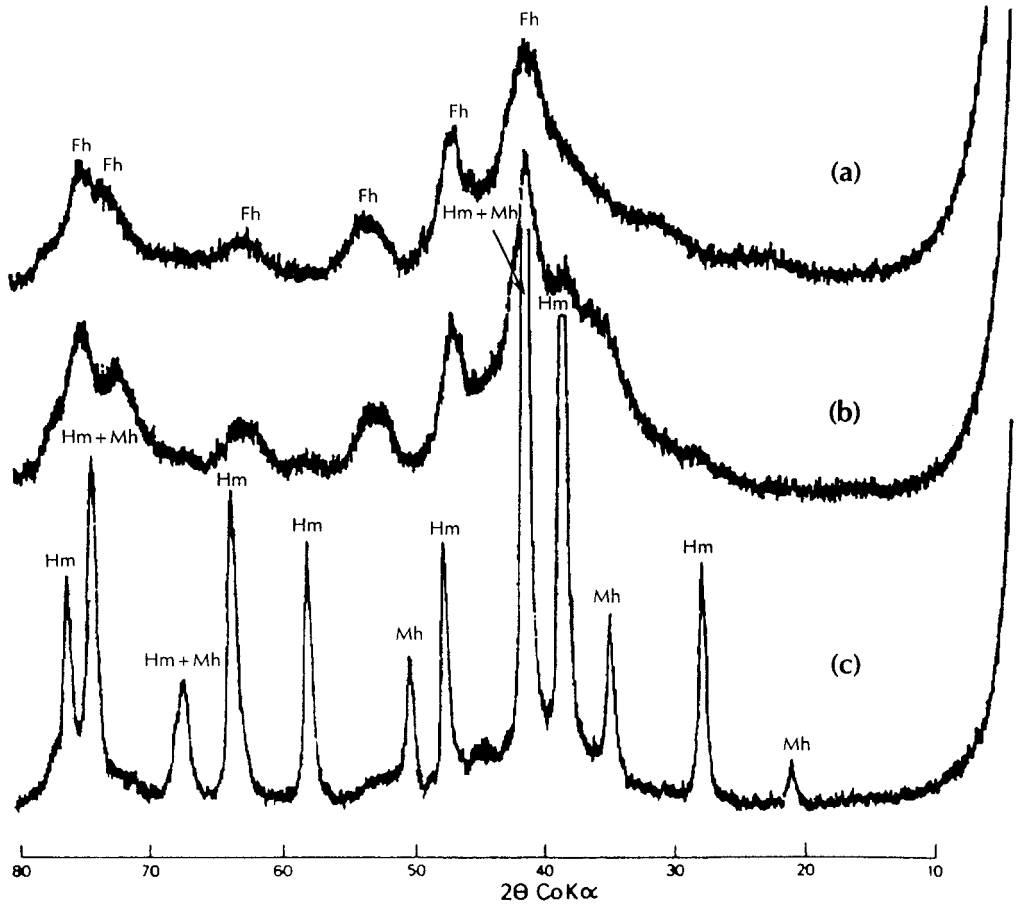

Figure 19. X-ray powder diffraction traces for 6-line ferrihydrite: (a) unheated, (b) heated to 310 °C, and (c) heated to 400 °C. Abbreviations: Fh, ferrihydrite; Hm, hematite; Mh, maghemite. (Slightly modified from ref 15.)

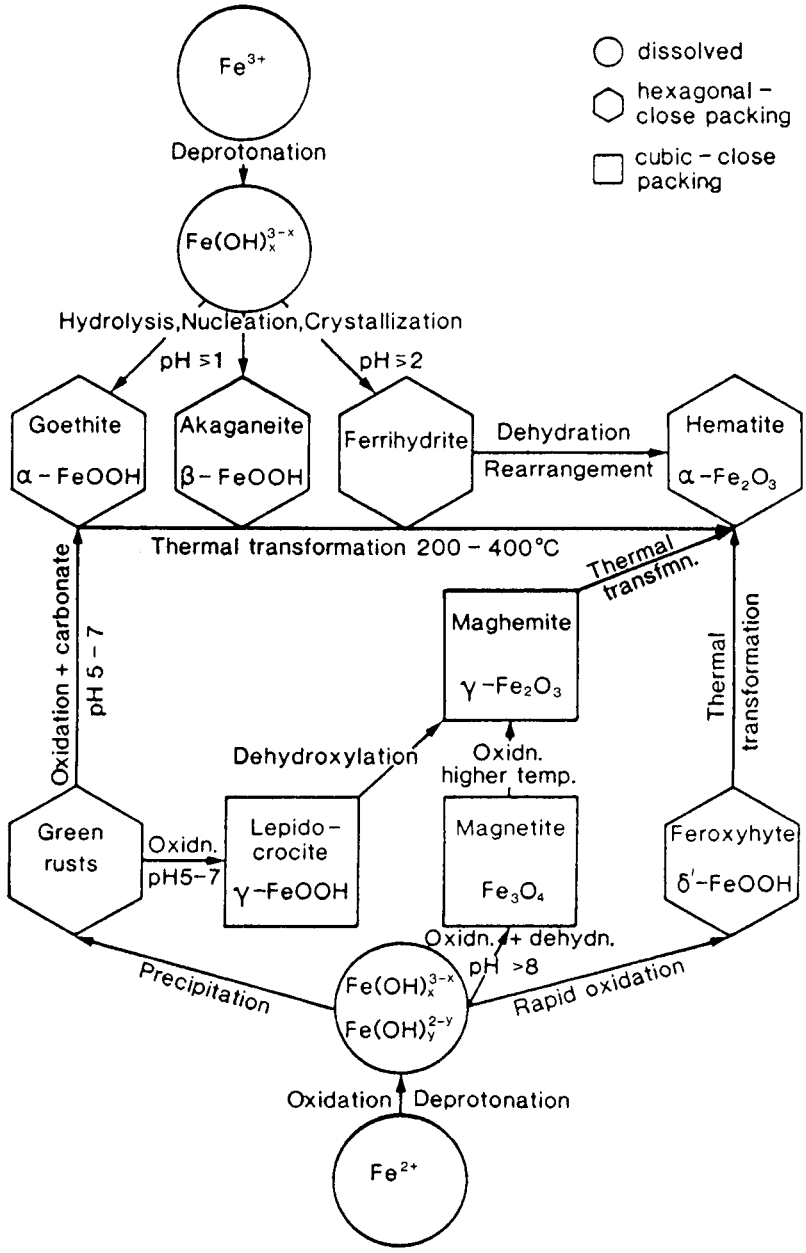

Figure 20. Schematic representation of formation and transformation pathways of common iron oxides, together with the approximate transformation conditions. (Slightly modified from ref 13.)

the X-ray diffraction patterns showed changes that were interpreted to correspond to a partial conversion to maghemite (Figure 19). At 400 °C the X-ray patterns contained relatively sharp peaks for maghemite and hematite, but at 500, 600, and 1000 °C only hematite was detectable. Thus, on the DTA pattern the exotherm at 350 °C, which occurs just as the last 2% of the water is lost from the sample, and which was interpreted by Schwertmann[187] to be due to the crystallization of hematite, was attributed by Eggleton and Fitzpatrick[123] to be largely the result of the growth of maghemite; the smaller exotherm at 482 °C was interpreted by Eggleton and Fitzpartick to result from the conversion of maghemite to hematite. In recent experiments by Campbell et al.,[188] however, only hematite was detected even where two exothermic peaks were present; magnetite−maghemite formed during heating only when a carbon reductant was present.

The occurrence of exothermic peaks at about 300 and 400 °C has in some cases been used as an indication of the presence of ferrihydrite in soils.[10,51] The absence of these peaks in siliceous ferrrihydrite indicates that DTA alone is not a reliable detection method for ferrihydrite in soils.[158,189]

VII. Synthesis

Rapid hydrolysis of Fe(III) solutions commonly leads to the formation of ferrihydrite. Brief heating of the solutions to about 80 °C typically produces 6-line ferrihydrite, whereas the 2-line variety is produced at ambient temperatures by the addition of alkali to raise the pH to about 7. Descriptions of the ferrihydrite products, and explicit procedures for their synthesis from $Fe(NO_3)_3 \cdot 9H_2O$ solutions using both of the above techniques, are given by Schwertmann and Cornell.[13] Schwertmann and Cornell[13]

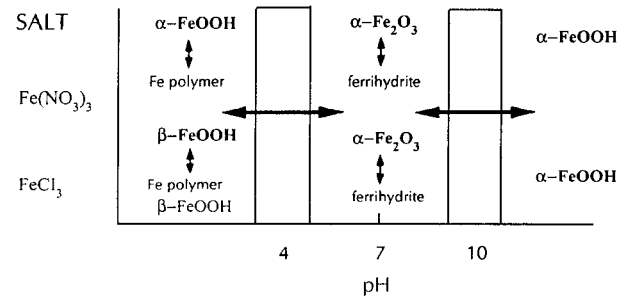

Figure 21. Schematic representation of stability domains for hematite, akaganéite, goethite, and associated hydrous oxides formed by the hydrolysis of an Fe(III) solution at room temperature. Bold text indicates well-crystallized minerals; plain text, local structure of their corresponding poorly crystallized phases (when existing). (Adapted from ref 133.)

noted that the length of time of hydrolysis is critical, and that goethite and hematite will form if the hydrolysis time is extended. Figure 20 is a schematic representation of the proposed pathways that lead to the formation of the various iron oxyhydroxides; earlier versions were presented by Schwertmann and Taylor[99] and Murray,[116] and the hydrolysis of Fe(III) to form polynuclear species was reviewed in detail by Cornell et al.[190] Ferrihydrite has been obtained both by oxidizing Fe(II) solutions and by precipitation from Fe(III) solutions containing a variety of anions (chloride, perchlorate, sulfate, nitrate). For nitrate solutions at 60 °C, Šubrt et al.[191] determined that ferrihydrite samples prepared in an approximately neutral medium are less crystalline than those prepared in either the acidic or alkaline regions. That the formation of different ferrihydrite products, such as the 2-line versus 6-line varieties, is related to the conditions of synthesis is not unexpected. Different starting materials or slight variations in conditions within the stability field of a precipitate are well-known to affect the physical properties of the product, especially the morphology, and for the iron oxides/oxyhydroxides the latter has been a topic within, or the focus of, numerous studies.[118,192−198]

Figure 21 represents the general stability fields of the various iron oxides/oxyhydroxides as outlined by Manceau and Drits.[133] Ferrihydrite and hematite are within the same stability field, whereas that of goethite is at higher and lower pH. Thus, the strong influence of solution pH is readily evident, as has also been reported by Zinck and Dutrizac.[199] In the low-pH field, akaganéite will form only in the presence of chloride solutions. Although Post and Buchwald[11] concluded that chlorine may be an essential constituent in akaganéite, which therefore would not be a polymorph of FeOOH and would be purged from the diagram,[200] this issue has not been resolved.[201] The formation of ferrihydrite and hematite in the same pH field is thought by Manceau and Drits[133] to provide an explanation of why ultradispersed hematite might coexist with ferrihydrite proper.

In summary, 2-line ferrihydrite is prepared by the rapid oxidation of Fe(II) solutions, or by the rapid neutralization of Fe(III) solutions. The 6-line variety of ferrihydrite forms by hydrolysis of Fe(III) solutions, typically at elevated temperatures and low pH. Precipitation is initially accompanied by a rapid pH change, which slows after the first hour, and aging for 2−4 h is necessary to stabilize the suspensions.

VIII. Adsorption and Solid Solution

A. General Observations

In contrast to goethite and hematite, in which at least partial solid solution of several metals has been unequivocally demonstrated,[202−208] it has not been shown that corresponding substitutions occur in ferrihydrite. That ferrihydrite would be completely devoid of substitutions is improbable, but the poor X-ray diffracting properties of the mineral, and the related uncertainties about the interpretation of the X-ray data even when adsorbed species are absent, seem to have deterred claims about observed solid solution, other than for Cr[143] and tellurate.[209] Thus, adsorption on ferrihydrite is employed as an explanation for the intimate association and behavior of various ions and molecules, although in some cases, the foreign species may be present in double-digit percentages (e.g., 35% Si[210]). For dissolved anions of equal charge and similar geometry, Harrison and Berkheiser[209] reported that, in general, suspension pH determines the adsorption capacity.

The adsorption of any species is directly dependent on the particle size or surface area of the adsorbing substrate. The particle sizes of ferrihydrite and other fine-grained minerals can be determined by measuring the ratio of the height and width of X-ray peaks; the premise is that the wider the peak relative to its height, the finer the grain size. Broad peaks are typical for ferrihydrite, and the particle size of the aggregates is reported to be generally 30-100 Å.[99,170] Murphy et al.[194] found the sizes to be 15−40 Å in the intial stages of polymerization, and Waychunas et al.[137] suggested crystallite coherence lengths in the range 8−15 Å. Ferrihydrite thus has a high surface area, and values of 200−350 m^2/g seem to be typical of the values obtained by BET analysis using nitrogen gas as the adsorbent (Table 9). Dzombak and Morel[211] list values up to 720 m^2/g obtained by various other techniques and adsorbents. If the particles are assumed to be spherical and the thickness of the surface layer is taken as ∼2 Å, which is roughly the length of the Fe(III)−O bonds, the surface area of ferrihydrite constitutes a substantial part of the total volume. For example, the surface layer of a sphere 30 Å in diameter makes up roughly 19% of the total volume, and a sphere 15 Å in diameter would have 35% of its volume represented by the surface layer. Moreover, any particle shape deviating from spherical will lead to an even greater surface area. Thus, because the stoichiometry of a surface is generally different from that of the interior, it is evident that a significant fraction of the bulk composition of ferrihydrite always represents that of the surface rather than that of the core structure. As noted previously, this duality has important implications with respect to interpretation of the composition and structure of ferrihydrite.

The large surface area and high reactivity of ferrihydrite make it an important adsorbent of trace

Table 9. Some Representative BET Surface Area Measurements of Ferrihydrite

type	area, m^2/g	ref
3-line; atomic Si/Fe 0.23, natural	240	Childs et al.[31]
6-line; atomic Si/Fe 0.37, natural	230	Childs et al.[31]
3-line; atomic Si/Fe 0.50, natural	120	Childs et al.[31]
6-line; synthetic	249	Saleh and Jones[186]
6-line; Si/Fe 0.02, synthetic	233	Saleh and Jones[186]
6-line; Si/Fe 0.16, synthetic	279	Saleh and Jones[186]
2-line; synthetic	340	Eggleton and Fitzpatrick[123]
6-line; synthetic	225	Eggleton and Fitzpatrick[123]
2-line; synthetic	260	Liaw et al.[212]
6-line; synthetic	203	Stanjec and Weidler[213]
2-line; synthetic	339	Postma[214]
2-line; synthetic	269	Bruun Hansen et al.[215]
2-line; synthetic	230	Axe and Anderson[216]
synthetic "amorophous"	159−234	Crosby et al.[217]

Table 10. Some Pre-1990 References to Adsorption by Ferrihydrite

sorbate	ref
Cd, Pb, Cu, Zn, Ag	Davis and Leckie[219]
Ca, Zn,	Kinniburgh and Jackson[222] and Kinniburgh[223,224]
Cd, Cu, Zn, Pb	Benjamin and Leckie[225]
Cd, Cu, Zn, Co, Se	Anderson and Benjamin[210]
As	Pierce and Moore[226]
Cr	Zachara et al.[227]
Cd, Zn, Ag, Cu, Pb, Hg, Cr, S, As, Se	Leckie et al.[228]
S	Parfitt and Smart[229]
Se, Si	Anderson and Benjamin[210]
U	Langmuir[230] and Hsi and Langmuir[231]

metals in surface and groundwater systems. How these ions interact with ferrihydrite is a topic beyond the scope of this review. In general, however, adsorption that is independent of the ionic strength of the solutions is attributed to the formation of an inner-sphere surface complex.[102] Various adsorption models are discussed by Dzombak and Morel,[211] and new models continue to be proposed.[218] Values adopted for some of the fundamental parameters of ferrihydrite vary. For example, none of the measured surface-area values given in Table 9 exceeds 340 m^2/g, but most authors recently seem to favor the adoption of a surface area of 600 m^2/g, which is the value recommended by Davis and Leckie[219] and Dzombak and Morel,[211] and which seems to give better results in computed models. The mean value of the conventional solubility product of ferric hydroxide, $K = (Fe^{3+}_{(aq)})(OH^-_{(aq)})^3$ is 10^{-39}, but Fox[220] recommended that it be replaced by the ion activity product $(Fe^{3+}_{(aq)})(OH^-_{(aq)})^{2.35} = 10^{-31.7}$. This replacement was questioned by Bruun Hansen et al.,[221] who nevertheless adopted it for their calculations. These aspects are not dealt with further in this review, and for cation and anion sorptive behavior of ferrihydrite, the reader is referred to Dzombak and Morel.[211]

B. Adsorption of Specific Species

Some of the early work relating to the adsorption of Ca, Zn, Pb, Cu, borate, and molybdate on ferrihydrite is summarized in Schwertmann and Taylor.[99] Table 10 gives a few references to studies that were done prior to 1990. A much more comprehensive review, and assessment of the data, is given in the book by Dzombak and Morel,[211] which discusses the sorption of Ba^{2+}, Ca^{2+}, Sr^{2+}, Co^{2+}, Ni^{2+}, Cd^{2+}, Zn^{2+}, Cu^{2+}, Pb^{2+}, Hg^{2+}, Ag^+, and Cr^{3+} cations, and PO_4, AsO_4, VO_4, AsO_3, BO_3, SO_4, SeO_4, SeO_3, S_2O_3, and CrO_4 anions. In addition, results from the experimental data for these various ions have permitted the prediction of the surface complexation constants for numerous additional cations and anions. Thus, the following brief notes only point out germane references that have appeared since the publication of Dzombak and Morel,[211] or include peripheral topics such as the adsorption of organic compounds.

1. Various Cations

The kinetics of Cd and Co desorption from ferrihydrite and goethite were investigated by Backes et al.,[232] whose "ferrihydrite" consisted of a mixture of feroxyhite and ferrihydrite. It was found that, at pH 6, increased contact times between the metal ions and the oxides decreased the subsequent rate of desorption, and that substantial proportions of the metal could not be readily desorbed into solution.

Uptake of Cd and Cu by sand sediments to which organic matter and ferrihydrite had been added was investigated at pH 6.5 by Warren et al.[233] Copper fractionation was strongly influenced by the organic matter (peat), and in its presence, neither Cu nor Cd was adsorbed by ferrihydrite to an appreciable degree. The ineffectiveness of ferrihydrite as an adsorbent may have been related to its transformation to more crystalline phases during the course of the experiments.

Up to 9.4 wt % Cd was adsorbed on ferrihydrite at pH 6.7−9.5 in the experiments by Spadini et al.[144] EXAFS spectroscopy indicated that Cd−Fe atomic distances for ferrihydrite are similar to those for Cd-sorbed goethite, but the density ratio of high-affinity to low-affinity surface sites is much greater on ferrihydrite than on goethite.

Adsorption of Mn(VI) by ferrihydrite over the pH range 3.5 to 8 attained a maximum of 0.6 mmol/g or 2.4 μmol/m^2, which was achieved at pH 4.5.[234] A similar study of Co, Cu, and Mn adsorption by ferrihydrite over almost the same pH range (3.8−8.2) was reported by Bibak.[235] The amount of metal adsorption was in the order Cu $\gg$ Co > Mn, and the relative adsorption decreased in the order humic acid → Al oxide → ferrihydrite → goethite.

Combes et al.[236] studied the sorption of Np(V) on goethite in pastes, and Sakamoto et al.[237] examined the redistribution of Np(V) during the alteration of ferrihydrite to goethite and hematite. These studies have relevance to the storage and potential mobilization and transportation of deleterious elements from radionuclide wastes. At pH 7.7, Np(V) adsorbed on ferrihydrite remained constant during alteration, but at pH 6.0 the Np abundance decreased drastically during alteration. The difference is thought to be related to the presence of adsorbed NpO_2 at the lower pH, and to NpO_2OH at higher pH.

Sakamoto et al.[237] cite references to 1993 and 1984 publications by Sakamoto and Senoo in which the redistribution behavior of Sr, Cs, and Li during the alteration of ferrihydrite to goethite was investigated. The rate of Sr diffusion within ferrihydrite was described by Axe and Anderson,[216] who observed that Sr followed the standard profile in which rapid initial adsorption was followed by much slower uptake through intraparticle diffusion.

The deportment of Zn, Cd, Tl, Sn, selenite, selenate, and sulfate in laboratory-precipitated ferrihydrite was reported by Zinck and Dutrizac.[199] Sulfate and Zn adsorption were reported to have been affected by solution pH.

The use of sequential extractions in general, and the inferences commonly drawn from such extractions, were reviewed by Whalley and Grant.[238] They found that Cu, Ni, and Zn adsorbed on laboratory-prepared spiked ferrihydrite samples could be removed simply by treatment with acetic acid.

The mechanism by which various metals bind to ferrihydrite surfaces has been examined by EXAFS spectroscopy in several studies. Manceau et al.[239] determined that both Pb and U adsorb as inner-sphere complexes that are edge-linked to the $Fe(O,OH)_6$ octahedra of ferrihydrite. Chromium, however, behaves differently. Coprecipitated ferrihydrite with high Cr/Fe contents has a solubility that is an order of magnitude lower than that of a surface precipitate.[239] EXAFS spectroscopy showed that Cr(III) and Fe(III) have similar local structures, thus indicating that a solid solution is present. In addition to this mutual substitution, Cr(III) adsorbed on the ferrihydrite surface occurs as multinuclear complexes that subsequently act as nucleation sites for the formation of Cr-bearing surface precipitates. Manganese oxides, which have an even higher affinity than ferrihydrite for Cr(III), tend to oxidize the Cr to Cr(VI), thus increasing its solubility and toxicity.[239]

2. Various Anions

Infrared spectra for freshly precipitated ferric oxides that were reacted with $NaNO_3$, Na_2SO_4, Na_2SeO_4, Na_2HAsO_4, or $Na_2H_4TeO_6$ were presented by Harrison and Berkheiser.[209] Because the resulting precipitates were not specifically characterized, conclusions about the extent of involvement of ferrihydrite is arguable; nevertheless, the IR curves provide useful comparisons of the adsorption effects. Monovalent oxyanions (nitrate, perchlorate) were concluded by Harrison and Berkheiser to adsorb through an electrostatic interaction with the hydrated hydrous oxide surface, whereas divalent oxyanions (carbonate, sulfate, arsenate, selenate) coordinate directly with surface iron cations. Tellurate, however, was concluded to incorporate in the hydrous oxide structure.

Selenite is known to adsorb on goethite by bonding to two OH surface groups,[240] and EXAFS spectroscopy[239] has indicated that the coordination with ferrihydrite surfaces occurs similarly. The possibility that the different results reported for sulfate versus selenate surface bonding might be due to hydration levels (use of dry versus wet samples) was investigated by Manceau and Charlet,[241] who concluded that selenate always forms inner-sphere surface complexes, regardless of the hydration state. It was further concluded that selenate attachment occurs by the sharing of edges of the $Fe(O,OH)_6$ octahedra and that a similar sorption mechanism operates for selenite, sulfate, arsenate, and phosphate. The details of arsenate binding on ferrihydrite have been controversial.[137−141]

It has long been known that ferrihydrite is an effective adsorbent for inorganic phosphate in soils.[242] This knowledge was applied in a practical way by Freese et al.,[243] who designed a system that utilizes a synthetic ferrihydrite suspension in a dialysis membrane to act as a sink for the phosphorus contained in soils. Measurement of "reversibly adsorbed" phospate; i.e., that which can be desorbed readily, is a parameter commonly determined in soil science. Among the advantages cited for the proposed system is that no desorption plateaus were detected in experimental tests, thus indicating that ferrihydrite acts as a very large sink for phosphate.

Studies of P adsorption on ferrihydrite have been conducted using both natural[69,244] and synthesized material.[245] Parfitt[69] observed that at high levels of P (>10 μmol/L), phosphate sorption was in the order hematite < goethite < ferrihydrite < allophane (an amorphous hydrous aluminum silicate). Adsorption of P was accompanied by desorption of Si.

Uptake of phosphate by ferrihydrite in groundwater systems was suggested by Griffloen[246] to be dependent on the pH and the Fe(II):PO_4 ratio. Various mechanisms of phosphate sorption have been discussed by Ryden et al.,[247] Parfitt et al.,[248] Willett et al.,[245] and Manceau and Charlet.[241] Reactions between tripolyphosphate and ferrihydrite were examined by Lin and Benjamin.[249,250] The high sorptive capacity of ferrihydrite for phosphate led van Riemsdijk et al.[251] to conclude that surface precipitates of ferric phosphate are formed, but this has not been proved.

Infrared spectra of P-bearing ferrihydrite show a broad absorption band at 1030 cm^{-1} that has been

attributed to the P−O stretching vibrations of phosphate;[245] the broadness of the band suggests that phosphate group oxygens are involved in bonding with the surface OH groups of ferrihydrite. Manceau and Charlet[241] suggested that, as with sulfate[229] and selenate, the phosphate adsorbs onto ferrihydrite by forming binuclear bridging complexes that bond with two singly coordinated OH groups. The phosphate adsorbed on ferrihydrite is readily desorbed, and despite the uptake of percentage quantities of P, no crystal-structure changes indicative of solid-solution-type incorporation have been demonstrated. Adsorption of P inhibits the transformation of ferrihydrite to other oxyhydroxides.[252,253]

3. Organic Species

Adsorption of insecticides and herbicides applied subaerially or directly on soils is of environmental concern because the accumulation of these compounds may be detrimental to the habitat or to organisms within the habitat. Accumulation and transportation of the agents in groundwaters can also impose hazards in environments distant from a dosed site.

Although most studies of insecticide and herbicide adsorption in soils have dealt with interactions with clay minerals, Schwandt et al.[254] tested the adsorption of quinmerac herbicide (7-chloro-3-methylquinoline-8-carboxylic acid) on synthetic 6-line ferrihydrite, and on natural ochreous ferrihydrite sludge. At low pH, up to 1.19 mg of quinmerac were adsorbed per gram of synthetic ferrihydrite (dry weight), but sorption decreased with increasing pH, and at pH >5.5 no adsorption was observed. Adsorption on goethite and hematite was poor, and because the amount of ferrihydrite in arable soils is low, it was concluded that iron oxides are not likely to be a sink for quinmerac if pH conditions are neutral to slightly acidic.

Cox et al.[255] used synthetic 2-line ferrihydrite to study the uptake of thiazafluron, a nonselective herbicide that is derived from urea and is applied to the soil in large doses for industrial weed control. Illitic clays were found to be the principal thiazafluron adsorbent, with less adsorption by montmorillonite, and none by ferrihydrite.

Ferrihydrite, lepidocrocite, hematite, and goethite were used by Inoue et al.[256] to study the reactions with mugineic acid, a non-protein-building amino acid that is excreted by the roots of rice and oat, as a strategy for Fe uptake when conditions are Fe-deficient. The mugineic acid evidently interacts with soil Fe oxides, thereby facilitating adsorption into the root system. Both the amount of mugineic acid adsorbed on the Fe oxides, and the amount of Fe dissolved from them, depended on the pH, the concentration of mugineic acid, and the type and amount of Fe oxides added to the system. Mugineic acid was not adsorbed above pH 10, but over the pH range 3−10 the acid adsorption was related to the specific surface area, following the order: ferrihydrite ≫ goethite ≥ lepidocrocite ≥ hematite. The amount of Fe dissolution followed the order: ferrihydrite ≫ lepidocrocite ≥ hematite = goethite.

Ferrihydrite and other Fe oxides were investigated by Kung and McBride[257] as adsorbents of *p*-hydroxybenzoic acid, one of the most common of the natural, simple phenolic acids in soils. At the pH 5.5 of the experiments, the amount of organic adsorbed was in the order: ferrihydrite > hematite ≫ goethite, and adsorption per unit of surface area was in the same order. All of the above studies in which the pH was variable indicated that adsorption of anionic organic chemicals is strongly dependent on the pH of the system.

C. Environmental Implications

Large surface area, strong adsorptive effects, high adsorption capacity, and low cost are properties that make ferrihydrite an attractive material for the treatment of wastewaters from various industries. Leckie et al.[228] concluded, on the basis of experimental results, that adsorption/coprecipitation with ferrihydrite is a feasible process for the removal of trace elements from a variety of power-plant waste streams. Schultz et al.[258] determined that soluble Cu, Pb, Ni, Cd, Zn, and Cr(III) could be adsorbed onto ferrihydrite at pH 9.5, and could be substantially desorbed at pH 4.5. For the same metals, Edwards and Benjamin[259] found that ferrihydrite added to waste solutions from a plating shop was a highly efficient sorbant over the pH range 8−12.5. Moreover, the ferrihydrite adsorption properties could be regenerated by acid treatment, and no measurable loss in metal-removal efficiency for either industrial or synthesized wastes was detected over 50 cycles of reuse.

Ferrihydrite-coated sand has been determined to be an effective, efficient water filtrant, especially at pH 7.[260] Tests by Edwards and Benjamin[261] showed that ferrihydrite-coated sand outperformed uncoated sand in removing not only particulate metals, but also uncomplexed and ammonia-complexed soluble metals. Despite these positive aspects, the total metal-removal capacity of such systems is relatively low because the sand particles themselves play a negligible role in adsorption. Nevertheless, ferrihydrite-coated sand (0.6 mass % ferrihydrite) has been found to be an efffective adsorbent of $Co^{II}EDTA^{2-}$ and $Ni^{II}EDTA^{2-}$ (ethylenediaminetetraacetic acid) complexes.[262] In this regard, EDTA has been used as a chelating agent for complexing radionuclides at waste-disposal facilities.

Ferrihydrite precipitated onto magnetite was reported by Chen et al.[263] to remove >90% of the soluble Cr(VI) and Zn from test solutions. This result is significant in that although Cr(III) was effectively adsorbed in the experiments by Schultz et al.[258] and Edwards and Benjamin,[259] Cr(VI) was not removed efficiently either by coprecipitation or adsorption. Chen et al.[263] found, however, that chromium recovery decreased after the first cycle of attempted desorption. The decline in performance was attributed to cumulative adsorption that slowed the reversibility (desorption).

The sorptive capacity of ferrihydrite decreases markedly at low pH,[210] and the extent of removal of heavy metals below pH 5.0 is severely attenuated. To overcome this problem Gao et al.[264] used a hybrid

sorbent, produced at high temperature, consisting largely of ferrihydrite and akermanite ($Ca_2MgSi_2O_7$) that together form porous aggregates of microparticles. The akermanite serves as a source of hydroxyl ions in accordance with the reaction of water with $Ca_2MgSi_2O_7 \rightleftharpoons 2Ca^{2+} + Mg^{2+} + 6OH^- + 2SiO_2$, thus helping to neutralize the aqueous-phase hydrogen ions and enabling ferrihydrite to adsorb in its more effective pH range. Column tests showed that the hybrid sorbent achieved almost complete removal of heavy metals (Cd = Ni = Pb $\approx$ 2.0 mg/L, Cu = 0.1 mg/L, Na = 250 mg/L, pH 4.0) for up to 5000 bed volumes. At higher metal concentrations the number of bed volumes decreased. The selectivity sequence (binding strength) was in the order Pb > Cu $\gg$ Ni > Cd. The hybrid sorbent loaded with heavy metals can be desorbed in situ for a number of cycles by washing with ammonia/amine solutions.

IX. Transformation of Ferrihydrite

A. Dry Thermal Transformation

Until the paper by Eggleton and Fitzpatrick[123] there was general agreement that dry heating of ferrihydrite resulted in a simple transformation: ferrihydrite → hematite. The principal, moderate exothermic peak noted by Towe and Bradley[4] at ~400 °C (Figure 16) was thought to reflect the conversion to hematite, or to energy released during hematite recrystallization. Eggleton and Fitzpatrick[123] observed two exotherms (Figure 18), the first of which was attributed to the onset of maghemite growth, and the second to the conversion of maghemite to hematite (Figure 18). Although maghemite had been detected as a conversion product many years earlier,[158,265] its presence was attributed to the effect of organic matter, and it seems not to have been discussed in later papers. As was mentioned in the section dealing with the ferrihydrite structure, however, the presence of maghemite was cited by Eggleton and Fitzpatrick[123] as indirect evidence to support the existence of tetrahedral Fe in ferrihydrite. The dual exothermic peaks were also the focus of discussion by Prasad and Sitakara Rao,[266] but the peaks were attributed to the conversion of ferrihydrite to hematite and to the crystallization of hematite at the higher temperature.

Drits et al.[132] reported that ferrihydrite heated in air at 350 °C for 1 h was converted to hematite and that subsequent heating of this hematite by the electron beam in the vacuum chamber of an electron microscope resulted in the formation of magnetite. This seems plausible in that the transformation of hematite to magnetite represents a deoxygenation reaction; i.e., $Fe_2O_3 \rightarrow Fe_3O_4 = Fe_2O_{2.67}$. Under vacuum conditions, microbeam heating of ferrihydrite resulted in the transformation: ferrihydrite → magnetite (Fe_3O_4) → wüstite (FeO). Drits et al.[132] thus argued that the tetrahedral iron inherent in maghemite is the result of the partial reduction of Fe^{3+}, and not, as Eggleton and Fitzpatrick[123] had proposed, the consequence of an inherited structural configuration from ferrihydrite.

Lewis[267] oven-heated synthetic 2-line and 6-line ferrihydrite and found that the 2-line phase transformed to hematite, whereas the more ordered variety formed goethite with little or no hematite. The different conversions were attributed to the size of the initial polymers, with the small polymers (2-line ferrihydrite) converting to hematite. In 6-line ferrihydrite the supply of small polymers is limited, and it was thought that there might also be concomitant growth of goethite nuclei within the ferrihydrite, thus "seeding" the preferred transformation to goethite. Of particular interest in Lewis's study[267] is a paragraph in which the work of Johnston and Lewis[268] is cited. This paragraph is given in its entirety as follows:

> The influence of polymer size on some crystallographic characteristics was investigated by Johnston and Lewis(268) who examined a series of molecular weight (MW) fractions obtained from a partially hydrolyzed Fe(III) solution by filtering through a sequence of Amicon Diafilters of decreasing pore size. Fractions with a nominal MW greater than 50,000 made up more than 75% of the iron in the system, and these were shown by XRD and Mössbauer studies to increase in goethitic character with size. Nearly 20% of the iron remained in the low MW fraction (nominally less than 500) and consisted only of monomeric and dimeric species. Intermediate-sized material from 1,000 to 50,000 MW (about 5%) showed no detectable goethitic character, resembling rapidly precipitated ferrihydrite by both techniques. When stored at 55° in 0.1 KOH (Lewis, unpublished) all fractions greater than 50,000 MW [75% of the iron] quickly formed fine-grained goethite as the sole product. However, transformation was much slower for the fractions less than 50,000 MW in which well crystalline hematite was produced as well as fine-grained goethite. For the fraction 1000 to 10,000 MW [*x* fraction] hematite was dominant (95%) and formed approximately 50% of the product from the 20,000 to 50,000 [*y* fraction] [$x + y = <5\%$ of the iron]; i.e. the smaller the polymer the greater the likelihood of hematite formation.

A significant aspect of the study by Johnston and Lewis,[268] as quoted above, is that not only were hematite-like and goethite-like fractions distinguishable, but they apparently could be discriminated with a high degree of sensitivity. The early-precipitated material did not possess features characteristic of hematite. This is in contrast to the ferrihydrite structural model of Drits et al.,[121,132] wherein ultradispersed hematite is considered to make up about 25% of the bulk ferrihydrite. If this were so, the high-molecular weight fraction examined by Johnston and Lewis[268] should have shown the presence of abundant hematite; the absence of hematite is not in accord with the proposal of Drits et al.[132] that ultradispersed hematite provides a seed or embryonic phase in the conversion of ferrihydrite.

Also of interest in the paper by Lewis[267] is the proposal that only the smaller polymers transform readily to hematite. In the CUS model of Zhao et al.,[95,96] these smaller polymers would have a high

surface area and would be the most amenable to dehydroxylation. The larger polymers would have proportionally fewer surface sites because linkages of the dioctahedral chains had advanced to form a goethite-like array.[137]

The dry heating of 2-line and 6-line ferrihydrite was also examined by Stanjek and Weidler,[213] whose work was contemporaneous with, but independent of, that of Lewis.[267] From their observations, Stanjek and Weidler[213] concluded that it was possible to dehydrate 6-line ferrihydrite, without the occurrence of significant changes in cell parameters or structure, to a composition corresponding to $Fe_{1.75}O_{2.26}(OH)_{0.74}$. It was proposed that:

> Continuous removal of OH from the ferrihydrite structure necessarily reduces the average coordination number of oxygens and OH around iron. Thus charge imbalance and structural distortion would increase up to a level where it is no longer possible to form further defects in the structure. If this model is valid, a ratio [of structural OH] can be expected where further removal of OH results in major structural rearrangement (to hematite). A temperature of 400 K [maximum OH loss without conversion occurring], however, it is probably too low to enable sufficient cations diffusion, because of [the required] high activation energy...A plateau is therefore expected, at which the dehydration reaction comes almost to a stop. This plateau was observed for the series SF2...

Stanjek and Weidler's observations indicated that the BET-determined surface areas decreased with increasing heating time, but that the mean coherence lengths of the ferrihydrite particles were not affected significantly.[213] To index an additional peak at 2.7 Å observed in the X-ray powder pattern, Stanjek and Weidler adopted a cell with $c = \sim 14$ Å. It should be noted, however, that the 2.7 Å diffraction line is at the position assigned by Drits et al.[121,132] to ultradispersed hematite.

The ideas expressed by Stanjek and Weidler[213] concerning the thermal conversion of ferrihydrite are of particular interest in that they can be construed to coincide with the structural concept which was derived independently. The minimum-OH formula $Fe_{1.75}O_{2.26}(OH)_{0.74}$ of Stanjek and Weidler can be rewritten as $Fe_2[O_{2.58}(OH)_{0.85}]_{\Sigma 3.43} = Fe_2O_2[O_{0.58}(OH)_{0.42}] = Fe_2(O,OH)_3$, in which the sum of O = 2.58. Wolska[269] reported that the thermal dehydration of goethite led to the initial formation of $Fe_{1.6}(OH)O_2$, and subsequently to "hydroxyhematite", and then to hematite.[270,271] The initially formed compound was concluded to have the structure of hematite. Although the validity of "hydrohematite" has been questioned, if not refuted,[272] if for the present purposes the composition is rewritten as $Fe_{1.67}(OH)O_2 = Fe_2(OH)_{1.200}O_{2.395}$, the following comparisons ensue:

$$Fe_2[O_{2.58}(OH)_{0.85}]_{\Sigma 3.43} \quad \text{(Stanjek and Weidler[213])}$$

$$Fe_2[O_{2.395}(OH)_{1.200}]_{\Sigma 3.595} \quad \text{(Wolska[269])}$$

Thus, the compositions of the two phases, one with the structure of ferrihydrite and the other with the structure of hematite, are roughly similar. One could infer, therefore, that the composition at which ferrihydrite transforms to hematite is approximately $Fe_2O_{2.5}(OH)$. The formula of the end-member dehydrated ferrihydrite thus becomes $Fe_4O_5(OH)_2$, which is more appropriately generalized as $Fe_4O_4(O,OH)_3$. Upon any further loss of hydroxyl the structure converts to hematite. If the proportion of OH is high, as occurs under conditions in which polymerization increases and the ferrihydrite structure takes on a more goethite-like character, then conversion to goethite is facilitated. Neither the conversion to hematite nor that to goethite would be expected to be topotactic, but the O−OH adjustments apparently are greater to achieve the transformation to goethite than to hematite.

B. Aqueous Transformation

Johnston and Lewis[273] examined the conversion of ferrihydrite in solution at 92 °C and concluded that direct formation of hematite occurred in the experimental conditions used. It was noted, however, that at 85 °C the hematite was preceded by goethite and that at even lower temperatures the period of production of goethite was extended. The experimental temperature of 92 °C was, in essence, a selection to eliminate the formation of goethite.

The effect of pH on the transformation of ferrihydrite at 24 °C was reported by Schwertmann and Murad,[274] who observed that ferrihydrite converted to hematite at pH 7−8, whereas at straddling pH values the product was goethite. The effect was attributed to the availability of Fe(III) in solution; maximum activity of Fe(III) as $Fe(OH)_2^+$ and $Fe(OH)_4^-$ were calculated to be at pH 4 and pH 12, respectively, and it was at these pH values that maximum goethite abundances were achieved. Minimum activity of Fe(III) ions was near pH 8, coinciding with the most prolific development of hematite. These results were interpreted to be an indication that goethite formed from ferrihydrite by dissolution, thereby providing the Fe(III) ions, whereas hematite formed by internal rearrangement and dehydration within the ferrihydrite aggregates.

The preceding experiments by Schwertmann and Murad[274] were conducted at 24 °C. For alkaline media at 70 °C, Cornell and Giovanoli[196] observed that ferrihydrite transformed to goethite at pH 11.2−14, whereas at straddling pH values the product was a mixture of goethite and hematite. The "goethite-only" pH range was narrowed if the temperature was increased. Limited experiments also showed that the ionic strength of the solutions and the suspension concentration affected the reaction products. The morphology of goethite in such systems was concluded to be influenced by, above all, the pH of the system.[197,198]

Torrent et al.[275] used dried samples of ferrihydrite to determine the effect of relative humidity on ferrihydrite conversion. Although one might question whether it is appropriate to include their studies in a section that purports to deal with aqueous

transformations, it can be argued that the only variable being introduced is the activity of water. At 45 and 55 °C and relative humidities close to 100%, ferrihydrite was found to transform to hematite and goethite, but goethite development decreased at lower humidities and at the higher temperatures. Subsequent experiments by Torrent and Guzman[276] to determine the effect of water activity confirmed that, in the conversion of ferrihydrite, goethite needs the presence of water more than does hematite. These results were considered to support the concept of different pathways for the ferrihydrite → hematite and the ferrihydrite → goethite conversions, as was outlined in the preceding paragraph[274,277] and was elaborated upon by Combes et al.[129]

As noted by Manceau and Drits,[133] the conversion of Fe oxyhydroxides has been well-studied by solution chemistry; in alkaline media, the formation of goethite from ferrihydrite is thought to involve dissolution and reprecipitation, whereas conversion to hematite is thought to more closely simulate a solid-state rearrangement.[198,277,278] Manceau and Drits[133] concluded that for structural reasons, major reconstruction (solution−reprecipitation) was required to achieve the ferrihydrite → goethite transformation, but that the transformation to hematite also would require dissolution and reprecipitation:

> That the formation of hematite and goethite from ferrihydrite appears macroscopically to follow two different pathways can be accounted for by the fact that these two transformations differ in the extent to which the dissolution−reprecipitation process affects the ferrihydrite framework. This process would operate solely during the formation of goethite, whereas both dissolution and the solid-state transformation would take place during the formation of hematite (from ref 133).

C. Effects of Various Ions on the Aqueous Transformation of Ferrihydrite

The adsorption of various ions can drastically modify the properties of ferrihydrite. A notable example is the substantial increase in the temperature required to convert silica-bearing ferrihydrite to hematite. The presence of foreign ions in solution can also influence the kinetics of ferrihydrite transformation, thereby altering the proportions of the goethite and hematite end products, or initiating the crystallization of new end products such as lepidocrocite. For example, addition of the reducing organic ligand L-cysteine to ferrihydrite-bearing solutions at pH 6−6.5 and 25 or 70 °C not only accelerated the rate of transformation of ferrihydrite, but determined the conversion product. At pH 6 and 70 °C, a cysteine:Fe ratio of 0.1 in the system led to a conversion mixture of hematite and lepidocrocite, a ratio of 0.2 resulted in lepidocrocite with a trace of goethite, and a ratio of 0.4 resulted in goethite only.[279] At pH 7.5−9, cysteine:Fe ratios ≥ 0.2 rapidly converted ferrihydrite to goethite.[280] The results were considered to be significant in that all organic ligands studied previously had suppressed the transformation of ferrihydrite to goethite, which is in accord with the observations that organic compounds retard or inhibit the conversion of ferrihydrite in soils. These previous experiments, and others, are briefly summarized below. Numerous other references to the effects of organic compounds, particularly in soils, can be found in the papers cited; as well, the influence of inorganic ions on ferrihydrite conversion is commonly mentioned in papers whose focus is on the adsorptive properties of ferrihydrite.

Table 11. Extent and Products of the Conversion of Ferrihydrite in the Presence of Simple Ions and Molecules (L) (after ref 283)

	%		
species	goethite	hematite	ferrihydrite
control	97	3	0
lactate	95	5	0
L-tartrate	0	100	0
meso-tartrate	5	15	80
citrate	0	10	90
sucrose[a]	10	85	5
glucose	5	45	50
maltose	0	30	70
silicate	0	0	100
Al	95	5	0
Mn	100	0	0
control	100	0	0
silicate[b]	0	0	100
silicate[c]	40	10	50
Al	40	60	0
Mn[d]	95	0	0

[a] pH 10, L:Fe = 0.01. [b] L:Fe = 0.01. [c] pH 12, L:Fe = 0.2, 24 h. [d] Jacobsite = 5%.

1. Various Organic Anions

Hydroxyl carboxylic acids inhibit the crystallization of ferrihydrite in the pH range 9−11 in the order citric > *meso*-tartaric > L-tartaric ≫ lactic.[281] Oxalate also favors hematite crystallization over that of goethite,[277] and the same effect of hematite promotion occurs with simple sugars in the order maltose > glucose > sucrose.[282] Retardation of the transformation of ferrihydrite was attributed to adsorption, which impeded ferrihydrite aggregation and dissolution, limiting the release of ferric species into solution and creating conditions favorable for the nucleation of hematite. Thus, the presence of organic anions in the system usually leads to an increase in the proportion of hematite relative to goethite in the transformation product (Table 11). The retarding power of the organic species generally falls as the pH rises, and the retarding power also falls with decreasing concentrations of the interfering ion or molecule.

The aging of ferrihydrite in the presence of different amounts of acetate was monitored for two years, mainly by Mössbauer spectroscopy, using ferrihydrite powders that had been dried at 120 °C after washing with ammonium acetate solutions of different concentrations.[284] High acetate concentrations led to the crystallization of goethite, whereas hematite was formed at low levels. Thus, acetate was concluded to inhibit the crystallization of hematite in favor of goethite.

2. Ionic Environment

Crystallization of goethite and/or hematite from ferrihydrite was retarded more in sulfate systems

than in chloride or nitrate media, possibly because of sulfate adsorption onto the ferrihydrite surface.[276] Although goethite and hematite both formed in NaCl, KCl, LiCl, and $CaCl_2$ solutions, the proportion of goethite in all the tests was lower than that in water. The degree of transformation was highest for chloride solutions and was higher for Ca than for Mg or Na. Calcium and magnesium favored the crystallization of hematite over that of goethite. Thus, it was concluded that the ionic environment must modify the activity of water in saline environments, and this in turn affects the nature of the conversion of ferrihydrite. At relatively low water activities, development of hematite is favored over that of goethite.

3. Silicon

Incorporation of Si in ferrihydrite affects several of its properties, some to a notable extent. Silica variably increases or impedes ferrihydrite dissolution,[189,285] variably changes its surface area (Table 9[186]), and lowers its point of zero charge as the Si content increases.[210,286] The quality of the X-ray patterns has been observed to decrease with increased Si content[287] or to remain largely unaffected,[186] but the best patterns of natural material seem to be from siliceous varieties (Figure 4). In this regard, Soma et al.[288] and Vempati et al.[289] used XPS to determine the bonding of silica in both natural and synthetic ferrihydrite. For the five natural samples studied,[288] there was little evidence of bonding of the three-dimensional SiO_4 anion. The Fe:Si ratio determined by XPS was comparable to the analytical ratio in the bulk material, suggesting that the Si was dispersed throughout the material, presumably via Fe−O−Si bonding. In contrast, there was strong evidence that the XPS-determined Fe:Si ratio in the synthetic ferrihydrite studied was higher than the analytical ratio of the sample. The conclusion was that the level of Si adsorption was enhanced on the surface of the synthetic ferrihydrite, and that the Si was present as a SiO_4-type ion. The implication is that natural and synthetic ferrihydrites, having comparable analytical Si contents, could have markedly different levels of bulk Si incorporation. The infrared spectrum of ferrihydrite shows an increased intensity of Si−O−Fe bands as the Si content increases (Figure 14),[287,290,291] and one of the most impressive changes is the increase in temperature required to convert siliceous ferrihydrite to hematite by dry thermal transformation (Table 8).[146,189]

Increased Si concentrations in 0.0125 M ferric chloride solutions at pH 7 were observed by Schwertmann and Thalman[157] to increase the relative formation of ferrihydrite precipitates at the expense of lepidocrocite; when the oxide contained >1.45 wt % Si, lepidocrocite was no longer formed. The effect of decreasing pH was also to increase ferrihydrite at the expense of lepidocrocite; moreover, the uptake of Si from the same solution increased from 3.14 wt % at pH 7.5 to 4.35% at pH 5.0. A possible explanation for the transformation trend observed by Schwertmann and Thalman was provided by Karim,[292] who showed that partly oxidized Si-free iron chloride solutions initially crystallize as a green rust phase that is the precursor to lepidocrocite. When Si is present, however, the formation of the green rust precursor is inhibited, and ferrihydrite is the ultimate oxidation product.

The transformations of lepidocrocite[293,294] and ferrihydrite[210,253] to goethite are retarded by Si. Although Si hinders the nucleation of goethite, the effect is outweighed by the even stronger stabilizing action on ferrihydrite.[253] Dissolution and conversion of akaganéite are also retarded by Si, but to a lesser extent than the effect on ferrihydrite.[198,253]

The relative inhibiting power of Si on the transformation of ferrihydrite is shown in Table 12, and is schematically illustrated in Figure 22. The L(1) ions and molecules include Si, citrate, *meso*-tartrate, and maltose, as can be discerned from Table 11; examples in the L(2) group are sucrose and lactate, those in the L(3) group include L-tartrate and oxalate, and examples in the L(4) group are Al and Mn.[283]

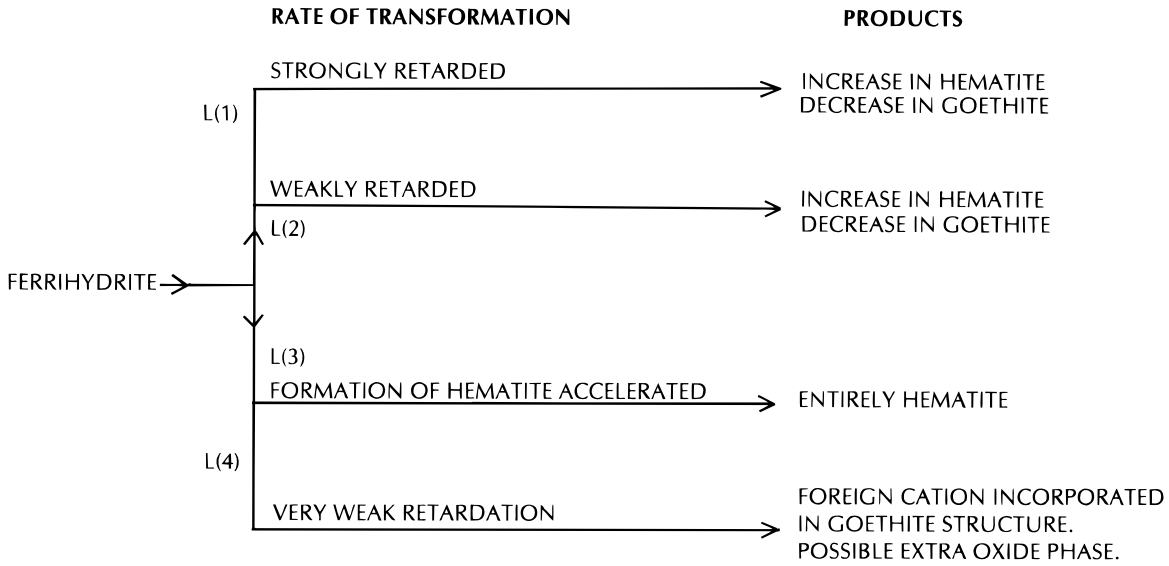

Figure 22. Schematic classification of the effects of ions and molecules (L = foreign species) on the kinetics and products of the transformation of ferrihydrite in alkaline media. (Adapted from ref 283.)

Table 12. Inhibitor Power of Silicate in the System Compared with That of Other Inhibitors[253]

	ferrihydrite untransformed after 24 h (%)	
species[a]	pH 11	pH 13
silicate	100	100
Al^{3+}	5	0
citrate	100	10
phosphate	100	25
maltose	100	100

[a] Concentration = 10^{-3} M, 70 °C.

In general, the presence of anions increases the proportion of hematite relative to goethite in the transformation product, and ligands that adsorb on ferrihydrite have a stronger effect than those that act only in solution.[283] Because slow dissolution favors the development of hematite over that of goethite, and because Si retards the transformation of ferrihydrite (Table 13), conversion of siliceous ferrihydrite to hematite rather than goethite is indirectly favored.

The remarkable effect of Si in elevating the temperature at which ferrihydrite converts to hematite has already been mentioned. Childs et al.[149] observed that it was possible to reduce the OH:Fe ratios of siliceous ferrihydrite to the order of 1:10 without an apparent phase change, and thus questioned the essentiality of H_2O and OH in the ferrihydrite structure. Feng et al.[93] and Zhao et al.[94] suggested that dehydroxylation of ferrihydrite improves its catalytic properties because H_2O adsorbs onto sites that are otherwise coordination-unsaturated. Adsorption of H_2O leads to particle linkages, and when this H_2O is evolved at elevated temperatures the small particles agglomerate, thereby facilitating the transformation to hematite. The coordination-unsaturated sites can therefore be considered as growth sites. If part of the H_2O is replaced by Si to form Fe−O−Si bonds, then particle linkages and ferrihydrite transformation would be retarded, as has been observed.

4. Germanium

Silicon- and germanium-bearing 7-line ferrihydrite precipitates were synthesized by Yoshinaga and Kanasaki,[147] who could detect no difference in the X-ray patterns of the two precipitate types even though the Fe:Si and Fe:Ge ratios were 10:1. Consequently, because the ionic radii for 6-fold-coordinated Si (0.40 Å) and Ge (0.53 Å) are so different, it was concluded that these elements must be adsorbed or surface-bonded rather than incorporated within the ferrihydrite structure. Heating of a Ge-bearing sample, comparable in Ge content to those synthesized by Yoshinaga and Kanasaki, showed that it transformed to hematite by 300 °C.[149]

5. Aluminum

The influence of Al on the formation of various iron oxides from Fe(II) chloride, sulfate, and carbonate solutions oxidized in air at pH 5.5−7 and 20 °C was investigated by Taylor and Schwertmann.[296] Formation of ferrihydrite was favored when the mol ratio of Al/(Al+Fe) exceeded 0.30, and lower ratios (0.09−0.30) inhibited the formation of lepidocrocite and maghemite in favor of goethite. That incorporation of Al in ferrihydrite stabilizes the mineral is evident from its DTA response; the exothermic peak temperature of 316 °C at zero Al was observed by Schwertmann et al.[297] to increase gradually with Al content, moving to 564 °C at 25 mol % added Al.

In their experiments on the effect of relative humidity on the transformation of ferrihydrite, Torrent et al.[276] determined that Al substitution in ferrihydrite caused a blockage in the formation of goethite, and also impeded the conversion to hematite. Incorporation of Al in ferrihydrite seems to stabilize the mineral,[298] and the reduced susceptibility to dissolution thereby kinetically favors the conversion of aluminous ferrihydrite to hematite rather than to goethite.[299,300] Ferrihydrite-derived synthetic hematite samples containing up to 18 mol % Al were described by Stanjek and Schwertmann.[301]

6. Soil Minerals

Suspensions of ferrihydrite and several soil-type minerals held at pH 7 and 40 °C for up to 210 days were found to affect the rate of conversion of ferrihydrite, which was to mixtures of goethite and hematite.[302] Crystallization of the iron oxides was retarded by deferrated soil clay > kaolinite > gibbsite > quartz, whereas muscovite accelerated the conversion. All substances except the soil clay had the effect of promoting hematite development over that of goethite, and it was thought that a template effect might have been the cause. Earlier experiments by Schwertmann[187] at different pH values and temperatures had also shown preferential crystallization of hematite, at least in part because the aluminum released by clay−mineral dissolution favored the formation of hematite over goethite. Schwertmann's experiments at 25 °C and pH 5 were terminated after 8.4 years,[187,303] at which time it was found that ferrihydrite conversion had been retarded by gibbsite, kaolinite, illite, and smectite, and had been blocked almost completely by allophane and a smectitic soil clay. The presence of the clay minerals had also resulted in higher ratios of hematite to goethite. The

Table 13. Effect of Different Ions on the Kinetics and Products of the Transformation of Ferrihydrite at pH 12.2 and 70 °C (after Cornell and Giovanoli, ref 295)

ion	[ion] (M)	induction time (h)	rate (min^{-1})	products
control	0	0.5	0.002	goethite
Al	10^{-3}	1.0	0.002	goethite
Al	2×10^{-3}	2.5	0.0035	goethite + hematite (10%)
Mn	10^{-3}	0.5	0.002	goethite
Si	4×10^{-4}	50.0	0.00016	goethite + hematite (15%)
Cu	10^{-3}	6.0	0.00030	hematite + goethite (3−5%)

conversion rate was inversely related to the final Si concentration in the solution. The extent of transformation was in the order: ferrihydrite control sample < gibbsite ≈ illite < kaolinite < smectite ≪ soil smectite < allophane ≈ aluminous ferrihydrite, with the last two completely blocking conversion.

7. Arsenic

Adsorption of arsenate while ferrihydrite is polymerizing interferes with the chain-building process, thereby retarding further polymerization and the transformation to hematite.[137,141] EXAFS As−Fe correlations indicated that arsenate adsorption on ferrihydrite is principally as an inner-sphere bidentate complex, but monodentate complexes also are present.[137,138]

8. Uranium

Manceau et al.[239] reported that the adsorption of uranyl ions (UO^{2+}) prevented the transformation of coprecipitated ferrihydrite. The results of EXAFS spectroscopy indicated that the high affinity of ferrihydrite for uranyl ions exists because these ions share edges with the $Fe(O,OH)_6$ octahedra, thus bonding to the surface functional groups of ferrihydrite as mononuclear bidentate inner-sphere complexes.[239] This type of surface bonding was confirmed by Waite et al.[142]

9. Ferrous Iron

The products of the air oxidation of $Fe^{II}-Fe^{III}$ chloride solutions at pH 6 and 7, at 20 and 60 °C, were investigated by Taylor and Schwertmann[304] to define the experimental conditions conducive for the precipitation of maghemite. Maghemite formation was determined to be favored by a slow oxidation rate, high total Fe concentration, the presence of small amounts of Fe(III) in the predominantly Fe(II) solution, higher temperatures, and the lower pH (6). At higher Fe(III) proportions, however, ferrihydrite was formed. The results were similar to those obtained earlier by Schwertmann and Thalman[157] in less extensive experiments.

Divalent transition-metal cations in concentrations in which, roughly, $M^{II}/Fe^{III} > 2$ have been shown to convert ferrihydrite to a spinel phase.[305−307] Tronc et al.[308] and Jolivet et al.[309] demonstrated that Fe(II) had the same effect, regardless of whether the $Fe^{II}-Fe^{III}$ phases were coprecipitated or Fe(II) was added after precipitation. When the ratio (x) of $Fe^{II}/Fe^{III} \geq 0.35$, a nonstoichiometric magnetite was formed; at $x = 0.10-0.33$ for the system, the magnetite phase coexisted with another spinel-type phase low in Fe(II), with $x \approx 0.07$. At the experimental conditions (pH 11, room temperature), ferrihydrite converted to goethite. The presence of Fe(II) accelerated the conversion, but at $x > 0.1$ only magnetite was formed.

10. Copper and Zinc

Cornell and Giovanoli[295] observed that the presence of Cu in alkaline media retarded the transformation of ferrihydrite (Figure 23) by hindering its dissolution. This in turn suppressed the formation of goethite, and at 9 mol % Cu concentration only cuprian hematite was formed. Higher Cu concentrations (9−23 mol %) led to the formation of cuprian hematite and cuprian magnetite (Table 14). Stabilization of ferrihydrite was far greater if Cu was coprecipitated with the ferrihydrite rather than added subsequently, thus suggesting some solid-solution incorporation by coprecipitation. With experimental conditions similar to those used to obtain the results for Cu, Cornell[305] determined that ferrihydrite containing 9 mol % Zn converted to a mixture of goethite and about 15% hematite. Upon the addition of 18 mol % Zn, the ferrihydrite converted to goethite, hematite, and spinel; at 23 mol % Zn the products were spinel and hematite. Both Cu and Zn extended the induction (nucleation) period and also retarded the subsequent conversion.

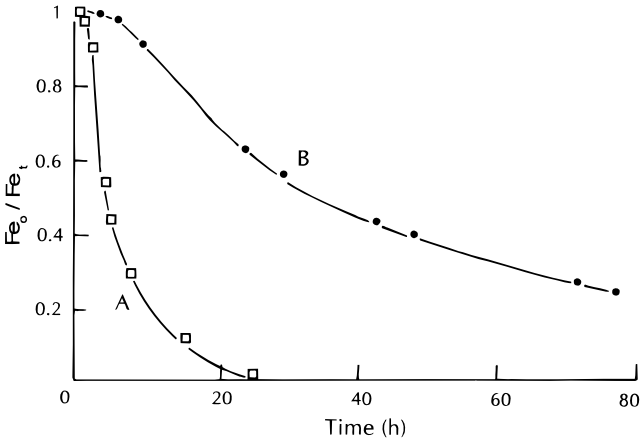

Figure 23. Fe_o/Fe_t (ferrihydrite/total Fe) as a measure of the degree of transformation of ferrihydrite into crystalline oxides vs time: (A) Cu absent, product goethite; (B) 10^{-3} M Cu coprecipitated with ferrihydrite, product Cu hematite. Conditions: pH 12.2, 70 °C. (Redrawn from ref 295.)

Table 14. Effect of Cu Concentration on the Transformation Products of Ferrihydrite at pH 12.2 and 70 °C (after Cornell and Giovanoli, ref 295)

Cu (M)	initial mol % Cu	product
0	0	goethite
1×10^{-4}	0.9	goethite
2.5×10^{-4}	2.43	goethite + hematite (30%)
5×10^{-4}	4.5	goethite + hematite (85%)
1×10^{-3}	9.09	hematite
2×10^{-3}	16.6	hematite + magnetite
3×10^{-3}	23.0	magnetite
5×10^{-2}	33.0	magnetite + tenorite
1×10^{-3} [a]	100.0	tenorite
1×10^{-3} [b]	9.09	hematite (60%) + goethite
1×10^{-3}	9.09	hematite (55%) + goethite
1×10^{-3} + 1×10^{-3} Mn[c]	9.09	hematite (95%) + goethite

[a] 6% goethite seed added. [b] Cu added to ferrihydrite. [c] Cu−Mn ferrihydrite coprecipitate.

11. Manganese

Goethite containing up to 15 mol % Mn can be formed from ferrihydrite in alkaline solutions containing divalent Mn.[310] The effects of pH, Mn concentration, and the initial source of the Mn are summarized in Table 15. Manganese, in general,

Table 15. Effect of pH, Mn Concentration, and Source of the Mn on the Transformation Products of Ferrihydrite[a] (after Cornell and Giovanoli, ref 310)

		pH					
[Mn] (M)	x[b]	8	10	11	12	13	14
0	0	Hm, g	Hm, g	G, Hm	G	G	G
				Manganese (II) Nitrate			
1.5×10^{-3}	0.15	Hm, g	G, hm	G	G	G	G
1.9×10^{-3}	0.18		G, hm	G, j	G, j	G, j	
4.4×10^{-3}	0.30		J, G	J, G	J, G	J, G	
1.0×10^{-2}	0.50	G, j		J, g	J, g	J, g	J, g
				Manganese (III) Acetate			
1.5×10^{-3}	0.15				G	G	
4.4×10^{-3}	0.30				G, 7-Å phase		
1.0×10^{-2}	0.50				G, ha, 7-Å phase		
				Manganese (II) Oxalate			
1.5×10^{-3}	0.15	Hm		G	G		
1.0×10^{-2}	0.50	Hm		G, J, Ha	J, Ha, g		

[a] Abbreviations: G, g = goethite; J, j = jacobsite; Hm, hm = hematite; Ha, ha = hausmannite; 7-Å phase = 7-Å phyllomanganate. Capital letter indicates dominant phase, lower case letter indicates minor phase. [b] x = Mn/(Mn + Fe) in the system.

Table 16. Effect of the Concentration of Co and the Order of Precipitation on the Transformation Products of Ferrihydrite at pH 12 and 70 °C (after Cornell and Giovanoli, ref 311)

method of precipitation	mol % Co added	product
Co + Fe coprecipitated	0	Co goethite
	0.9	Co goethite
	4.5	Co goethite
	9.0	Co goethite
	18.0	Co goethite + some Co magnetite
	23.0	Co magnetite
	33.0	Co magnetite
	50.0	Co magnetite
Co added to ferrihydrite	9.0	Co goethite
	23.0	Co goethite + trace Co magnetite
	33.0	Co goethite + trace Co magnetite
Co^{2+} solution alone	100.0	Co_3O_4 + CoOOH

suppressed the formation of hematite, but at low concentrations of Mn(II) in the system there was little retardation effect on the transformation of ferrihydrite. At sufficiently high levels of Mn, the Mn analogue of magnetite (jacobsite) was formed.

12. Cobalt

Transformation of ferrihydrite to more crystalline oxides is retarded by Co, which stabilizes ferrihydrite against dissolution.[311] The effects of Co concentration and the method of Co (i.e., cobalt) precipitation are summarized in Table 16. No hematite formed at pH >11.5, but at lower pH values the formation of goethite was suppressed relative to that of hematite or magnetite.

13. Manganese–Cobalt–Nickel

Metal−ferrihydrite coprecipitates simultaneously containing Mn, Co, and Ni converted to goethite at pH 12 and 70 °C.[306] The metal/(Fe + metal) mole fractions were up to 0.13 for mixtures of the three substituting ions, and 0.165 for two substituting ions. Because the conversion of ferrihydrite to goethite involves a solution−reprecipitation process, the soluble metal species can be readsorbed on the remaining ferrihydrite; readsorption was observed to be in the order Ni ≫ Co > Mn. Conversion of the enriched residual (10−15%) ferrihydrite was retarded, and the final stages of the transformation to goethite were extended over weeks.

Table 17. Products of Crystallization of Ferrihydrite Coprecipitated with Different Levels of Divalent Ions at pH 12, 70 °C, and 50 Days Aging[307]

		product upon addition of [a]		
ion	radius (Å)	9 mol %	18 mol %	33 mol % metal
control		G	G	G
Mn^{2+}	0.82	G	G + S	S + G
Co^{2+}	0.74	G	G + S	S
Ni^{2+}	0.69	G	G + S	α-3Ni(OH)$_2$·2H$_2$O + S
Cu^{2+}	0.73	H	H + S	S + CuO
Zn^{2+}	0.74	G + H	H + S	S

[a] Abbreviations: G, goethite; H, hematite; S, spinel.

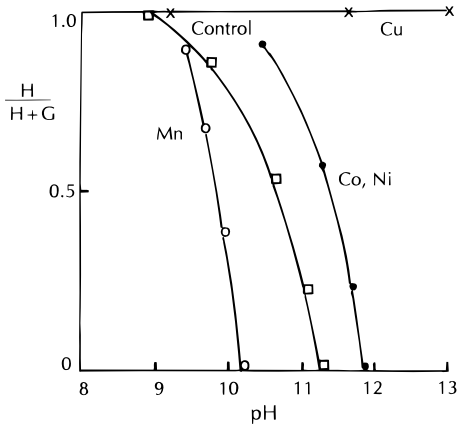

Figure 24. Effect of pH and the nature of M^{2+} on the proportions of goethite (G) and hematite (H) in the crystallization product of metal-bearing ferrihydrite. (Redrawn from ref 307.)

The influences of divalent Mn, Co, Ni, Cu, and Zn on the crystallization products formed from ferrihydrite were reviewed by Giovanoli and Cornell.[307] The effects of the various metals are summarized in Table 17, which shows clearly that the products are dependent on the concentration of the metal, and on the pH of the system (Figure 24). Copper and Zn have the strongest influence in forming hematite, and

Mn is the least effective. The kinetics of ferrihydrite transformation are altered, with metals (M) usually extending the induction period and, except for Mn, retarding the conversion (recrystallization) process. Retardation increased with increased amounts of M, but the effects were apparent even at levels as low as 2 mol % M.

14. Molybdenum

Ferrihydrite used as a catalyst in coal liquefaction is less than ideal because at high temperatures it does not maintain its dispersion, but quickly agglomerates during its transformation to hematite. The presence of adsorbed Mo inhibits the crystallization of hematite, thus maintaining the ferrihydrite dispersion.[95] EXAFS results indicated that Mo is probably chemisorbed at coordination-unsaturated sites, probably in tetrahedral coordination as MoO^{2-}, but with no extensive coordination shells beyond the nearest oxygen shell.

15. Gold

The transformation of ferrihydrite to goethite is retarded in the presence of colloidal gold at pH 7.[312,313] It is thought that the dissolution−reprecipitation step in the formation of goethite is slowed because goethite nuclei are adsorped at the surface of the gold colloids, thus slowing goethite growth. The transformation of ferrihydrite to hematite involves a less extensive dissolution−reprecipitation mechanism; hence, the formation of hematite is not affected. Some gold combines with ferrihydrite as Au(III), but whether the effect is through electrostatic interactions or specific bindings is not known.[314]

X. Conclusions

Although ferrihydrite is of considerable importance in metallurgical processing and in the natural environment, often its presence is greatly underestimated because of the difficulty in its definitive identification and because of its common designation as amorphous iron hydroxide, colloidal ferric hydroxide, $Fe(OH)_3$, etc. Nevertheless, ferrihydrite has been identified as a preterrestrial component of meteorites, and may be a constituent of the soils of Mars. On Earth, ferrihydrite occurs widely in natural waters, in the sediments derived from these waters, and is a constituent of a wide variety of soils, especially those formed rapidly under cool and moist conditions. Ferrihydrite is abundantly present, although difficult to identify, in sulfide oxidation products and in the precipitates resulting from acid mine drainage. Ferrihydrite is believed to be the dominant constituent of some metallurgical processing residues, but this conclusion requires direct confirmation. In all its occurrences, ferrihydrite precipitation controls the level of dissolved iron in solution and also regulates the concentration and distribution of a host of impurity species.

Ferrihydrite is generally classified according to the number of X-ray diffraction lines that the material gives: typically "2-line" ferrihydrite for material that exhibits little crystallinity and "6-line" ferrihydrite for that which is best crystallized. Several models of the structure of ferrihydrite have been developed, and the tempo of proposals has increased in the past few years. In one model, ferrihydrite consists of three components: (1) a defect-free structure, which has ordered, three-dimensional anion packing, (2) a defective structure in which the anion packing is nonperiodic, and (3) ultradispersed hematite. Dimensions of the coherent scattering domains in 2-line ferrihydrite are 10−20 Å, whereas much larger domains (40−60 Å) are characteristic of 6-line ferrihydrite. In another structure that was derived largely from the results of EXAFS spectroscopy, the fundamental units consist of microdomains of goethite. However, it was subsequently observed, also from EXAFS spectroscopy, that although the Fe−O bond lengths in ferrihydrite have their greatest similarity to those of goethite, the Fe−Fe bond distances are similar to those of akaganéite rather than goethite. Accordingly, it was concluded that the FeO_6 polyhedra in ferrihydrite must be systematically different from those in goethite. Nevertheless, the structures of goethite, akaganéite, and ferrihydrite are similar in that all consist of edge-sharing Fe octahedra cross-linked by double corners to form chains. In ferrihydrite, however, the length of the chains is extremely short, thereby resulting in a tremendous increase in chain terminations and in a commensurate increase in unshared sites available for adsorption.

Because the structure of ferrihydrite has not been incontrovertibly solved, the composition of the mineral remains enigmatic. The widely accepted nominal formula of ferrihydrite, $5Fe_2O_3{\cdot}9H_2O$, seems to be excessively hydrous. Ferrihydrite with adsorbed Si or Ge and a negligibly small OH content is known, and an arsenate-bearing ferrihydrite having the composition $Fe_{0.206}As_{0.139}O_{0.655}H_{0.000}$ has been synthesized. If the nominal formula of ferrihydrite is recast to a hematite-like form, the result is $Fe_2O_3{\cdot}1.8H_2O$. The calculated formula for one ordered ferrihydrite is $Fe_{0.282}O_{0.521}H_{0.197}$; when recast to the hematite-like form as above, this becomes $Fe_2O_3{\cdot}0.70H_2O$, which is a substantial decrease in water content. If the goethite-like structural units proposed for ferrihydrite are valid, the adopted density of 3.1−3.3 g/cm^3 seems to be rather low in comparison with the densities of goethite and lepidocrocite, both of which are in the range 4.0−4.2 g/cm^3. If the formula for goethite is used as an initial model for ferrihydrite, then the cell dimensions derived for "ordered" ferrihydrite (a = 2.96, c = 9.40 Å) yield a calculated density of 4.14 g/cm^3 for FeOOH and two formula weights per unit cell (Z = 2). For defective ferrihydrite, a cell with a = 5.126, c = 4.70 Å was calculated, which gives D_{calc} = 4.14 g/cm^3 for Z = 6, which is an appropriate Z value for a hexagonal cell. One could assume, therefore, that the periodic and nonperiodic phases correspond to hexagonal or pseudohexagonal units. Taking into account the possibility of excessive, nonessential water in the formula for ferrihydrite, it could be further speculated that the formula is of the type $FeO[(O,OH)_{1-x}\square_x]$ or FeO(O,OH). At the extreme, the latter would correspond to FeO-

($O_{0.5}\square_{0.5}$), yielding a density of 3.72 g/cm^3. The extreme composition corresponds to that of hematite or maghemite, so presumably the transformation from ferrihydrite would already have taken place. Intermediate compositions, however, would contain some OH, and would yield calculated densities between 3.72 and 4.14 g/cm^3. It is interesting to note that a density of 3.96 g/cm^3 was obtained by Towe and Bradley for ferrihydrite.

In the laboratory, 2-line ferrihydrite is prepared by rapid oxidation of Fe(II) solutions, or by rapid neutralization of Fe(III) solutions. The more crystalline 6-line variety of ferrihydrite forms by hydrolysis of Fe(III) solutions, typically at elevated temperature and low pH. Precipitation is initially accompanied by a rapid pH change, which slows after the first hour; aging for 2−4 h is necessary to stabilize the suspensions.

Because of their variable X-ray diffraction patterns and chemical compositions, both synthetic and natural ferrihydrites generally must be characterized using a variety of complementary techniques. Infrared spectroscopy is useful for identifying ferrihydrite and helping to differentiate it from the similar mineral, schwertmannite. Differential dissolution techniques help to separate ferrihydrite from a number of similar iron compounds, whereas both Mössbauer spectroscopy and TG-DTA analyses provide complementary and confirmatory evidence. It would, however, be useful to develop a single definitive characterization procedure for ferrihydrite.

The large surface area (>340 m^2/g) and high reactivity of ferrihydrite make it an important adsorbent of trace metals, anions, and organic species in both surface and groundwater systems. A wide range of metal ions has been adsorbed, commonly in amounts up to 10% of the dry mass of the ferrihydrite. The mechanism by which various metals bind to ferrihydrite has been examined by EXAFS spectroscopy. In many instances, the metal ions adsorb as inner-sphere complexes that are edge-linked to the $Fe(O,OH)_6$ octahedra of ferrihydrite. Ferrihydrite also adsorbs most of the common anions; the oxygens in the anion bond to the surface OH groups in the ferrihydrite. The adsorption of several percent of Si or P has been demonstrated, and in all instances the extent of species adsorption depends strongly on the concentration and pH of the solution. Adsorption on ferrihydrite helps to control the migration of a number of species in the environment.

The dry thermal transformation of ferrihydrite proceeds at <400 °C to either hematite or goethite. Fine particle sizes lead to direct hematite formation, whereas coarser material initially generates goethite. The presence of adsorbed species increases the transformation temperature; for example, 25 mol % Si in ferrihydrite elevates the transformation to 800 °C. The aqueous transformation of ferrihydrite is complex and depends on the temperature, pH, and the presence of various cations, anions, and organic species in the reaction slurry. Two different reaction pathways have been identified: a dissolution−reprecipitation mechanism for the transformation to goethite, and a dissolution−solid state transformation process to hematite. Generally, higher temperatures favor the transformation of ferrihydrite to hematite, but the reaction is dependent on the pH of the slurry. The presence of organic species usually leads to an increase in the relative proportions of hematite to goethite in the transformation slurry, and it is believed that the organic species adsorb on the ferrihydite, thereby retarding its dissolution and subsequent reprecipitation. Inorganic anions and cations also favor the transformation to hematite, and the effect is related to adsorption on ferrihydrite that retards its dissolution. Both phosphate and silica adsorb extensively, and both species signficantly stabilize ferrihydrite to aqueous transformation.

XI. Acknowledgments

M. Baker of the Waterloo Centre for Groundwater Research, and Dr. F. J. Wicks of the Royal Ontario Museum garnered several articles for the study, most of them through inter-library services. Dr. J. M. Bigham of The Ohio State University provided reprints, and generously granted permission to use information from a paper which was in press when preparaton of this review began. The authors are indebted to CANMET staff member L. Paquette for assistance in the preparation of the manuscript.

XII. References

(1) Chen, T. T.; Cabri, L. J. In *Iron Control in Hydrometallurgy*; Dutrizac, J. E., Monhemius, A. J., Eds.; Ellis Horwood; Chichester, 1986; p 19.
(2) Dutrizac, J. E. In *Lead−Zinc−Tin '80*; Cigan, J. M., Mackey, T. S., O'Keefe, T. J., Eds.; Metall. Soc. AIME; Warendale, PA, 1979; p 532.
(3) Dutrizac, J. E.; Chen, T. T.; Longton, R. J. *Metall. Trans.* **1996**, *27B*, 567.
(4) Towe, K. M.; Bradley, W. F. *J. Colloid Interface Sci.* **1967**, *24*, 384.
(5) Chukhrov, F. V.; Zvyagin, B. B.; Gorshkov, A. I.; Yermilova, L. P.; Rudnitskaya, E. S. *Izvest. Akad. Nauk SSSR* (*Geol Ser.*) **1971**, *1*, 3 (in Russian) .
(6) Chukhrov, F. V.; Zvyagin, B. B.; Yermilova, L. P.; Gorshkov, A. I. In *Proc. Int. Clay Conf., Madrid* **1972**, *1*, 397. (In ref 7).
(7) Schwertmann, U.; Fischer, W. R. *Geoderma* **1973**, *10*, 237.
(8) Childs, C. W. *Zeits. Pflanzenernär. Bodenk.* **1992**, *155*, 441.
(9) Fleischer, M.; Chao, G. Y.; Kato, A. *Am. Mineral.* **1975**, *60*, 485.
(10) Chukhrov, F. V.; Zvyagin, B. B.; Gorshkov, A. I.; Yermilova, L. P.; Balashova, V. V. *Int. Geol. Rev.* **1973**, *16*, 1131.
(11) Post, J. E.; Buchwald, V. F. *Am. Mineral.* **1991**, *76*, 272.
(12) Schwertmann, U. In *Soil Color*; Bigham, J. M., Ciolkosz, E. J., Eds.; Soil Sci. Am. Special Pub. 31; SSSA: Madison, WI, 1993; p 51.
(13) Schwertmann, U.; Cornell, R. M. *Iron Oxides in the Laboratory*; VCH: New York, 1991, 137 pp.
(14) Birch, W. D.; Pring, A.; Reller, A.; Schmalle, H. W. *Naturwissenschaften* **1992**, *79*, 509.
(15) Birch, W. D.; Pring, A.; Reller, A.; Schmalle, H. W. *Am. Mineral.* **1993**, *78*, 827.
(16) McCammon, C. A.; de Grave, E.; Pring, A. *J. Magn. Magn. Mater.* **1996,** *152*, 33.
(17) McCammon, C. A.; Pring, A.; Keppler, H.; Sharp, T. *Phys. Chem. Miner.* **1995**, *22*, 11.
(18) Tomeoka, K.; Buseck, P. R. *Meteoritics* **1986**, *21*, 526.
(19) Tomeoka, K.; Buseck, P. R. *Geochim. Cosmochim. Acta* **1988**, *52*, 1627.
(20) Keller, L. P.; Buseck, P. R. *Geochim. Cosmochim. Acta* **1990**, *54*, 1155.
(21) Brearley, A. J. *Geochim. Cosmochim. Acta* **1989**, *53*, 2395.
(22) Brearley, A. J.; Prinz, M. *Geochim. Cosmochim. Acta* **1992**, *56*, 1373.
(23) Bishop, J. L.; Pieters, C. M.; Burns, R. G. *Geochim. Cosmochim. Acta* **1993**, *57*, 4583.
(24) Bishop, J. L.; Pieters, C. M.; Burns, R. G.; Edwards, J. O.; Mancinelli, R. L.; Froeschl, H. *Icarus* **1995**, *117*, 101.

(25) Morris, R. V.; Golden, D. C.; Bell, J. F. iii; Lauer, H. V., Jr.; Adams, J. B. *Geochim. Cosmochim. Acta* **1993**, *57*, 4597.
(26) Tipping, E.; Woof, C.; Cooke, D. *Geochim. Cosmochim. Acta* **1981**, *45*, 1411.
(27) Fortin, D.; Leppard, G. G.; Tessier, A. *Geochim. Cosmochim. Acta* **1993**, *57*, 4391.
(28) Manning, P. G.; Lum, K. R.; Birchall, T. *Can. Mineral.* **1983**, *21*, 121.
(29) Manning, P. G.; Lum, K. R.; Kwong, H. K. T.; Birchall, T. *Can. Mineral.* **1985**, *23*, 103.
(30) Manning, P. G.; Murphy, T. P.; Prepas, E. E. *Can. Mineral.* **1991**, *29*, 77.
(31) Childs, C. W.; Downs, C. J.; Wells, N. *Austral. J. Soil Res.* **1982**, *20*, 119.
(32) Schwertmann, U.; Carlson, L.; Murad, E. *Clays Clay Miner.* **1987**, *35*, 297.
(33) Carlson, L.; Schwertmann, U. *Water Res.* **1987**, *21*, 165.
(34) Fuller, C. C.; Davis, J. A. *Nature* **1989**, *340*, 52.
(35) Cho, B.; Fujita, K.; Oda, K.; Ino, H. *Nucl. Instrum. Methods Phys. Res.* **1993**, *B76*, 415.
(36) Tuhela, L.; Carlson, L.; Tuovinen, O. H. *Water Res.* **1992**, *26*, 1159.
(37) Childs, C. W.; Matsue, N.; Yoshinaga, N. *Clay Sci.* **1990**, *8*, 9.
(38) Schwertmann, U.; Friedl, J. *Neues Jahrb. Mineral. Monatsch.* **1998**, 63.
(39) Ivarson, K. C.; Sojak, M. *Can. J. Soil Sci.* **1978**, *58*, 1.
(40) Henmi, T.; Wells, N.; Childs, C. W.; Parfitt, R. L. *Geochim. Cosmochim. Acta* **1980**, *44*, 365.
(41) Chukhrov, F. V. *Chem. Geol.* **1973**, *12*, 67.
(42) Canfield, D. *Geochim. Cosmochim. Acta* **1989**, *53*, 619.
(43) Murad, E.; Schwertmann, U. *Am. Mineral.* **1988**, *73*, 1395.
(44) Xiao, Xuqi; Guo, Lihe *Yanshi Kuangwuxue Zashi* **1997** *16*, 255−259 (in Chinese); *Chem. Abstr.* **1998**, *128*, 77691v.
(45) Dill, H. G.; Siegfanz, G.; Marchig, V. *Mar. Georesour. Geotechnol.* **1994**, *12*, 159.
(46) Marumo, K. *Kobutsugaku Zasshi* **1996**, *25*, 198−210; *Chem. Abstr.* **1997**, *126*, 133618z.
(47) Stoffers, P.; Glasby, G. P.; Stüben, D.; Renner, R. M.; Pierre, T. G.; Webb, J.; Cardile, C. M. *Mar. Georesour. Geotechnol.* **1993**, *11*, 45.
(48) Brown, D. A.; Kamineni, D. C.; Sawicki, J. A.; Beveridge, T. J. *Appl. Environ. Microbiol.* **1994**, *60*, 3182.
(49) Sawicki, J. A.; Brown, D. A.; Beveridge, T. J. *Can. Mineral.* **1995**, *33*, 1.
(50) Brown, D. A.; Gross, G. A.; Sawicki, J. A. *Can. Mineral.* **1995**, *33*, 1321.
(51) Jackson, T. A.; Keller, W. D. *Am. J. Sci.* **1970**, *269*, 446.
(52) Johnson, M. G.; McBride, M. B. *Soil Sci. Am. J.* **1989**, *53*, 482.
(53) Kodama, H.; Wang, C. *Soil Sci. Soc. Am. J.* **1989**, *53*, 526.
(54) Shoji, S.; Yamada, H.-O. *Soil Sci.* **1991**, *152*, 162.
(55) Parfitt, R. L.; Saigusa, M.; Eden, D. N. *J. Soil Sci.* **1984**, *35*, 625.
(56) Michalet, R.; Guillet, B.; Souchier, B. *Clay Miner.* **1993**, *28*, 233.
(57) Schwertmann, U.; Murad, E. *Clay Miner.* **1988**, *23*, 291.
(58) De Geyter, G.; Vandenberghe, R. E.; Verdoncke, L.; Stoops, G. *Neues Jahrb. Mineral. Abh.* **1985**, *153*, 1.
(59) Torrent, J.; Schwertmann, U.; Barrón, V. *Clays Clay Miner.* **1992**, *40*, 14.
(60) Birnie, A. C.; Paterson, E. *Geoderma* **1991**, *50*, 219.
(61) Fitzpatrick, R. W.; Naidu, R.; Self, P. G. In *Biomineralization Processes of Iron and Manganese*: *Modern and Ancient Environments*; Skinner, H. C. W., Fitzpatrick, R. W., Eds.; Catena Supplement 21; Catena-Verlag: Cremlingen-Destedt, 1992; p 263.
(62) Johnston, J. H.; Cardile, C. M.; Coote, G. E.; Sparks, R. J.; Wallace, G.; McMillan, J. W.; Pummery, F. C.; Longworth, G. *Chem. Geol.* **1984**, *42*, 189.
(63) Schwertmann, U. In *Iron in Soils and Clay Minerals*; Stucki, J. W., Goodman, B. A., Schwertmannn, U., Eds.; NATO-ASI Ser. 217; D. Reidel: Dordrecht, 1988; p 267.
(64) Campbell, A. S.; Schwertmann, U. *J. Soil Sci.* **1984**, *35*, 569.
(65) Kassim, J. K.; Gafoor, S. M.; Adams, W. A. *Clay Miner.* **1984**, *19*, 99.
(66) Fitzpatrick, R. W. In *Iron in Soils and Clay Minerals*; Stucki, J. W., Goodman, B. A., Schwertmann, U., Eds.; NATO-ASI Ser. 217 D. Reidel: Dordrecht,1988; p 351.
(67) Arnalds, O.; Hallmark, C. T.; Wilding, L. P. *Soil Sci. Soc. Am. J.* **1995**, *59*, 161.
(68) Wang, H. D.; White, G. N.; Turner, F. T.; Dixon, J. B. *Soil Sci. Soc. Am. J.* **1993**, *57*, 1381.
(69) Parfitt, R. L. *J. Soil Sci.* **1989**, *40*, 359.
(70) Schwertmann, U. In *Advances in Soil Science*; Stewart, B. A., Ed.; Springer-Verlag: New York, 1985; Vol. 1, p 171.
(71) Bartoli, F.; Philippy, R.; Rotal, J. M.; Gerard, B. *J. Soil Sci.* **1992**, *43*, 47.
(72) Bartoli, F.; Philippy, R.; Burtin, G. *J. Soil Sci.* **1992**, *43*, 59.
(73) Jones, A. A.; Saleh, A. M. *Mineral. Magn.* **1987**, ***51***, 87.
(74) Bigham, J. M.; Schwertmann, U.; Carslon, L.; Murad, E. *Geochim. Cosmochim. Acta* **1990**, *54*, 2743.
(75) Bigham, J. M.; Schwertmann, U.; Carlson, L. In *Biomineralization Processes of Iron and Manganese*: *Modern and Ancient Environments*; Skinner, H. C. W., Fitzpatrick, R. W., Eds.; Catena Supplement 21; Catena-Verlag: Cremlingen-Destedt, 1992; p 219.
(76) Hudson-Edwards, K. A.; Macklin, M. G.; Curtis, C. D.; Vaughan, D. J. *Environ. Sci. Technol.* **1996**, *30*, 72.
(77) Airey, P. L. *Chem. Geol.* **1986**, *55*, 255.
(78) Payne, T. E.; Davis, J. A.; Waite, T. D. *Radiochim. Acta* **1994**, *66/67*, 297.
(79) Brown, L. J.; Gutsa, E. H.; Cashion J. D.; Fraser, J. R.; Coller, B. A. W. *Hyperfine Interact.* **1990**, *57*, 2159.
(80) Jambor, J. L. In *Environmental Geochemistry of Sulfide Mine-wastes*; Jambor, J. L., Blowes, D. W., Eds. *Short Course Handb. Mineral. Assoc. Can.* **1994**, *22*, 59.
(81) Jambor, J. L. *Natural Resources Canada, CANMET Report* **1987**, *MSL 87−97* (*IR*).
(82) Jambor, J. L.; Owens, D. R. *Natural Resources Canada, CAN-MET Report* **1993**, *94−4* (*CF*).
(83) Milnes, A. R.; Fitzpatrick, R. W.; Self, P. G.; Fordham, A. W.; McClure, S. G. In *Biomineralization Processes of Iron and Manganese*: *Modern and Ancient Environments*; Skinner, H. C. W., Fitzpatrick, R. W., Eds.; Catena Supplement 21; Catena-Verlag: Cremlingen-Destedt, 1992; p 233.
(84) Ferris, F. G.; Tazaki, K.; Fyfe, W. S. *Chem. Geol.* **1989**, *74*, 321.
(85) Johnson, C. A. *Geochim. Cosmochim. Acta* **1986**, *50*, 2433.
(86) Mann, H.; Fyfe, W. S. *Can. J. Earth Sci.* **1989**, *26*, 2731.
(87) Bowell, R. J.; Bruce, I. *Appl. Geochem.* **1995**, *10*, 237.
(88) Karanthanasis, A. D.; Thompson, Y. L. In *Proc. Int. Conf. Abatement Acidic Drainage* Montreal, Canada.; MEND, Natural Resources Can.; **1991**, *2*, 485.
(89) Karanthanasis, A. D.; Thompson, Y. L. *Soil Sci. Soc. Am. J.* **1995**, *59*, 1771.
(90) Misawa, T.; Hashimoto, K.; Shimodaira, S. *Corros. Sci.* **1974**, *14*, 131.
(91) Music, S.; Gotic, M.; Popovic, S. *J. Mater. Sci.* **1993**, *28*, 5744.
(92) Jaén, J. A.; Aceveda, E.; González, M. *Hyperfine Interact.* **1994**, *88*, 59.
(93) Feng, Z.; Zhao, J.; Huggins, F. E.; Huffman, G. P. *J. Catal.* **1993,** *143*, 510.
(94) Zhao, J.; Feng, Z.; Huggins, F. E.; Huffman, G. P. *Energy Fuels* **1994**, *8*, 38.
(95) Zhao, J.; Feng, Z.; Huggins, F. E.; Shah, N.; Huffman, G. P.; Wender, I. *J. Catal.* **1994**, *148*, 194.
(96) Zhao, J.; Huggins, F. E.; Feng, Z.; Huffman, G. P. *Clays Clay Miner.* **1994**, *42*, 737.
(97) Zhao, J.; Huggins, F. E.; Feng, Z.; Lu, F.; Shah, N.; Huffman, G. P. *J. Catal.* **1993**, *143*, 499.
(98) Hawkins, C.; Williams, J. M.; Hudson, A. J.; Andrews, S. C.; Traffry, A. *Hyperfine Interact.* **1994**, *91*, 827.
(99) Schwertmann, U.; Taylor, R. M. In *Minerals in Soil Environments*; Dixon, J. B., Weed, S. B., Eds.; Soil Sci. Soc. Am.: Madison, WI, 1977; p 145.
(100) Erel, Y.; Morgan, J. J. *Geochim. Cosmochim. Acta* **1992**, *56*, 4157.
(101) Coston, J. A.; Fuller, C. C.; Davis, J. A. *Geochim. Cosmochim. Acta* **1995**, *59*, 3535.
(102) Davis, D. B.; Kent, D. B. In *Mineral-Water Interface Geochemistry*; Hochella, M. F., White, A. F., Eds. *Rev. Mineral.* **1990**, *23*, 177.
(103) Belzile, N.; Tessier, A. *Geochim. Cosmochim. Acta* **1990**, *54*, 103.
(104) Biber, M. V.; Dos Sabtis Afonso, M.; Stumm, W. *Geochim. Cosmochim. Acta* **1994**, *58*, 1999.
(105) Kimball, B. A.; Callender, E.; Axtmann, E. V. *Appl. Geochem.* **1995**, *10*, 285.
(106) McKnight, D. M.; Kimball, B. A.; Bencala, K. E. *Science* **1988**, *240*, 637.
(107) Waite, T. D.; Torikov, A. *J. Colloid Interface Sci.* **1987**, *119*, 228.
(108) Waite, T. D.; Morel, F. M. M. *Environ. Sci. Technol.* **1984**, *18*, 860.
(109) Moffett, J. W.; Zika, R. G. *Environ. Sci. Technol.* **1987**, *21*, 804.
(110) Finden, D. A. S.; Tipping, E.; Jaworski, G. H. M.; Reynolds, C. S. *Nature* **1984**, *309*, 783.
(111) Wells, M. L.; Mayer, M. *Deep-Sea Res.* **1991**, *39*, 1379.
(112) Wells, M. L.; Mayer, L. M.; Donard, O. F. X.; de Souza Sierra, M. M.; Ackelson, S. G. *Nature* **1991**, *353*, 248.
(113) Miles, C. J.; Brezonik, P. L. *Environ. Sci. Technol.* **1981**, *15*, 1089.
(114) Millero, F. J.; Sotolongo, F. J. *Geochim. Cosmochim. Acta* **1989**, *53*, 1867.
(115) Waychunas, G. A. In *Oxide Minerals*: *Petrologic and Magnetic Significance*; Lindsley, D. H., Ed. *Rev. Mineral.* **1991**, *25*, 11.
(116) Murray, J. W. In *Marine Minerals*; Burns, R. G., Ed. *Rev. Mineral.* **1979**, *6*, 47.
(117) Van der Giessen, A. A. *J. Inorg. Nucl. Chem.* **1966**, *28*, 2155.
(118) Atkinson, R. J.; Posner, A. M.; Quirk, J. P. *J. Inorg. Nucl. Chem.* **1968**, *30*, 2371.
(119) Harrison, P. M.; Fischbach, F. A.; Hoy, T. G.; Haggis, G. H. *Nature* **1967**, *216*, 1188.
(120) Brady, G. W.; Kurkjian, C. R.; Lyden, E. F. X.; Robin, M. B.; Saltman, P.; Spiro, T.; Terzis, A. *Biochemistry* **1968**, *7*, 2185.

(121) Drits, V. A.; Sakharov, B. A.; Salyn, A. L.; Manceau, A. *Clay Miner.* **1993**, *28*, 185.
(122) Russell, J. L. *Clay Miner.* **1979**, *14*, 109.
(123) Eggleton, R. A.; Fitzpatrick, R. W. *Clays Clay Miner.* **1988**, *36*, 111.
(124) Coey, J. M. D.; Readman, P. W. *Earth Planet. Sci. Lett.* **1973**, *21*, 45.
(125) Cardile, C. M. *Clays Clay Miner.* **1988**, *36*, 537.
(126) Pankhurst, Q. A.; Pollard, R. J. *Clays Clay Miner.* **1992**, *40*, 268.
(127) Manceau, A.; Combes, J.-M.; Calas, G. *Clays Clay Miner.* **1990**, *38*, 331.
(128) Combes, J. M.; Manceau, A.; Calas, G.; Bottero, J. Y. *Geochim. Cosmochim. Acta* **1989**, *53*, 583.
(129) Combes, J. M.; Manceau, A.; Calas, G. *Geochim. Cosmochim. Acta* **1990**, *54*, 1083.
(130) Eggleton, R. A.; Fitzpatrick, R. W. *Clays Clay Miner.* **1990**, *38*, 335.
(131) Manceau, A.; Combes, J. M. *Phys. Chem. Miner.* **1988**, *15*, 283.
(132) Drits, V. A.; Gorshkov, A. I.; Sakharov, B. A.; Salyń, A. L.; Manceau, A.; Sivtsov, A. B. *Lithol. Miner. Resour.* **1995**, *1*, 76.
(133) Manceau, A.; Drits, V. A. *Clay Miner.* **1993**, *28*, 165.
(134) St. Pierre, T. G.; Sipos, P.; Chan, P.; Chua-Anusor, A.; Bauchspiess, K. R.; Webb, J. In *Nanophase Materials*: *Synthesis*−*Properites*−*Applications*; Hadjipanayis, G. C., Siegel, R. W., Eds.; NATO-ASI Series, Kluewer Academic Publishers: Dordrecht, 1993; p 49. (In Bocquet and Hill, *Phys. Chem. Miner.* **1995**, *22*, 524.)
(135) Manceau, A.; Gates, W. P. *Clays Clay Miner.* **1997**, *45*, 448.
(136) Shinoda, K.; Matsubara, E.; Muramatsu, A.; Waseda, Y. *Mater. Trans., JIM* **1994**, *35*, 394.
(137) Waychunas, G. A.; Rea, B. A.; Fuller, C. C.; Davis, J. A. *Geochim. Cosmochim. Acta* **1993**, *56*, 2251.
(138) Waychunas, G. A.; Davis, J. A.; Fuller, C. C. *Geochim. Cosmochim. Acta* **1995**, *59*, 3655.
(139) Waychunas, G. A.; Fuller, C. C.; Rea, B. A.; Davis, J. A. *Geochim. Cosmochim. Acta* **1996**, *60*, 1765.
(140) Fuller, C. C.; Davis, J. A.; Waychunas, G. A. *Geochim. Cosmochim. Acta* **1993**, *57*, 2271.
(141) Manceau, A. *Geochim. Cosmochim. Acta* **1995**, *59*, 3647.
(142) Waite, T. D.; Davis, J. A.; Payne, T. E.; Waychunas, G. A.; Xu, N. *Geochim. Cosmochim. Acta* **1994**, *58*, 5465.
(143) Charlet, L.; Manceau, A. *J. Colloid Interface Sci.* **1992**, *148*, 443.
(144) Spadini, L.; Manceau, A.; Schindler, P. W.; Charlet, L. *J. Colloid Interface Sci.* **1994**, *168*, 73.
(145) Rea, B. A.; Davis, J. A.; Waychunas, G. A. *Clays Clay Miner.* **1994**, *42*, 23.
(146) Vempati, R. K.; Loeppert, R. H.; Sittertz-Bhatkar, H.; Burghardt, R. C. *Clays Clay Miner.* **1990**, *38*, 294.
(147) Yoshinaga, N.; Kanasaki, N. *Clay Sci.* **1993**, *9*, 43.
(148) Childs, C. W.; Wells, N.; Downes, C. J. *J. R. Soc. N. Z.* **1986**, *16*, 85.
(149) Childs, C. W.; Kanasaki, N.; Yoshinaga, N. *Clay Sci.* **1993**, *9*, 65.
(150) Bigham, J. M.; Schwertmann, U.; Traina, S. J.; Winland, R. L.; Wolf, M. *Geochim. Cosmochim. Acta* **1996**, *60*, 2111.
(151) Schwertmann, U.; Bigham, J. M.; Murad, E. *Eur. J. Mineral.* **1995**, *7*, 547.
(152) Bigham, J. M.; Carlson, L.; Murad, E. *Mineral. Magn.* **1994**, *58*, 641.
(153) Murad, E.; Schwertmann, U.; Bigham, J. M.; Carlson, L. In *Environmental Geochemistry of Sulfide Oxidation*; Alpers, C. N., Blowes, D. W., Eds.; ACS Symp. Ser. 550; American Chemical Society: Washington DC, 1994; p 190.
(154) Brown, G. In *Crystal Structures of the Clay Miner. and Their X-ray Identification*; Brindley, G. W., Brown, G., Eds.; *Mineral. Soc. Monogr.* **1980**, *5*, 361.
(155) Farmer, V. C. *Clay Miner.* **1992**, *27*, 373.
(156) Manceau, A.; Ildefonse, P.; Hazemann, J.-L.; Flank, A.-M.; Gallup, D. *Clays Clay Miner.* **1995**, *43*, 304.
(157) Schwertmann, U.; Thalmann, H. *Clay Miner.* **1976**, *11*, 189.
(158) Carlson, L.; Schwertmann, U. *Geochim. Cosmochim. Acta* **1981**, *45*, 421.
(159) Murad, E.; Schwertmann, U. *Am. Mineral.* **1980**, *65*, 1044.
(160) Murad, E. In *Iron in Soils and Clay Miner.*; Stucki, J. W., Goodman, B. A., Schwertmann, U., Eds.; NATO-ASI Ser. 217; D. Reidel; Dordrecht, 1988; p 309.
(161) Murad, E. *Phys. Chem. Miner.* **1996**, *23*, 248.
(162) Chadwick, J. C.; Jones, D. H.; Thomass M. F.; Devinish, M. *Hyperfine Interact.* **1986**, *28*, 541.
(163) Madsen, M. B.; Mørup, S.; Koch, C. J. W. *Hyperfine Interact.* **1986**, *27*, 329.
(164) Arshed, M.; Butt, N. M.; Siddique, M.; Anwar-ul Islam, M. *Phys. Status Solidi* **1993**, *137*, K33.
(165) Cianchi, L.; Mancini, M.; Spina, G.; Tang, H. *J. Phys.: Condens. Matter* **1992**, *4*, 2073.
(166) Cianchi, L.; Gulisano, F.; Spina, G. *J. Phys.: Condens. Matter* **1994**, *6*, 2269.
(167) Pollard, R. J.; Cardile, C. M.; Lewis, D. G.; Brown, L. G. *Clay Miner.* **1992**, *27*, 57.
(168) Chadwick, J. C.; Jones, D. H.; Thomass M. F.; Devenish, M. *Hyperfine Interact.* **1986**, *28*, 537.
(169) Chadwick, J.; Jones, D. H.; Thomas, M. F.; Tatlock, G. J.; Devenish, R. W. *J. Magn. Magn. Mater.* **1986**, *61*, 88.
(170) Murad, E. *Neues Jahrb. Mineral. Monatsh.* **1982**, 45.
(171) Murad, E. *J. Magn. Magn. Mater.* **1988**, *74*, 153.
(172) Murad, E.; Schwertmann, U. *Hyperfine Interact.* **1988**, *41*, 835.
(173) Murad, E.; Bowen, L. H.; Long, G. J.; Quin, T. G. *Clay Miner.* **1988**, *23*, 161.
(174) Borggaard, O. K. In *Iron in Soils and Clay Miner.*; Stucki, J. W., Goodman, B. A., Schwertmann, U., Eds.; NATO-ASI Ser. 217; D. Reidel; Dordrecht, 1988; p 83.
(175) Mehra, O. P.; Jackson, M. L. *Clays Clay Miner.* **1960**, *7*, 317.
(176) Schwertmann, U. *Z. Pflanzenernähr. Bodenkd.* **1964**, *105*, 194.
(177) Schwertmann, U. *Can. J. Soil Sci.* **1973**, *53*, 244.
(178) Adams, W. A.; Kassim, J. K. *J. Soil Sci.* **1984**, *35*, 117.
(179) Ryan, J. N.; Gschwend, P. M. *Clays Clay Miner.* **1991**, *39*, 509.
(180) Schulze, D. G. *Soil Sci. Soc. Am. J.* **1981**, *45*, 437.
(181) Schwertmann, U.; Schulze, D. G.; Murad, E. *Soil Sci. Soc. Am. J.* **1982**, *46*, 869.
(182) Rhoton, F. E.; Bigham, J. M.; Norton, L. D.; Smeck, N. E. *Soil Sci. Soc. Am. J.* **1981**, *45*, 645.
(183) Golden, D. C.; Ming, D. W.; Bowen, L. H.; Morris, R. V.; Lauer, H. V., Jr. *Clays Clay Miner.* **1994**, *42*, 53.
(184) Borggaard, O. K. *Clays Clay Miner.* **1991**, *39*, 324.
(185) Borggaard, O. K. *Z. Pflanzenernähr. Bodenkd.* **1992**, *155*, 431.
(186) Saleh, A. M.; Jones, A. A. *Clay Miner.* **1984**, *19*, 745.
(187) Schwertmann, U. *Soil Sci.* **1979**, *128*, 195.
(188) Campbell, A. S.; Schwertmann, U.; Campbell, P. A. *Clay Miner.* **1997**, *32*, 615.
(189) Karim, Z. *Clays Clay Miner.* **1984**, *32*, 181.
(190) Cornell, R. M.; Giovanoli, R.; Schneider, W. *J. Chem. Technol. Biotechnol.* **1989**, *46*, 115.
(191) Šubrt, J.; Štengl, V.; Skokánek, M. *Thermochim. Acta* **1992**, *211*, 107.
(192) Schwertmann, U.; Cambier, P.; Murad, E. *Clays Clay Miner.* **1985**, *33*, 369.
(193) Matijevic, E.; Scheiner, P. *J. Colloid Interface Sci.* **1978**, *63*, 509.
(194) Murphy, P. J.; Posner, A. M.; Quirk, J. P. *J. Colloid Interface Sci.* **1976**, *56*, 312.
(195) Lewis, D. G.; Schwertmann, U. *J. Colloid Interface Sci.* **1980**, *78*, 543.
(196) Cornell, R. M.; Giovanoli, R. *Clays Clay Miner.* **1985**, *33*, 424.
(197) Cornell, R. M.; Giovanoli, R. *Clays Clay Miner.* **1986**, *34*, 557.
(198) Cornell, R. M.; Giovanoli, R. *Clays Clay Miner.* **1990**, *38*, 469.
(199) Zinck, J. M.; Dutrizac, J. E. *CIM Bull.* **1998**, *91* (No. 1009) , 94.
(200) Singh, S. S.; Kodama, H. *Clays Clay Miner.* **1994**, *42*, 606.
(201) Bland, P. A.; Kelly, S. P.; Berry, F. J.; Cadogan, J. M.; Pillinger, C. T. *Am. Mineral.* **1997**, *82*, 1187.
(202) Schulze, D. G.; Schwertmann, U. *Clay Miner.* **1984**, *19*, 521.
(203) Stiers, W.; Schwertmann, U. *Geochim. Cosmochim. Acta* **1985**, *49*, 1909.
(204) Schwertmann, U.; Gasser, U.; Sticher, H. *Geochim. Cosmochim. Acta* **1989**, *53*, 1293.
(205) Gerth, J. *Geochim. Cosmochim. Acta* **1990**, *54*, 363.
(206) Wolska, E.; Schwertmann, U. *Neues Jahrb. Mineral. Monatsch.* **1993**, p 213.
(207) Ruan, H. D.; Gilkes, R. J. *Clays Clay Miner.* **1995**, *43*, 196.
(208) Bibak, A.; Gerth, J.; Borggaard, O. K. *Clays Clay Miner.* **1995**, *43*, 141.
(209) Harrison, J. B.; Berkheiser, V. E. *Clays Clay Miner.* 1982, *30*, 97.
(210) Anderson, P. R.; Benjamin, M. M. *Environ. Sci. Technol.* **1985**, *19*, 1048.
(211) Dzombak, D. A.; Morel, F. M. M. *Surface Complexation Modeling. Hydrous Ferric Oxide*; Wiley-Interscience: New York, 1990; 331 pp.
(212) Liaw, B. J.; Cheng, D. S.; Yang, B. L. *J. Catal.* **1989**, *118*, 312.
(213) Stanjek, H.; Weidler, P. G. *Clay Miner.* **1992**, *27*, 397.
(214) Postma, D. *Geochim. Cosmochim. Acta* **1993**, *57*, 5027.
(215) Bruun Hansen, H. C.; Raben-Lange, B.; Raulund-Rasmusssen, K.; Borggaard, O. K. *Soil Sci.* **1994**, *158*, 40.
(216) Axe, L.; Anderson, P. R. *J. Colloid Interface Sci.* **1995**, *175*, 157.
(217) Crosby, S. A.; Glasson, D. R.; Cuttler, A. H.; Butler, I.; Turner, D. R.; Whitfield, M.; Millward, G. E. *Environ. Sci. Technol.* **1983**, *17*, 709.
(218) Hiemstra, T.; van Riemsdijk, W. H. *J. Colloid Interface Sci.* **1996**, *179*, 488.
(219) Davis, J. A.; Leckie, J. O. *J. Colloid Interface Sci.* **1978**, *67*, 90.
(220) Fox, L. E. *Geochim. Cosmochim. Acta* **1988**, *52*, 771.
(221) Bruun Hansen, H. C.; Borggaard, O. K.; Sørensen, J. *Geochim. Cosmochim. Acta* **1994**, *58*, 2599.
(222) Kinniburgh, D. G.; Jackson, M. L. *Soil Sci. Soc. Am. J.* **1982**, *46*, 56.
(223) Kinniburgh, D. G. *J. Soil Sci.* **1983**, *34*, 759.
(224) Kinniburgh, D. G. *Environ. Sci. Technol.* **1986**, *20*, 895.
(225) Benjamin, M. M.; Leckie, J. O. *J. Colloid Interface Sci.* **1981**, *79*, 209.
(226) Pierce, M. L.; Moore, C. B. *Water Res.* **1982**, *16*, 1247.

(227) Zachara, J. M.; Girvin, D. C.; Schmidt, R. L.; Resch, C. T. *Environ. Sci. Technol.* **1987**, *21*, 589.
(228) Leckie, J. O.; Benjamin, M. M.; Hayes, K.; Kaufman, G.; Altman, S. *Electr. Power Res. Inst.* **1980**, *C3*−*1513*.
(229) Parfitt, R. L.; Smart, R. S. C. *Soil Sci. Soc. Am. J.* **1978**, *42*, 48.
(230) Langmuir, D. *Geochim. Cosmochim. Acta* **1978**, *42*, 547.
(231) Hsi, C. D.; Langmuir, D. *Geochim. Cosmochim. Acta* **1985**, *49*, 1931.
(232) Backes, C. A.; McLaren, R. G.; Rate, A. W.; Swift, R. S. *Soil Sci. Soc. Am. J.* **1995**, *59*, 778.
(233) Warren, L. A.; Outridge, P. M.; Zimmerman, A. P. *Hydrobiologia* **1995**, *304*, 197.
(234) Bibak, A.; Borggaard, O. K. *Soil Sci.* **1994**, *158*, 323.
(235) Bibak, A. *Soil Sci. Plant Anal.* **1994,** *25*, 3229.
(236) Combes, J. M.; Chisholm-Brause, C. J.; Brown, G. E., Jr.; Parks, G. A.; Conradson, S. D.; Eller, P. G.; Triay, I. R.; Hobart, D. E.; Meijer, A. *Environ. Sci. Technol.* **1992**, *26*, 376.
(237) Sakamoto, Y.; Ohnuki, T.; Senoo, M. *Radiochim. Acta* **1994**, *66*/*67*, 285.
(238) Whalley, C.; Grant, A. *Anal. Chim. Acta* **1994**, *291*, 287.
(239) Manceau, A.; Charlet, L.; Boisset, M. C.; Didier, B.; Spadini, L. *Appl. Clay Sci.* **1992**, *7*, 201.
(240) Hayes, K. F.; Roe. A. L.; Brown, G. E., Jr.; Hodgson, K. O.; Leckie, J. O.; Parks, G. A. *Science* **1987**, *238*, 783.
(241) Manceau, A.; Charlet, L. *J. Colloid Interface Sci.* **1994**, *168*, 87.
(242) Eynard, A. *Mineral. Petrogr. Acta* **1993**, *36*, 343.
(243) Freese, D.; Lookman, R.; Merckx, R.; van Riemsdijk, W. H. *Soil Sci. Soc. Am. J.* **1995**, *59*, 1295.
(244) Fordham, A. W.; Schwertmann, U. *J. Environ. Qual.* **1977**, *6*, 133.
(245) Willett, I. R.; Chartres, C. J.; Nguyen, T. T. *J. Soil Sci.* **1988**, *39*, 275.
(246) Griffloen, J. *Environ. Sci. Technol.* **1994**, *28*, 675.
(247) Ryden, J. C.; McLaughlin, J. R.; Syers, J. K. *J. Soil Sci.* **1977**, *28*, 72.
(248) Parfitt, R. L.; Atkinson, R. J.; Smart, R. S. C. *Soil Sci. Soc. Am. Pro.* **1975**, *39*, 837.
(249) Lin, C. F.; Benjamin, M. M. *Environ. Sci. Technol.* **1990**, *24*, 126.
(250) Lin, C. F.; Benjamin, M. M. *Water Res.* **1992**, *26*, 397.
(251) Van Riemsdijk, W. H.; Boumans, L. J. M.; de Haan, F. A. M. *Soil Sci. Soc. Am. J.* **1984**, *48*, 537.
(252) Barrón, V.; Gálvez, N.; Hochella, M. F., Jr.; Torrent, J. *Am. Mineral.* **1997**, *82*, 1091.
(253) Cornell, R. M.; Giovanoli, R.; Schindler, P. W. *Clays Clay Miner.* **1987**, *35*, 21.
(254) Schwandt, H.; Kögel-Knaber, I.; Stanjek, H.; Totsche, K. *Sci. Total Environ.* **1992**, *123*/*124*, 121.
(255) Cox, L.; Hermosin, M. C.; Cornejo, J. *Eur. J. Soil Sci.* **1995**, *46*, 431.
(256) Inoue, K.; Hiradate, S.; Takagi, S. *Soil Sci. Soc. Am. J.* **1993**, *57*, 1254.
(257) Kung, K.-H.; McBride, M. B. *Clays Clay Miner.* **1989**, *37*, 333.
(258) Schultz, M. F.; Benjamin, M. M.; Ferguson, J. F. *Environ. Sci. Technol.* **1987**, *21*, 863.
(259) Edwards, M. M.; Benjamin, M. M. *J.*—*Water Pollut. Control Fed.* **1989**, *61*, 481.
(260) Stenkamp, V. S.; Benjamin, M. M. *J. Am. Water Works Assoc.* **1994**, *86*, 37.
(261) Edwards, M. M.; Benjamin, M. M. *J.*—*Water Pollut. Control Fed.* **1989**, *61*, 1523.
(262) Zachara, J. M.; Gassman, P. L.; Smith, S. C.; Taylor, D. *Geochim. Cosmochim. Acta* **1995**, *59*, 4449.
(263) Chen, W. Y.; Anderson, P. R.; Holsen, T. M. *Res. J.*—*Water Pollut. Control Fed.* **1991**, *63*, 958.
(264) Gao, Y.-M.; Sengupta, A. K.; Simpson, D. *Water Res.* **1995**, *29*, 2195.
(265) Schwertmann, U.; Heinemann, B. *Neues Jahrb. Mineral. Monatsch.* **1959**, p 174.
(266) Prasad, S. V. S.; Sitakara Rao, V. *J. Mater. Sci.* **1984**, *19*, 3266.
(267) Lewis, D. G. *Z. Pflanzenernähr. Bodenkd.* **1992**, *155*, 461.
(268) Johnston, J. H.; Lewis, D. G. In *Industrial Applications of the Mössbauer Effect*; Long, G. J., Stevens, J. G., Eds.; Plenum Publishing: New York, 1986; p 565. (In ref 267.)
(269) Wolska, E. *Solid State Ionics* **1988**, *28*−*30*, 1349.
(270) Wolska, E. *Z. Kristallogr.* **1981**, *154*, 69.
(271) Wolska, E.; Szajda, W. *J. Mater. Sci.* **1985**, *20*, 4407.
(272) Serna, C. J.; Iglesias, J. E. *J. Mater. Sci. Lett.* **1986**, *5*, 901.
(273) Johnston, J. H.; Lewis, D. G. *Geochim. Cosmochim. Acta* **1983**, *47*, 1823.
(274) Schwertmann, U.; Murad, E. *Clays Clay Miner.* **1983**, *31*, 277.
(275) Torrent, J.; Guzman, R.; Parra, M. A. *Clays Clay Miner.* **1982**, *30*, 337.
(276) Torrent, J.; Guzman, R. *Clay Miner.* **1982**, *17*, 463.
(277) Fischer, W.; Schwertmann, U. *Clays Clay Miner.* **1975**, *23*, 33.
(278) Andreeva, D.; Mitov, I.; Tabakova, T.; Mitrov, V.; Andreev, A. *Mater. Chem. Phys.* **1995**, *41*, 146.
(279) Cornell, R. M.; Schneider, W.; Giovanoli, R. *Clay Miner.* **1989**, *24*, 549.
(280) Cornell, R. M.; Schneider, W. *Polyhedron* **1989**, *8*, 149.
(281) Cornell, R. M.; Schwertmann, U. *Clays Clay Miner.* **1979**, *27*, 402.
(282) Cornell, R. M. *Clays Clay Miner.* **1985**, *33*, 219.
(283) Cornell, R. M. *Z. Pflanzenernähr. Bodenkd.* **1987**, *150*, 304.
(284) Carmo Rangel Varela, M. do; Francisco de Jesus Filho, M.; Galembeck, F. *Hyperfine Interact.* **1994**, *83*, 161.
(285) McBride, M. B.; Farmer, V. C.; Russell, J. D.; Tait, J. M.; Goodman, B. A. *Clay Miner.* **1984**, *19*, 1.
(286) Schwertmann, U.; Fechter, H. *Clay Miner.* **1982**, *17*, 471.
(287) Vempati, R. K.; Loeppert, R. H. *Clays Clay Miner.* **1989**, *37*, 273.
(288) Soma, M.; Seyama, H.; Yoshinaga, N.; Theng, B. K. G.; Childs, C. W. *Clay Sci.* **1996**, *9*, 385.
(289) Vempati, R. K.; Loeppert, R. H.; Dufner, D. C.; Cocke, D. L. *Soil Sci. Am. J.* **1990**, *54*, 695.
(290) Parfitt, R. L.; Van Der Gaastt, S. J.; Childs, C. W. *Clays Clay Miner.* **1992**, *40*, 675.
(291) Hansen, H. C. B.; Wetche, T. P.; Raulund-Rasmussen, K.; Borggaard, O. K. *Clay Miner.* **1994**, *29*, 341.
(292) Karim, Z. *Soil Sci. Soc. Am. J.* **1986**, *50*, 247.
(293) Schwertmann, U.; Taylor, R. M. *Clays Clay Miner.* **1972**, *20*, 159.
(294) Schwertmann, U.; Fechter, H. *Clay Miner.* **1994**, *29*, 87.
(295) Cornell, R. M.; Giovanoli, R. *Polyhedron* **1988**, *7*, 385.
(296) Taylor, R. M.; Schwertmann, U. *Clays Clay Miner.* **1978**, *26*, 373.
(297) Schwertmann, U.; Fitzpatrick, R. W.; Taylor, R. M.; Lewis, D. G. *Clays Clay Miner.* **1979**, *27*, 105.
(298) Colombo, C.; Violante, A. *Clays Clay Miner.* **1996**, *44*, 113.
(299) Lewis, D. G.; Schwertmann, U. *Clay Miner.* **1979**, *14*, 115.
(300) Lewis, D. G.; Schwertmann, U. *Clays Clay Miner.* **1979**, *27*, 195.
(301) Stanjek, H.; Schwertmann, U. *Clays Clay Miner.* **1992**, *40*, 347.
(302) Boero, V.; Franchini-Angela, M. *Eur. J. Miner.* **1992**, *4*, 539.
(303) Schwertmann, U. *Soil Sci. Soc. Am. J.* **1988**, *52*, 288.
(304) Taylor, R. M.; Schwertmann, U. *Clay Miner.* **1974**, *10*, 299.
(305) Cornell, R. M. *Clay Miner.* **1988**, *23*, 329.
(306) Cornell, R. M. *Clay Miner.* **1991**, *26*, 427.
(307) Giovanoli, R.; Cornell, R. M. *Z. Pflanzenernähr. Bodenkd.* **1992**, *155*, 455.
(308) Tronc, E.; Belleville, P.; Jolivet, J. P.; Livage, J. *Langmuir* **1992**, *8*, 313.
(309) Jolivet, J. P.; Belleville, P.; Tronc, E.; Livage, J. *Clays Clay Miner.* **1992**, *40*, 531.
(310) Cornell, R. M.; Giovanoli, R. *Clays Clay Miner.* **1987**, *35*, 11.
(311) Cornell, R. M.; Giovanoli, R. *Clays Clay Miner.* **1989**, *37*, 65.
(312) Greffié, C.; Parron, C.; Benedetti, M.; Amouric, M.; Marion, P.; Colin, F. *Chem. Geol.* **1993**, *107*, 292.
(313) Greffié, C.; Benedetti, C. P.; Hiemstra, T. *C. R. Acad. Sci. Paris, Ser. IIa* **1996**, *332*, 197.
(314) Greffié, C.; Benedetti, M. F.; Parron, C.; Amouric, M. *Geochim. Cosmochim. Acta* **1996**, *60*, 1531.

CR970105T